



## SYSTEMS





# TECHNOLOGY RESEARCH INSTITUTE

## LETI AT A GLANCE

Founded in **1967**

Based in **France** (Grenoble)  
with offices in **USA** (Silicon Valley)  
and **Japan** (Tokyo)

**330**  
industrial partners

**1,900**  
researchers

Committed to innovation, Leti's teams create **differentiating solutions in miniaturization and energy-efficient technologies** for its industrial partners.

Leti is a technology research institute at CEA Tech and a recognized global leader focused on miniaturization technologies enabling energy-efficient and secure IoT. Leti delivers solid expertise throughout the entire IoT chain, from sensors to data processing and computing solutions. Leti pioneered FDSOI low power platform for IoT, M&NEMS technology for low cost multisensors solutions, CoolCube™ integration for highly connected and cost effective devices.

Leti's mission is to pioneer new technologies, enabling innovative solutions to ensure Leti's industrial partners competitiveness while creating a better future. It tackles most current global issues such as the future of industry, clean and safe energies, health and wellness, sustainable transport, information and communication technologies, space exploration and safety & security.

For 50 years, the institute has built long-term relationships with its partners: global industrial companies, SMEs and startups. It tailors innovative and differentiating solutions that strengthen their competitiveness and contribute to creating new jobs. Leti and its partners work together through bilateral projects, joint laboratories and collaborative research programs. Leti actively contributes to the creation of startups through its startup program.

Leti has signed partnerships with major research technology organizations and academic institutions. It is a member of the Carnot Institutes network\*.

\*Carnot Institutes network: French network of 34 institutes serving innovation in industry.


**2,760**  
patents in portfolio

**60**  
startups created

**€315**  
million budget

**700**  
publications each year

**ISO 9001**  
certified since 2000



Based on MINATEC Campus, Systems Integration Division (DSYS) is at the strategic core of Leti's technological solutions, adding a "system perspective" on technological trends. Our research activities focus on the design and integration of innovative solutions based on emerging electronic technologies for a wide panels of applications such as factory of the future, multimedia, smart energy, smart transport, e-health, sports and leisure.

DSYS's expertise is based on four major pillars which are (i) wireless communications, (ii) innovative sensor-system design, (iii) power-management systems and (iv) security solutions for electronics and components. Our teams are using tools and know how inherited from physic, electromagnetism and electronic areas but also from signal and data processing domain ; they also take profit from state of the art facilities for achieving simulation, characterization and prototyping steps.

Thanks to its capability to work on specific application barriers, DSYS Division is particularly attractive for industrial partners who are facing the challenges of IoT , 5G and cybersecurity. It can be either SME or big companies which are looking for a high level expertise in a businesslike environment.



## SYSTEMS







## CONTENTS

Edito	05
Key figures	07
Scientific activity	08
<b>01 / Wireless Mobile Communications</b>	<b>11</b>
<b>02 / Wireless Short-Range and Contactless Systems</b>	<b>21</b>
<b>03 / Antennas and Propagation</b>	<b>31</b>
<b>04 / Sensors and Systems, Energy and Nano technologies</b>	<b>45</b>
<b>05 / Security</b>	<b>55</b>
<b>06 / PHD Degree awarded</b>	<b>63</b>





## EDITO

**SÉBASTIEN DAUVÉ**  
**HEAD OF THE SYSTEMS DIVISION**

This document publishes our most significant technological achievements of 2016 selected among a wide variety of scientific results, some of them conducted jointly with external partners who gave their agreement.

2016 has been very fruitful for DSYS, with more than 130 publications, 50 patents and tens of prototypes. In this report, chapter 1 details our scientific finding on both below 6 GHz and millimeter wave wireless communications that have today strong relevance for the forthcoming 5G and beyond systems. In addition, in chapter 2 we present our research on short range communications and in-door localization solutions. In chapter 3 we detail our proposed innovation, its technological implementation and performance measurements on wideband and reconfigurable antennas, including our work on precise propagation characterization. Our continuous efforts on innovative sensors' design and their dedicated signal processing are detailed in chapter 4 where we propose to exploit



either MEMs capabilities for applications where low power or advanced integration present critical constraints or, to explore capabilities of nanotechnology where MEMs do not provide efficient solutions. 2016 has been notably marked by a significant increase of our investigations on hardware enabled cyber security and on the identification of countermeasures to threats for the applications related to massive IoT which have a critical impact on vertical industry needs. Our proposed solutions are detailed in chapter 5. I hope you enjoy reading this report.

Sébastien Dauvé









## KEY FIGURES



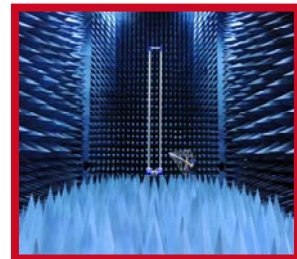
**230** researchers  
**35** PhD students and post-docs

**27 M€** budget  
**90%** external funding



**50** patents granted in 2016  
**445** patents portfolio  
**29** book chapters and journal papers  
**136** communications in conferences and workshops

Research facilities:  
**23** testing and experimentation labs  
**3** anechoic chambers  
Magnetometer test ground  
Information Technology Security  
Evaluation Facility (ITSEF)



**250** industrial partners



## SCIENTIFIC ACTIVITY

### Publications

**165 publications** in 2016 including 29 book chapters and top journals, 136 international conference communications. These include IEEE Transactions on Wireless Communications, IEEE Transactions on Antenna and Propagation, IEEE Transactions on Electromagnetic Compatibility, IEEE Transactions on Communications, IEEE Sensors & Transducers journal, IEEE Transaction on Haptics, IEEE Transactions on Very Large Scale Integration Systems, IEEE Transactions on vehicular Technology, Smart Materials and Structures journal, IEEE VTC, IEEE ICC, IEEE PIMRC, IEEE WCNC, IEEE GlobeCom, Physiological computing conference; International Workshop on SHM, PowerMEMS, etc.

### Prize and awards

- **Best paper award:** R. Gerzaguet, et al., "Performance of Fractional Delay Estimation in Joint Estimation Algorithm Dedicated to Digital Tx Leakage Compensation inn FDD Transceivers", EAI International Conference on Cognitive Radio Oriented Wireless Networks 2016 (EAI CROWNCOM'16), Grenoble, May-June 2016
- **Best paper award:** B. Denis et al., "Cooperative Localization in GNSS-aided VANETs with Accurate IR-UWB Range Measurements", IEEE Workshop on Positioning, Navigation and Communications 2016 (IEEE WPNC'16), Bremen, Oct. 2016
- **Best paper award:** D. Noguet et al., "Advances in opportunistic radio technologies for TVWS", EURASIP Journal on Wireless Communications and Networking, vol. 2011:170, 2011. Award granted in 2016.
- **Best paper award:** S. Thibert, A. Ghis, and M. Delaunay, "AFM study of 2D resonators based on Diamond Like Carbon", IEEE NANO 2016 conference, Sendai, Japan.
- **Best poster award:** M. Ranieri, D. Alberto, H. Piret, V. Cattin, "Electronic Module for the Thermal Monitoring of a Li-ion Battery Cell through the Electrochemical Impedance Estimation", Thermionic Workshop, Budapest, Hungary, 2016.
- **Celtic Plus Excellence Award 2016: best Smart City Project** for the Celtic Plus research project 'TILAS' - Technology Improvements for Large Scale Smart Cities Deployments.



## SCIENTIFIC ACTIVITY

### Experts

1 International Expert, 16 Senior Experts, 12 Experts, 7 of them holding an HDR.

### Scientific committees

- National Research Agency "High performance infrastructures, software technology and science » committee.
- Technical Program committees of: JNM, COST 15104, EurAAP, IEEE EUROCON, IEEE GlobCom, EuCNC, IEEE VTC, IEEE PIMRC, IEEE WCNC, IEEE VTC, IEEE DySPAN.

### Conferences and Workshops organizations

CrownCom Conference Organization in Grenoble, Workshops, Panels and special sessions organized in the following conferences: EuCAP, EuMW, EuCNC, ISWCS, IEEE ICC, IEEE WCNC, IEEE PIMRC.

### International Collaborations

University of Rome (Italy) University of Bologna (Italy), University of Calgary (Canada), Université Catholique de Louvain (Belgium), Czech Technical University (Czech Republic), Fraunhofer Institute HHI (Germany), ETRI (South Korea), Tokyo Teck University (Japan).









## 1.

**WIRELESS MOBILE  
COMMUNICATIONS**

- Millimeter Waves
- Full Duplex
- Advanced Coding
- Spectrum and Heterogeneous  
Network Management

# WAVEFORM CANDIDATES FOR 5G MOBILE RADIO COMMUNICATIONS BELOW 6 GHz

## RESEARCH TOPIC:

5G, waveform, filtered OFDM, UFMC, FBMC

## AUTHORS:

D. Kténas, J.-B. Doré, R. Gerzaguet and N. Cassiau

## ABSTRACT:

5G will have to cope with a high degree of heterogeneity in terms of services and requirements. Flexible and efficient use of all available spectrums for different network deployment scenarios is one challenge for the future 5G. To maximize spectrum efficiency, the 5G air interface technology will also need to be flexible and capable of mapping various services to the best suitable combinations of frequency and time resources. In this work, we study and fairly compare the performance of different waveforms (UFMC, FBMC, and legacy LTE waveforms) in cellular networks under a common framework. We assess spectral efficiency, power spectral density, peak-to-average power ratio and robustness to asynchronous multi-user uplink transmission.

## Context and Challenges

Even though Orthogonal Frequency Division Multiplexing (OFDM) is the most prominent multicarrier modulation technique in wireless standards for below 6GHz transmission, it also exhibits some intrinsic drawbacks. An important frequency leakage is caused by its rectangular pulse shape; the cyclic prefix insertion drives to a spectral efficiency loss; and fine time and frequency synchronization is required to preserve the carrier orthogonality that guarantees a low level of interference. Several alternative candidates have been intensively studied in the literature in the past few years, such as Universal Filtered Multicarrier (UFMC) and Filter Bank Multicarrier (FBMC). However, to the best of our knowledge, a fair comparison between the different waveforms in the context of an asynchronous multi-user scenario is lacking.

## Main Results

CP-OFDM is a well-known multicarrier modulation (which serves as the physical layer for 3GPP-LTE or 802.11.a/g/n). A block of complex symbols is mapped onto a set of orthogonal carriers. A cyclic prefix (CP) is inserted, i.e. the end of the symbol is appended to its beginning. The CP guarantees circularity of the OFDM symbol (and thus no inter-carrier interference) if the delay spread of the channel is lower than the CP duration.

UFMC is a derivative of OFDM introduced by Alcatel-Lucent; in that case a group of carriers is filtered. The subband filtering has been motivated by the fact that the smallest unit used by the scheduling algorithm in frequency domain in 3GPP-LTE is a resource block (RB), which is a group of 12 carriers. The filtering operation leads to a good frequency localization of the RB resulting in a lower ACL (Adjacent Channel Leakage) compared to OFDM.

A multicarrier system can be described by a synthesis/analysis filter bank, i.e. a transmultiplexer structure. The synthesis filter bank is composed of a set of parallel transmit filters. FBMC waveforms utilize a prototype filter designed to give a good frequency localization of the carriers. The prototype filter considered in this paper is based on the frequency sampling technique. This technique gives the advantage of using a closed-

form representation that includes only a few adjustable design parameters. The most significant parameter is the duration of the impulse response of the prototype filter also called overlapping factor,  $K$ . The larger the overlapping factor  $K$ , the more localized the signal will be in frequency.

The performance of the different waveforms have been assessed by simulations in [1][2][3]. A summary of the comparison is depicted in Fig. 1. The benefits of new waveforms for the 5G use cases have been clearly highlighted. UFMC offers improvements keeping backward compatibility with legacy OFDM, while FBMC goes forward making this waveform particularly interesting for 5G scenarios. Last but not least, we demonstrated the benefits of the FBMC waveform compared to legacy LTE waveforms and UFMC both in terms of robustness against asynchronicity and in terms of spectral efficiency.

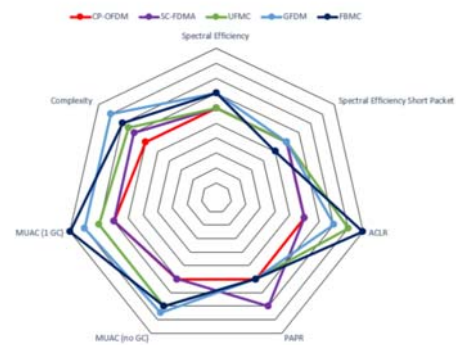


Fig.1: waveform comparison - synthesis.

## Perspectives

The main drawbacks of FBMC are: the long pulse shape impulse response that is not suitable for short bursts transmission, scattered pilot insertion and MIMO support due to the use of OQAM (real orthogonality). CEA is therefore already working on an adaptation of FBMC waveform, called Block Filtered (BF)-OFDM that is compatible with these concepts.

## RELATED PUBLICATIONS:

- [1] R.Gerzaguet, D.Ktenas, N.Cassiau, JB Doré., "Comparative study of 5G Waveform candidates for below 6GHz air interface", ETSI Workshop on Future Radio Technologies & Air Interfaces, 27-28 January 2016, Sophia Antipolis, France.
- [2] J-B. Doré, R. Gerzaguet, and D. Kténas, "5G Cellular Networks with Relaxed Synchronization: Waveform Comparison and New Results", IEEE VTC Spring 2016, 15-18 May 2016, Nanjing, China.
- [3] R. Gerzaguet et al., "The 5G candidate waveform race: A comparison of complexity and performance", Eurasip Journal on Wireless Communications and Networking, 2017:13 DOI: 10.1186/s13638-016-0792-0, 11th January 2017.

# MIMO FOR NEW 5G WAVEFORMS

## RESEARCH TOPIC:

5G, MIMO technologies, Spatial multiplexing

## AUTHORS:

D. Demmer, J-B Doré, R Gerzaguet, (D Le Ruyet)

## ABSTRACT:

With the increasing demand for mobile data traffic, multiple antennas as well as enhanced frequency localized transmissions are considered for the generation of wireless networks to come. Filter Bank Multi-Carrier modulation, with the use of Offset-QAM, proves to be an interesting candidate to satisfy those spectrum constraints. Contrary to CP-OFDM, FBMC does not use any CP. Its spectral efficiency is improved but it also weakens the transmissions over highly frequency selective channels. In this work, we extend probabilistic multiple antenna decoding to linear FBMC receivers. The performance of the two common FBMC receiver structures, PolyPhase Network and Frequency-Spreading, are assessed over frequency-selective LTE channel models and compared to state of the art CP-OFDM.

## Context and Challenges

It is a common consensus that mobile wireless standards to come are expected to support a large diversity of services ranging from the high-rate mobile broadband to ultra-high reliability communications. The multi-service dimension of the future mobile network implies tougher requirements in terms of spectrum localization or relaxed synchronous access which has encouraged the study of alternatives waveforms to CP-OFDM. A promising candidate is the Filter-Bank Multi-Carrier (FBMC) that can achieve maximum spectral efficiency with a tightly frequency-localized pulse shape filter. However, FBMC does not satisfy the complex orthogonality which generates inherent interference. Fitting the communication systems with multiple antennas is a common solution to improve the throughput and the transmission reliability. Although MIMO techniques are well suited with CP-OFDM, the application to FBMC systems is not straightforward mainly due to the inherent interference.

## Main Results

When associated with FBMC waveform, the Maximum-Likelihood detection (ML) requires an important complexity that cannot be practically implemented. Indeed, the inherent interference term generated by the 2-D transmultiplexer response requires a large computation overhead because of the ML full research process even for small constellation. This fact motivates the study of linear receivers.

When the carrier spacing widens, the channel variations may become appreciable at the layer band level. Consequently, with a simple 1-tap equalization stage the channel effects may not be properly compensated. Therefore the orthogonality would no longer be satisfied and the performance would considerably decrease. Using precoding at the transmitter side and/or multi-tap equalizers is an efficient way to significantly improve the performance for transmissions over highly frequency-selective channels.

In this work, we have considered an open-loop system, i.e. without any channel knowledge at the transmitter side. We have proposed to extend linear detectors to multi-tap equalizer using a frequency spreading (FS) based receiver. Indeed, as the symbols are spread over a set of subcarriers with the FS scheme, a per layer 1-tap detection can be seen as a multi-tap detection at the carrier level

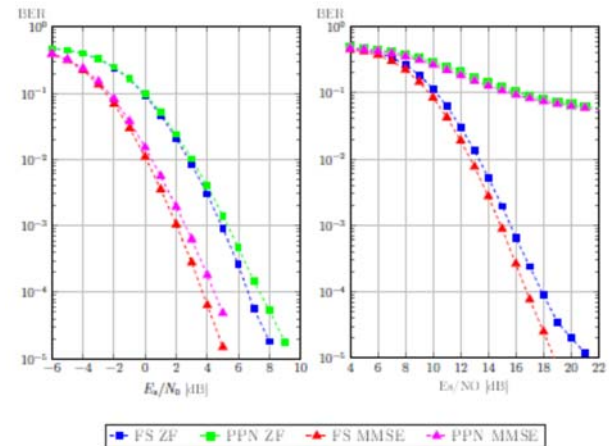


Figure 1 - Performance of the proposed scheme (red and blue curves) for QPSK and 64-QAM modulation with 2 transmit and receive antennas over LTE Vehicular A channel model.

Performance have been assessed by simulations and are depicted in Fig. 1. The FS scheme achieves better performances with both equalizer techniques (ZF and MMSE). Indeed for the PPN scheme, the variations of the channel at the carrier spacing level become appreciable and therefore the 1-tap equalizer does not fully compensate the channel effects. Therefore the orthogonality is not satisfied and the PPN exhibits an error floor due to the huge amount of residual interferences. This phenomenon is intensified for high throughput mode (64-QAM).

## Perspectives

The combination of MIMO schemes and FBMC waveform does not work well with reasonable complexity. We are currently working on the definition of a new waveform that combines good frequency localization and the compatibility with current MIMO technologies.

## RELATED PUBLICATIONS:

[1] D. Demmer, J-B Doré, R Gerzaguet, D Le Ruyet, "Performance of Soft-Decision Linear Receivers for Spatial-Multiplexing FBMC/OQAM ", International Symposium on Wireless Communication Systems. ISWCS 2016.



# MILLIMETER-WAVE AIR INTERFACE FOR 5G

## RESEARCH TOPIC:

5th generation of mobile communications, millimeter wave, physical layer

## AUTHORS:

R. Gerzaguet, J.B. Doré, A. De Domenico, V. Savin, N. Cassiau, D. Kténas

## ABSTRACT:

The rapid growing demand for high bandwidth applications has made it necessary to consider carrier frequencies above 6 GHz for 5G mobile radio networks. The main motivation is the huge amount of available bandwidth in the 6-100 GHz range, which can enable high capacity, high throughput services with low latency. CEA is currently studying the enabling technologies to make 5G mmWave a reality from the antennas to the radio frequency technologies and the mobile communication algorithms. For example, the challenges of mmW transmissions force to revisit most of the design of the radio interface. Alternative waveforms and optimized high throughput decoders have been extensively studied by CEA which paves the way for future efficient use of these bands.

## Context and Challenges

One challenge of 5G is the efficient and flexible use of all available non-contiguous spectrum above 6 GHz (also called millimeter-wave band) for different scenarios of network deployment. Massive data rates will also require significantly higher processing as compared to conventional solutions. This is especially challenging for Forward Error Correction (FEC) mechanisms, since FEC decoding is one of the most computationally intensive baseband processing tasks.

## Main Results

CEA has simulated several candidate air interfaces for 5G and has proposed a fair comparison between them. These multicarrier waveforms all try to reach a trade-off between a good time/frequency localization, while being energy efficient. For achieving this compromise, waveforms have been developed with optimized time/frequency shaping filters and/or symbol interleaving: Universal Filtered MultiCarrier (UFMC), FilterBank MC (FBMC) and (windowed) Generalized Frequency Division Multiplexing ((w)GFDM). These air interfaces have been assessed in [1][2]. Fig.1. shows for example their frequency response: the best spectral location is obtained with FBMC. GFDM has a slightly lower channel leakage compared to OFDM but is clearly outperformed by UFMC. With the addition of the windowing process, GFDM becomes comparable to UFMC.

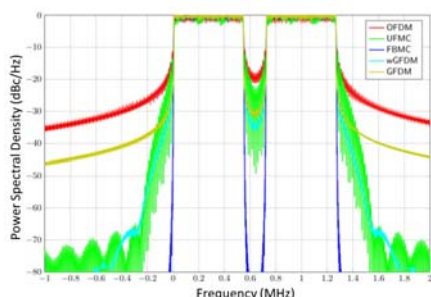


Fig.1: waveform comparison - synthesis.

CEA has investigated the design of Quasi-Cyclic (QC) LDPC codes and hardware architectures able to support very high-throughput applications. Cost-effective, high-throughput QC-LDPC decoders have been proposed, based on specific optimizations at both the algorithmic and architectural levels. ASIC post-synthesis implementation results (Fig. 2) show that the proposed designs achieve a Throughput to Area Ratio (TAR) up to 5.72 Gbps/mm<sup>2</sup> for regular LDPC codes, and 2.66 Gbps/mm<sup>2</sup> for WiMAX irregular LDPC codes, at 20 decoding iterations. These results compare favorably with the highest-throughput LDPC decoder implementations reported in the literature, as shown in [3].

	(3, 6) REGULAR QC-LDPC			WiMAX QC-LDPC, RATE=1/2		
Decoder	MS	NS-FAID-3	NS-FAID-2	MS	NS-FAID-3	NS-FAID-2
Max. Freq. (MHz)	125	147	172	161	178	200
Throughput (Mbps)	2700	3175	3715	1539	1701	1912
Area (mm <sup>2</sup> )	0.75	0.67	0.75	0.77	0.75	0.72
TAR (Mbps/mm <sup>2</sup> )	3600	4738	5715	1998	2268	2655
±% w.r.t. MS	0	+31.61	+58.75	0	+13.51	+32.88

Fig. 2: ASIC post-synthesis implementation results on 65nm-CMOS technology, for regular and WiMAX QC-LDPC codes

## Perspectives

The benefits of new waveforms for the 5G use cases have been highlighted in [1][2]. UFMC offers improvements keeping backward compatibility with legacy OFDM. FBMC goes forward making this waveform particularly interesting for 5G scenarios. However, we underlined that with FBMC, some concepts should be revisited for a future deployment. CEA is therefore already working on an adaptation of FBMC waveform, called Block Filtered (BF)-OFDM, that is compatible with these concepts, like MIMO and short packet adaptation for example. BF-OFDM will furthermore allow to design efficient hybrid beamforming (HB) schemes. HB is a promising technique for mmWave multiuser scenario, which makes possible to use larger beam and to null the inter-user interference through signal processing. CEA is currently focusing on demonstrating multiuser HB for mmWave systems.

## RELATED PUBLICATIONS:

- [1] R. Gerzaguet, D. Kténas, N. Cassiau and J-B. Doré, "Comparative study of 5G waveform candidates for below 6GHz air interface," ETSI WORKSHOP ON FUTURE RADIO TECHNOLOGIES – AIR INTERFACES, 27-28 January 2016, Sophia Antipolis France
- [2] A. A. Zaidi, J. Luo, R. Gerzaguet, H. Wang, X. Chen, Y. Qi, N. Cassiau et al., "Evaluation of Waveforms for Mobile Radio Communications Above 6 GHz," 2016 IEEE Globecom Workshops (GC Wkshps), Washington, DC, 2016, pp. 1-6.
- [3] A. De Domenico, R. Gerzaguet, N. Cassiau, A. Clemente, R. D'Errico, C. Dehos, J. L. González, D. Kténas, L. Marnat, V. Savin, and A. Siligaris, " Making 5G Millimeter Wave Communications a Reality," IEEE Wireless Communications Magazine, December 2016



# FLEXIBLE IN-BAND FULL DUPLEX TRANSCEIVERS

## RESEARCH TOPIC:

In-Band Full-Duplex transmission, Self-Interference Cancellation (SIC), Multiple Input Multiple Output architecture (MIMO), RF

## AUTHORS:

P. Rosson, D. Dassonville, V. Berg

## ABSTRACT:

In-band full-duplex transceivers are getting considered for future generations of cellular network systems. This work proposed to evaluate the performance of in-band full-duplex transceivers using a modified architecture based on hardware available for multiple-input multiple-output transceivers. A hybrid self-interference cancellation technique using an auxiliary transmitter is introduced. It is completed with a digital canceller. Performance are evaluated using simulation models and are confirmed by hardware experimentation. The main limiting factors of the architecture are analysed. Eventually, further improvements to the architecture are suggested.

## Context and Challenges

Wireless cellular operators are still looking for improving data rate or enhancing infrastructure capacity. Several solutions are currently operated to meet these requirements:

- ✓ Increase, or add new transmission bandwidths,
- ✓ Use Multiple Input Multiple Output (MIMO) techniques,
- ✓ Reduce radio path loss by making shorter the distance between the transmitter and the receiver (densification, relays).

Recently several In-Band Full-Duplex (IBFD) transceivers have been evaluated in the Wireless Local Area Network (WLAN) context. An IBFD transceiver transmits and receives simultaneously in the same frequency band. A maximum capacity gain of two is expected. The most important challenge of IBFD is the cancellation of the powerful self-interference (SI) generated by the transmitter. This undesired SI dazzles the lower received signal of interest. Antenna, RF and digital sub-systems are the three stages that can be concatenated to minimize this SI. In this first work, only the RF part and the digital aspect are considered.

## Main Results

Nowadays all cellular standards support MIMO communication, meaning that most of the transceiver supports multiple transmitters. Here the proposed work is based on current 2x2 MIMO transceiver architecture (see Fig.1). The original idea is to switch from a 2x2 MIMO configuration working in Frequency Division Duplex (FDD) to single ended IBFD transmission [1]. When IBFD mode is selected, the second transmitter generates the broadband analogue signal that mitigates the self-interference. This hybrid (i.e. digital and RF) self-interference Canceller is called HSIC.

The Radio Resource Management (RRM) selects between classical FDD MIMO or IBFD single-end transmissions. The transceiver becomes flexible and can switch from a configuration to another according to the scenario. If the channel conditions are favourable for MIMO transmission, MIMO operation is selected otherwise IBFD can be applied.

As mentioned previously, the most important challenge is the mitigation of the self-interference. To reach such objective, the linear and the nonlinear contributions of the desired transmitted

signal need to be estimated [2] [3] and subtracted to the received signal.

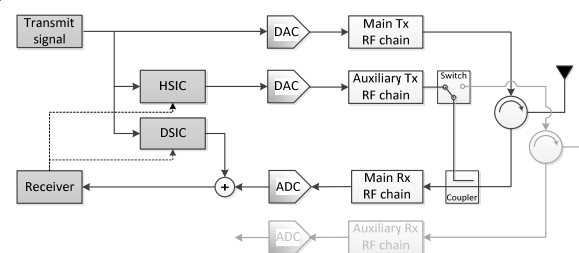


Figure 1: Modified MIMO architecture to support IBFD.

The following Fig.2 shows power spectrum density measured before and after our RF analogue canceller. It shows that 60 dB cancellation are achievable by the analogue canceller over 20 MHz.

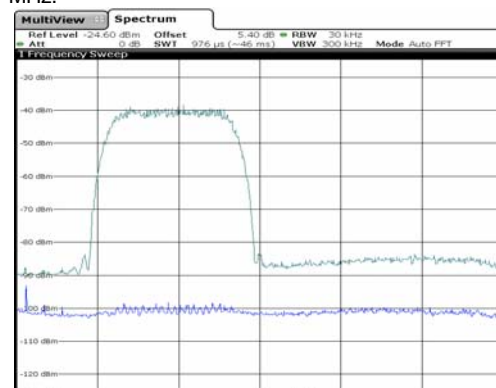


Figure 2: Analogue canceller performance.

## Perspectives

Future work will investigate an architecture that is based on 4x4 MIMO transmitters, including also a pure RF canceller. Fast tracking techniques with lower complexity algorithms are under studies.

## RELATED PUBLICATIONS:

- [1] A. Debar, P. Rosson, D. Dassonville, V. Berg, "Flexible In-Band Full-Duplex Transceivers Based on a Modified MIMO RF Architecture", chapter in Cognitive Radio Oriented Wireless Networks, 2016.
- [2] Zeleny J, Dehos C, Rosson P, Kaiser A. Receiver-aided predistortion of power amplifier non-linearities in cellular networks Iet Science, Measurement and Technology. 6: 168-175. DOI: 10.1049/iet-smt.2011.0016.
- [3] Zeleny J, Rosson P, Dehos C, Kaiser A. Digital compensation of the power amplifier nonlinearities at relay station receivers in 802.16j very high data rate systems 2010 IEEE Radio and Wireless Symposium, 2010 - Paper Digest. 244-247. DOI: 10.1109/RWS.2010.5434157.

# HIGH THROUGHPUT ARCHITECTURES FOR LDPC DECODERS

## RESEARCH TOPIC:

LDPC, NS-FAID, low-cost, high-throughput decoder

## AUTHORS:

V. Savin, T. Nguyen-Ly, M. Pezzin, X. Popon

## ABSTRACT:

The objective of this work is to contribute to the development of high-throughput, cost-effective, LDPC decoder designs, so that to address in the most suitable way the new generation of communication systems, requiring increased data rates and reduced energy footprint. The proposed approach is to exploit the robustness of message-passing LDPC decoders against computing inaccuracies. The use of approximate computing and storage in message passing LDPC decoders is seen as an enabler for throughput and cost optimization. By modeling such approximations in a specific way, we are actually able to address the multi-objective optimization of the design, with respect to cost, throughput, and error correction performance.

**SCIENTIFIC COLLABORATIONS:** D. Declercq (ENSEA), F. Ghaffari (ENSEA), O. Boncalo (UPT)

## Context and Challenges

The increasing demand of massive data rates in wireless communication systems will require significantly higher processing speed of the baseband signal, as compared to conventional solutions. This is especially challenging for Forward Error Correction (FEC) mechanisms, since FEC decoding is one of the most computationally intensive baseband processing tasks, consuming a large amount of hardware resources and energy. In this context, this work addresses the design of cost-effective, high-throughput LDPC decoders, through exploiting the robustness of message-passing decoding algorithms to computing inaccuracies.

## Main Results

We introduce a new family of Non-Surjective Finite Alphabet Iterative Decoders (NS-FAIDs) [1], characterized by specific processing rules, which can be theoretically analyzed and optimized for different trade-offs between hardware cost and error correction performance (Fig. 1). The proposed approach builds upon the approximate storage technique, and allows storing the exchanged messages using a smaller precision than the processing units. It is also shown to provide a unified approach for several designs previously proposed in the literature.

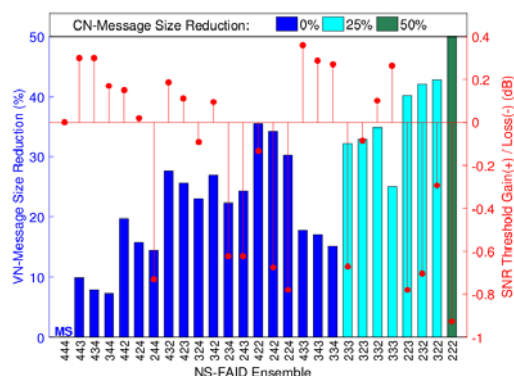


Fig. 1: Memory size reduction vs. decoding performance, for different NS-FAIDs, for the WiMAX LDPC code with rate 1/2.

We further propose three high-throughput hardware architectures, integrating both Min-Sum (MS) and NS-FAIDs decoding kernels. The proposed architectures implement layered scheduled decoding with fully parallel processing units. Throughput is further increased by making use of a specific design of the data path processing units [2], hazard-free pipelining, or maximum hardware parallelism [3]. Implementation results on both FPGA and ASIC technology show that NS-FAIDs allow significant improvements in terms of both throughput and hardware resources consumption, as compared to the MS decoder. Fig. 2 shows the area and throughput (at 20 decoding iterations) results of NS-FAID decoders, for the WiMAX LDPC code with rate 1/2. Two different implementations are considered, according to whether check-node messages are stored in an uncompressed (blue curve) or compressed (red curve) format. The increase in the Throughput to Area Ratio (TAR), with respect to the baseline MS decoder, is also shown. We note that the NS-FAID-222 decoder achieves a Normalized TAR of 5.46 Gbps/mm<sup>2</sup>/iteration.

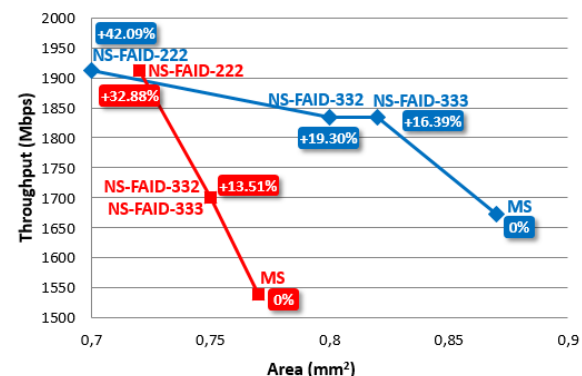


Fig. 2: ASIC post-synthesis implementation results on 65n-CMOS technology, for the WiMAX LDPC code with rate 1/2.

## Perspectives

The use of unrolled hardware architectures and the impact of the proposed solutions in terms of power consumption will be investigated in future work.

## RELATED PUBLICATIONS:

- [1] Truong Nguyen-Ly, Khoa Le, V. Savin, D. Declercq, F. Ghaffari, and O. Boncalo, "Non-Surjective Finite Alphabet Iterative Decoders", IEEE International Conference on Communications (ICC), Kuala Lumpur, Malaysia, May 2016.
- [2] T. Nguyen-Ly, T. Gupta, M. Pezzin, V. Savin, D. Declercq, and S. Cotoana, "Flexible, Cost-Efficient, High-Throughput Architecture for Layered LDPC Decoders with Fully-Parallel Processing Units", Euromicro Conference on Digital System Design (DSD), Limassol, Cyprus, September 2016.
- [3] T. Nguyen-Ly, V. Savin, X. Popon, D. Declercq, "High Throughput FPGA Implementation for Regular Non-Surjective Finite Alphabet Iterative Decoders", IEEE International Conference on Communications (ICC), Workshop on Channel Coding for 5G and Future Networks, Paris, France, May 2017.

# ADVANCED DECODERS FOR POLAR CODES

## RESEARCH TOPIC:

olar codes, 5G, Successive Cancellation (SC), SC-Flip

## AUTHORS:

L. Chandesaris, V. Savin, D. Declercq (ENSEA / UCP / CNRS)

## ABSTRACT:

In this work, we propose a generalization of the Successive Cancellation Flip (SCFlip) decoding of polar codes, characterized by a number of extra decoding attempts, where one or several positions are flipped from the standard SC decoding. To do so, we first introduce the concept of higher-order bit-flips, and propose a new metric to determine the bit-flips that are more likely to correct the trajectory of the SC decoding. We show that the proposed decoder, called Dynamic SCFlip, is an effective alternative to list decoding of polar codes, with an average computation complexity close to the one of the SC decoder.

**SCIENTIFIC COLLABORATIONS:** D. Declercq (ENSEA / UCP / CNRS)

## Context and Challenges

Polar codes recently emerged as the first construction that probably achieves the capacity of any binary-input memoryless symmetric channel, with log-linear encoding and decoding complexity. Their construction relies on a specific recursive encoding procedure, which can be reversed at the receiver end by applying a Successive Cancellation (SC) decoder. Besides their theoretical importance, the particularity of their construction makes them very attractive for practical applications, mainly due to the flexibility it provides in accommodating multiple coding rates or different transmission channels. This also explains the ongoing research effort, by both academia and industry, to investigate their use in 5G systems. Recently, 3GPP selected Polar codes as the official coding method for the control channel in the 5G enhanced mobile broadband use case.

## Main Results

Despite their capacity-achieving performance, Polar codes under SC decoding are known to provide rather modest error correction performance for short to moderate block-lengths, as compared to the ubiquitous LDPC and Turbo codes. This work is aimed at improving the error correction performance of Polar codes, especially at finite block-lengths. We introduce a new decoding algorithm, referred to as Dynamic SCFlip (D-SCFlip) [1, 2], characterized by a number of extra decoding attempts, where one or several positions are flipped from the standard SC decoding. D-SCFlip is based on a Cyclic Redundancy Check (CRC)-Polar concatenated scheme, where the CRC code is used to determine the success of a decoding attempt. Starting with the initial SC decoding, the D-SCFlip performs additional decoding attempts, until one of them passes the CRC test, or a maximum number of allowed attempts is reached. Each new decoding attempt amounts to performing a SC decoding, while flipping one or several hard decision estimates of the data bits. A specific metric is used to determine the flipping positions. Moreover, flipping positions are dynamically determined, by taking into consideration the previous decoding attempts, so that the next attempt is guaranteed to be the one with the best probability of success [2]. Fig. 1 provides a comparison of the SC, SC-List and D-SCFlip decoders for Polar codes with rate  $r = 1/2$  and length  $N = 1024$ , over the binary-input AWGN channel. For SC-

List and D-SCFlip decoders, a CRC of size 16 bits is concatenated to the Polar code. The D-SCFlip decoder has a maximum number of extra decoding attempts  $T_{\max} \in \{10, 50, 200\}$ , while the size of the list is set to  $L \in \{2, 16\}$  for the SC-List decoder. For comparison purposes, we have also included the Word Error Rate (WER) performance of a (3,6)-regular LDPC code, with the same  $(N, r)$  parameters, under Belief Propagation decoding, with maximum number of iterations set to  $I_{\max} = 100$ . It can be seen that the proposed D-SCFlip decoder with  $T = 50$  slightly outperforms the BP decoder, while for  $T = 200$  it closely approaches the performance of the SCL decoder with  $L = 16$ . However, we note that D-SCFlip provides a different trade-off, as compared to SC-List decoding, since it keeps both the space and the computational complexity close to the one of the SC decoding.

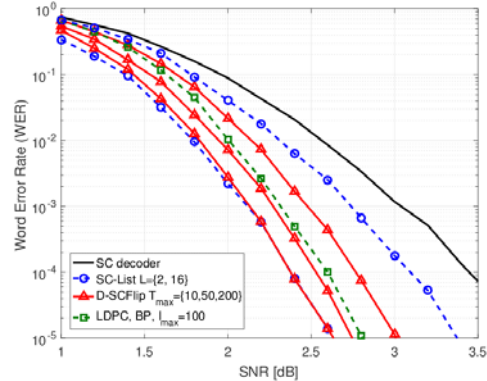


Fig. 1: Performance of Polar and LDPC decoders for codes with coding rate  $r=1/2$  and length  $N=1024$ .

## Perspectives

Future work will investigate the joint optimization of both the D-SCFlip decoder's parameters and the Polar code construction, in the context of multi-level and bit-interleaved Polar coded modulations.

## RELATED PUBLICATIONS:

- [1] L. Chandesaris, V. Savin, and D. Declercq, "An improved SCFlip decoder for Polar Codes", IEEE Global Communications Conference (GLOBECOM), Washington DC, USA, December 2016.
- [2] L. Chandesaris, V. Savin, and D. Declercq, "Dynamic SCFlip decoding for polar codes", IEEE Transactions on Communications, 2017, submitted. [Online]. Available: <https://arxiv.org/abs/1703.04414>.

# IEEE1900.7-2015 PHY EVALUATION ON TVWS SCENARIOS

## RESEARCH TOPIC:

In Cognitive radio, FBMC, IEEE1900.7-2015 standard

## AUTHORS:

J.-B. Doré and D. Noguét

## ABSTRACT:

White space communications have attracted a particular interest after some national regulators have authorized TVWS unlicensed secondary usage. The IEEE 1900.7 working group has defined a specific air interface tailored to these applications. The standard is based on a Filter Bank Multi Carrier (FBMC) physical layer and a CSMA-CA MAC sub-layer proposed by CEA Leti. In this paper, the Modulation and Coding Schemes (MCS) of the IEEE 1900.7-2015 are considered to assess simulated expectations on throughput and coverage under various typical TVWS deployment scenarios: Fixed Long Range Access, campus WLAN (in Fixed Urban/Suburban environments), Indoor Femtocells (a TVWS low power transceiver for WLAN-like applications). Expected rate and coverage maps are provided for these scenarios.

## Context and Challenges

In the recent years, there has been a worldwide concern related to spectrum shortage. One of the means to make new spectrum available is through sharing, and the Digital Switch Over (DSO) in TV bands, which has resulted in making the so-called TV White Space (TVWS) UHF spectrum available, was the first actual example where such a mechanism has been allowed. TVWS availability depends on TV broadcast frequency usage profile, thus changing across time and space. TVWS usage relies on unlicensed secondary Dynamic Spectrum Access (DSA) under the principle on a non-harmful interference with incumbent users. All broadband TVWS standards (ECMA 392, IEEE 802.22, IEEE 802.11af) are based on Cyclic Prefix - Orthogonal Frequency Division Multiplexing (CP-OFDM) physical layer (PHY), often inherited from previous standard developments such as IEEE 802.16e or IEEE 802.11a. These standards have been adapted to make them suitable for TVWS operation. Although this approach was the best to guarantee fast market readiness, it had some difficulties to face the TVWS specific requirements in terms of interference control.

## Main Results

IEEE DySPAN Standards Committee created an ad hoc group on White Space (WS) Radio in March 2010. The IEEE 1900.7-2015 standard is the result of a clean slate technology analysis where the working group tried to identify the most suitable technology to TVWS requirements [1]. The chosen technology is based on the Leti's Filter Bank Multi Carrier (FBMC) technology and a contention based CSMA-CA MAC also proposed and tuned by Leti.

In our work [2], our focus was to put the performance of the IEEE 1900.7-2015 PHY into the perspective of typical TVWS scenarios namely Rural Broadband Access and indoor TVWS Femtocells. This work investigates the standard modulation and coding schemes (MCS) and expresses throughput and coverage for these scenarios (see Fig 1). Performance evaluations have been carried out. In the case of the rural broadband access, transmit power has been set to 36dBm (4W). The path loss has been computed to maintain the minimal signal to noise ratio required to transmit with a given quality of service (throughput and BER).



Figure 1 - Rural broadband (left), campus (middle) and indoor (right) with indoor to outdoor coverage scenarios.

Figure 2 shows these range estimates for an 8MHz configuration. Simulations show that in the rural broadband access case, a range of 2km at 8Mbps to 23Mbps depending on channel conditions, with an 8MHz bandwidth.

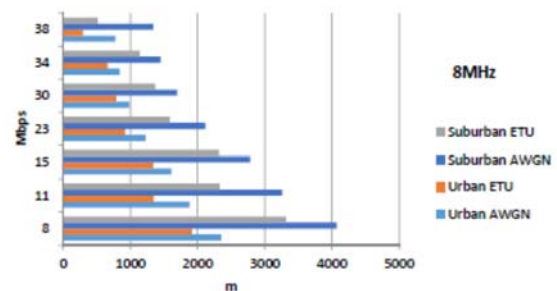


Figure 2 - Max. data rate [Mbps] vs. max. range [m] in rural broadband scenario.

In the indoor case, where TX power is limited to 100mw (similar to the Tx power of WiFi), range can reach 100m at 8Mbps when crossing 2 floors and 38Mbps when on the same floor (considering 8MHz bandwidth), making IEEE 1900.7-2015 suitable for indoor and indoor to outdoor connectivity, even in large building [2].

## Perspectives

Field tests using Leti's technology platform are planned mid 2017 in Scotland with local partners. The aim of this experiment is to assess performance on typical use cases (rural and maritime broadband internet access).

## RELATED PUBLICATIONS:

1) S. Filin, D. Noguét, J.-B. Doré, B. Mawlawi, O. Holland, M. Zeeshan Shakir, F. Kojima, H. Harada, IEEE 1900.7 standard for white space dynamic spectrum access radio systems, IEEE Conference on Standards for Communications and Networking (CSCN), Tokyo, 2015.

[2] Noguét D and Doré JB, "IEEE 1900.7-2015 PHY evaluation on TVWS scenarios" International Conference on Cognitive Radio Oriented Wireless Networks CROWNCOM 2016.



# COVERAGE ANALYSIS AND LOAD BALANCING IN HETNETS WITH MM-WAVE MULTI-RAT SMALL CELLS

## RESEARCH TOPIC:

Millimeter wave, Multi radio access technology, load balancing

## AUTHORS:

Gourab Ghatak, Antonio de Domenico and Marceau Coupechoux (Télécom ParisTech)

## ABSTRACT:

In this work we model and analyze a heterogeneous network, consisting of classical microwave macro cells, and multi Radio Access Technology (RAT) small cells that operate in microwave and millimeter-wave bands. We characterize the user performance in terms of signal to interference plus noise ratio (SINR) coverage probability and throughput and obtain the optimal biases that maximize either the SINR coverage or the downlink throughput. Our analysis highlights the importance of deploying dual band small cells in particular when small cells are sparsely deployed or in case of heavy traffic.

**SCIENTIFIC COLLABORATIONS:** Télécom ParisTech

## Context and Challenges

Future wireless networks will require a massive increase in data rates. For this, two techniques are particularly attractive: network densification and millimeter wave (mm-wave) wave communications. Densification of cellular networks consists of massive deployments of small cells, overlaying the existing macro cell architecture. Traditionally, small cells are deployed in microwave frequencies with the aim of offloading the underlying macro-cells [1]. This calls for inter-cell interference coordination and load balancing. On the other hand, due to the high path-loss and sensitivity to blockages, it is unrealistic to assume ubiquitous coverage with only mm-wave small cells, and it is envisioned that multiple radio access techniques (RATs) will co-exist in future cellular networks. In this context, we characterize a two tier heterogeneous network, consisting of classical microwave macro cells, and multi RAT small cells able to operate in microwave and mm-wave bands [2].

## Main Results

Fig. 1 shows the effect of the tier and RAT selection biases on the SINR coverage for a small cell to macro cell deployment density ratio of 50, i.e., 50 small cells per each macrocell.

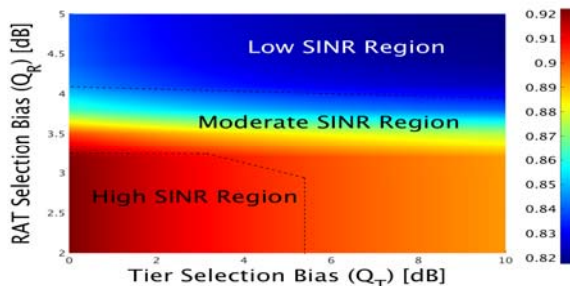


Fig 1: SINR Coverage Probability as a function of tier and RAT selection biases.

The high SINR regions occur for low tier and RAT selection biases. Increasing the tier selection bias decreases the SINR coverage probability because some users are forced to associate

with base stations providing less signal power. This holds true also for the case when the RAT selection bias is increased. For higher densities, however, increasing the RAT selection bias may increase the SINR coverage. This increase is because, with higher deployment densities, the user-small cell distance decreases, as a result of which, the useful signal power increases more in mm-wave than in microwave. Moreover, the mm-wave communications do not experience any cross-tier interference, resulting in an effective increase in SINR.

Next we show the user throughput as a function of the two biases in Fig 2. It must be noted that it may not be feasible to increase the RAT selection bias in an unconstrained manner so as to increase the user throughput. This is because the regions where the user throughput is high, the average SINR may be below a minimum desired value or the base stations may get overloaded by the user traffic. Thus, there is a need for maximizing the throughput under SINR outage and overloading constraints.

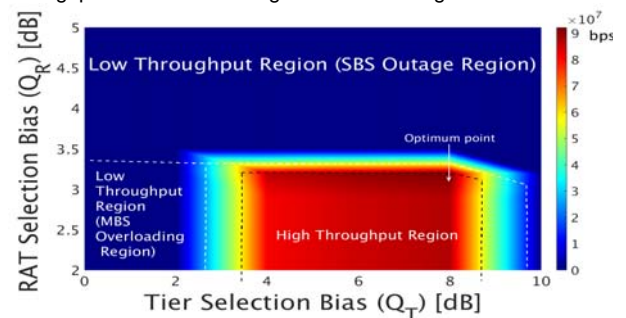


Fig 2: User throughput as a function of tier and RAT selection biases.

## Perspectives

Our study highlights the fundamental trade-offs between outage probability, user throughput, and overloading probability, and, thereby, underscores the necessity of the dual band small cells to maintain outage below a certain threshold, especially in sparse small cell deployments. The dual band nature of the base stations calls for advanced radio resource management, which is an interesting topic to be investigated in future works.

## RELATED PUBLICATIONS:

- [1] G. Ghatak, A. De Domenico, M. Coupechoux, "Performance Analysis of Two-Tier Networks with Closed Access Small-Cells", SPASWIN 2016.
- [2] G. Ghatak, A. De Domenico, M. Coupechoux, "Coverage Analysis and Load Balancing in HetNets with mmWave Multi-RAT Small Cells" submitted to IEEE Transaction on Wireless Communications, 2017.







## 2.

### WIRELESS SHORT-RANGE AND CONTACTLESS SYSTEMS

- Localization and Navigation Techniques
- Advanced Coding for LPWA Networks
- Body Area Networks

# HIGH-ACCURACY COOPERATIVE LOCALIZATION FOR CONNECTED VEHICLES WITH LOW COMMUNICATION FOOTPRINT

## RESEARCH TOPIC:

Intelligent Transportation Systems, Connected vehicles, Hybrid Data Fusion, Vehicular Networks, Cooperative Localization

## AUTHORS:

G.M. Hoang, B. Denis, J. Härrä (EURECOM), D. Slock (EURECOM)

## ABSTRACT:

Future intelligent transport systems will require very accurate, seamless and resilient localization capabilities in any operating condition. In vehicular networks, dedicated short range wireless communications can thus support new localization functionalities to improve nominal GPS capabilities, based on cooperative data fusion and vehicle-to-vehicle measurements. We propose solutions against specific issues inherent to this cooperative context, such as the extra communication cost of localization, harmful space-time measurement correlations over vehicle-to-vehicle links, or error propagation between cooperating vehicles.

**SCIENTIFIC COLLABORATIONS:** EURECOM, Sophie Antipolis, France

## Context and Challenges

High-precision vehicular localization (i.e., with errors of a few 10s of cm) is a key enabler for future intelligent transport systems (ITS) and their applications (e.g., autonomous driving, vulnerable road users' safety, automotive Internet of Things...). However, most Global Positioning Systems (GPS) commercialized today can neither fulfil such precision requirements, nor guarantee a true continuity of service or a sufficiently fast convergence time in harsh environments (tunnels, urban canyons...). Vehicle-to-x (V2x) communication standards (a.k.a. IEEE 802.11p or ITS-G5) have thus been recently considered to support new cooperative localization functionalities (Fig.1). Typically, each vehicle fuses its own GPS estimates with positional information contained in Cooperative Awareness Messages (CAMs) sent by neighboring vehicles, on V2V radio measurements (e.g., relying on the signal strength of received CAMs or on dedicated ranging technologies), as well as on on-board sensors (odometers, cameras...). Major challenges such as the communication footprint of cooperative localization or the effect of correlated V2V measurement noises still remain largely unexplored in the literature.

## Main Results

In a global fusion framework based on particle filtering and ITS-G5 V2V communications, message approximations (e.g., multimodal Gaussian) have been considered to reduce the amount of over-the-air information required for reconstructing the posterior density of neighbours' estimated positions & speeds, thus making it compatible with standardized CAM payloads (<800bytes) [1]. Complementary CAM control strategies have also been proposed (in terms of transmission power, mixed data traffic and refresh rate), conveying only the most informative positional data and taking benefits from mobility-based predictions. Simulation results show an accuracy comparable to that of nominal 10Hz transmission rates at much lower V2V channel load (e.g., 8% vs. 40%) and dually, a fine resilience to standardized V2V congestion control mechanisms when reducing the CAM rate to 2Hz (Fig.2).

In the same context, after modeling the impact of correlated noises affecting both GPS and V2V signal strength observations on fusion filters, complementary methods have been put forward in [2] to decorrelate measurement noises (e.g., adaptive observation covariance, mobility-based differential

measurements, decreased fusion rates, censoring...).

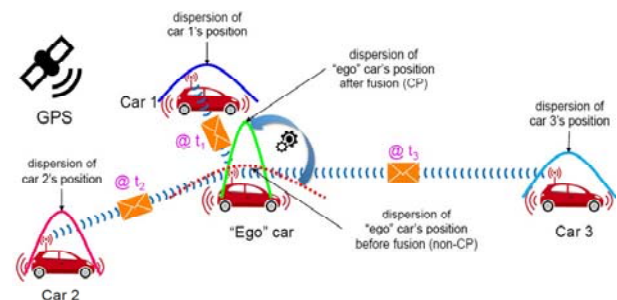


Figure 1. Vehicular cooperative positioning fusing awareness messages from neighbors and GPS data.

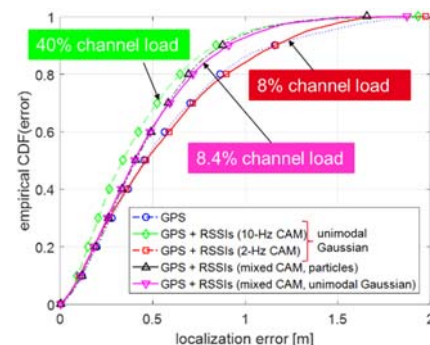


Figure 2. CDF of 2D location error with messages approximation and mixed data traffic (pink).

Such "decorrelation" methods contribute to improve accuracy by up to 60% in highly correlated environments.

## Perspectives

Other studies have been focusing on the mitigation of filter overconfidence and error propagation (e.g., scheduling [3], adaptive dithering of V2V ranging observation noise [4]), as well as on the fusion with other on-board sensors (e.g., inertial unit, lane detector) to improve performance orthogonally to the road [5] and/or in tunnels, while considering also road side units [6].

## RELATED PUBLICATIONS:

- [1] G.M. Hoang, B. Denis, et al. "On Communication Aspects of Particle-Based Cooperative Localization in GPS-aided VANETs", Proc. IEEE IV'16 - CCP, June 2016
- [2] G.M. Hoang, B. Denis, et al. "Breaking the Gridlock of Spatial Correlation in GPS-aided IEEE 802.11p-based Cooperative Positioning", IEEE Trans. VT, Aug. 2016
- [3] G.M. Hoang, B. Denis, et al. "Cooperative Localization in GNSS-aided VANETs with Accurate IR-UWB Range Measurements", Proc. IEEE WPNC'16, Oct. 2016
- [4] G.M. Hoang, B. Denis, et al. "Robust and Low Complexity Bayesian Data Fusion for Hybrid Cooperative Vehicular Localization", Proc. IEEE ICC'17, May 2017
- [5] G.M. Hoang, B. Denis, et al. "Mitigating Unbalanced GDoP Effects in Range-Based Vehicular Cooperative Localization", Proc. IEEE ICC'17 - ANLN, May 2017
- [6] G.M. Hoang, B. Denis, et al. "Robust Data Fusion for Cooperative Vehicular Localization in Tunnels", Proc. IEEE IV'17, June 2017



# OBSTRUCTION-RESILIENT PEDESTRIAN LOCALIZATION WITH WIRELESS ON-BODY NODES

## RESEARCH TOPIC:

Wearable Networks, Body Shadowing, Off-Body Radio Links, Orientation Estimation, Personal Navigation, Received Power

## AUTHORS:

B. Denis, R. D'Errico, B. Uguen (Univ. Rennes 1)

## ABSTRACT:

In the context of wearable networks, we propose a localization solution that benefits from body shadowing, rather than treating it as a nuisance. The relative orientation of the carrying body is determined out of differential received power measurements at back and front on-body nodes with respect to fixed infrastructure transmitters. Based on these relative angles, an algorithm jointly estimates the absolute position and orientation of the body. Experiments with IEEE 802.15.4-compliant devices illustrate the resilience of this proposal in the presence of strong shadowing caused by both the carrying body and other people moving in the vicinity.

**SCIENTIFIC COLLABORATIONS:** Université Rennes 1 - IETR, Rennes, France

## Context and Challenges

Wearable and body area networks support a variety of emerging user-centric applications, such as human-to-machine interfaces, smart/connected clothing, e-Health and e-Wellness, personal sports and nomadic social networking, personal safety... Besides, numerous mobile services based on physical activity detection or pedestrian navigation have been put forward recently. However, most of currently available low-power radiolocation solutions (e.g., based on Bluetooth Low Energy, WiFi, Zigbee...) and low-complexity metrics (e.g., received signal strength -RSS-) are subject to severe performance degradations due to large signal fluctuations, radio obstructions or unreliable a priori models. In the recent literature, a few original contributions aim at benefitting from orientation-dependent body shadowing effects, as a constructive and deterministic source of information. However, the latter still require a non-practical in-site model calibration.

## Main Results

In [1], a first solution has been proposed to estimate the relative orientation of human bodies based on differential RSS readings observed at on-body nodes in the back and on the torso, with respect to surrounding anchors set at known locations (Fig.1).

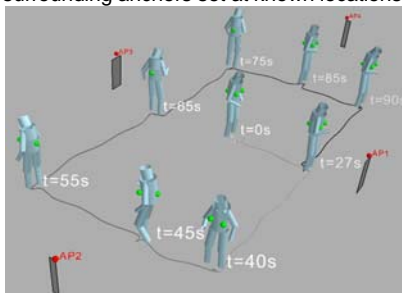


Figure 1. Snapshots of a few body poses, with back/front on-body radio nodes (green) and 4 anchor nodes (red).

Based on these relative measurements, an iterative linearized Least Squares (LS) algorithm jointly estimates the absolute position and absolute orientation (heading) of the carrying body. A light auto-calibration procedure makes the solution adapted to both the operating environment and the carrying body and thus,

improves performance over time without requiring costly preliminary measurements. First experimental validations based on IEEE 802.15.4-compliant devices have shown that, whereas heading is accurately retrieved, the absolute position still suffers from relatively large errors. An improved version of this algorithm enables to re-inject reliable heading estimates into the next estimation steps, based on an empirical mobility indicator. It thus benefits from body movement continuity over time, without requiring any a priori parametric mobility model.

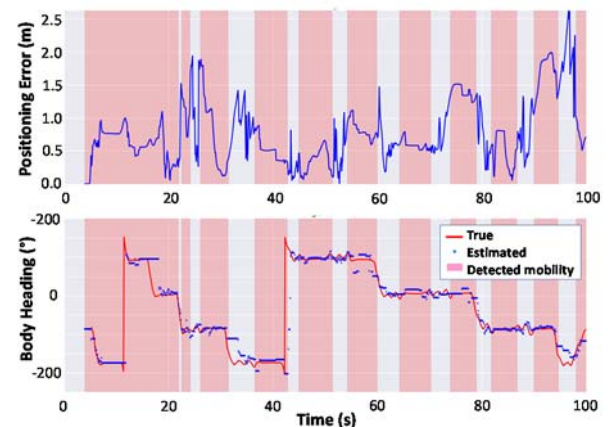


Figure 2. Positioning error (top) and true/estimated heading (bottom) vs. time along Fig.1 trajectory.

Performance has been assessed by means of experiments in both single-user and crowded scenarios, illustrating the robustness of the proposal against uncalibrated radiated powers, obstructions, as well as dispersed body/mobility characteristics, while using a low-cost, low-complexity and standard-compliant radio system (typically with a median positioning error of 0.5m).

## Perspectives

Future works will aim at a better disambiguation of relative angles [2], a better handling of false alarms triggered by noisy angle measurements, and finally, an extension into cooperative scenarios using complementary body-to-body links.

## RELATED PUBLICATIONS:

- [1] B. Denis, B. Uguen, F. Mani, R. D'Errico, N. Amiot, "Joint Orientation and Position Estimation from Differential RSS Measurements at On-Body Nodes", Proc. IEEE PIMRC'16, Sept. 2016.
- [2] B. Uguen, B. Denis, F. Mani, R. D'Errico, N. Amiot, "Differential Received Power Measurements over Off-Body Links for Obstruction-Resilient Navigation", submitted to Springer International Journal of Wireless Information Networks (IJWIN), Special Issue on Internet of Things and Machine-to-Machine Communications..

# MULTIPATH-AIDED LOCALIZATION FOR ROBUST INDOOR NAVIGATION

## RESEARCH TOPIC:

Indoor Localization, Multipath Channel, Non Line of Sight Mitigation, Time of Arrival Correction, Ultra Wideband

## AUTHORS:

J. Maceraudi, F. Dehmas, B. Denis, B. Uguen (Université Rennes 1)

## ABSTRACT:

Relying on integrated Impulse Radio - Ultra Wideband devices, we exploit the space-time correlation of received multipath components under mobility to improve indoor localization in case of generalized radio obstructions. More specifically, multiple hypothesis Kalman filters track the relative temporal variations of multipath components so as to "collectively" retrieve the missing direct path's delay in case of non-line of sight transition. The corrected observations finally feed a conventional Extended Kalman Filter to estimate the mobile's positions over time, showing promising gains in reasonably dense multipath environments.

**SCIENTIFIC COLLABORATIONS:** Université Rennes 1 - IETR, Rennes, France.

## Context and Challenges

Indoor localization appears as a key enabler for a plurality of applications including pedestrian navigation, house and building automation, smart factories, next generation human-machine interfaces, physical activity monitoring and learning... In this context, an Impulse Radio - Ultra Wideband (IR-UWB) receiver architecture endowed with high-resolution capabilities was successfully integrated in [1]. The latter can estimate the arrival times (ToA) of multipath echoes of the transmitted impulse signals within a time granularity of 1ns. Based on first path detection, this receiver theoretically enables accurate distance measurements (within centimetric errors). In uncontrolled indoor environments however, radio obstructions and dense multipath propagation significantly degrade ranging and accordingly, range-based localization performances. It has been also pointed out that the time/space correlation of multipath components under mobility could be beneficial to tracking [2,3], even though those concepts have not been demonstrated with integrated receivers.

## Main Results

For the sake of improving indoor localization robustness, we have proposed in [4] an algorithm that detects, associates and tracks (with parallel multi-hypothesis Kalman filters) the relative temporal variations of several multipath components, based on channel energy profiles estimated at real IR-UWB receivers.

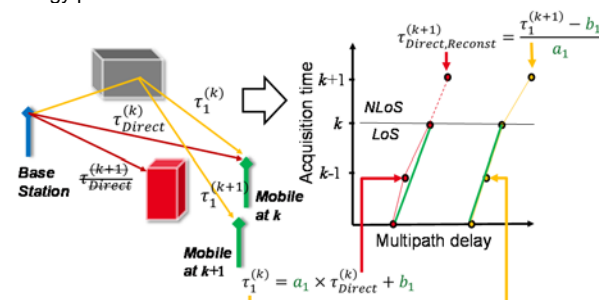


Figure 1. 1st path's Time of Arrival (ToA) reconstruction in Non-Line of Sight (NLoS).

Beyond, we estimate the parameters of locally linearized "relative

drift" functions binding the delays of channel's leading edge (first path) and secondary components in favorable line of sight conditions. Assuming the remanence of these functions over time, the missing direct path's arrival time is corrected out of the tracked components in case of detected non-line of sight (NLoS) transitions (Fig.2). This solution is suitable to receivers under stringent hardware and computational constraints (i.e., in terms of channel estimation dynamics, embedded computational resources and memory). It is also compatible with conventional low-complexity filter-based tracking architectures, which admit one single ToA estimate per radio link as input observation.

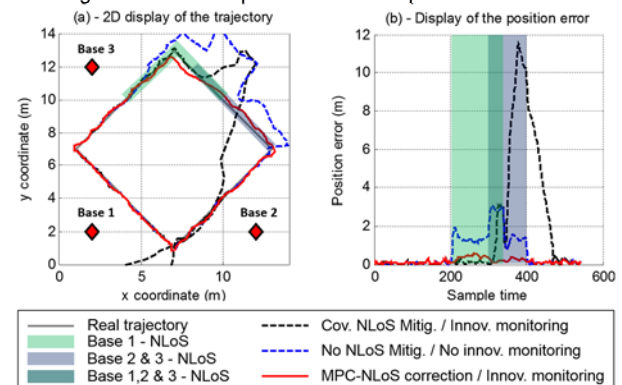


Figure 2. Estimated indoor trajectory (left) and location error as a function of time (right) under gradual non-line of sight (NLoS) conditions (solid red lines: proposal).

Assuming a simplified channel model between the mobile and 3 base stations (incl. four secondary components resulting from single-bounce reflections on the walls), preliminary simulations have shown the promising potential of the proposed technique in case of generalized NLoS with sparse multipath profiles (Fig.2).

## Perspectives

Current works have been focusing on improved multipath information recombination during the ToA reconstruction phase, on the continuous update of "relative drift" parameters, as well as on the pre-filtering of channel estimate to mitigate interferences in case of ultra-dense multipath profiles.

## RELATED PUBLICATIONS:

- [1] G. Masson, et al. "A 1nJ/b 3.2-to-4.7GHz UWB 50Mpulses/s Double Quadrature Receiver for Communication and Localization", Proc. ESSCIRC'10, Sept. 2010
- [2] J. Youssef, et al. "Enhanced UWB Indoor Tracking through NLOS TOA Bias Estimation", Proc. IEEE GLOBECOM'08, New-Orleans, Nov.-Dec. 2008
- [3] B. Uguen, et al. "Extraction and Characterization of Location-Dependent UWB Radio Features with Practical Implications for Indoor Positioning", Proc. European Wireless 2012, April 2012
- [4] J. Maceraudi, et al. "Multipath Components Tracking Adapted to Integrated IR-UWB Receivers for Improved Indoor Navigation", Proc. EUSIPCO'16, Special Session on Network Localization, Budapest, Aug.-Sept. 2016

# COMPARISON OF POST-PROCESSING ALGORITHMS FOR INDOOR NAVIGATION TRAJECTORIES

## RESEARCH TOPIC:

Indoor localization, Post-processing, real-time particle filter, Map-matching, sensor fusion

## AUTHORS:

Kersane Zoubert-Ousseni, Christophe Villien, François Le Gland (INRIA)

## ABSTRACT:

Most of the indoor localization studies are considering real-time processing to offer the user instantaneous positioning. However many applications only require post-processing analysis which allows for access to more powerful processing techniques. This first work compares smoothing algorithms that are applied on the top of a real-time particle filter (RT-PF) to further improve positioning performances. Viterbi algorithm has shown to have the best performances, but limited to an improvement of about 10% with respect to the RT-PF. We are now investigating new approaches that do not rely on a real-time algorithm, intended for crowd-sourcing applications.

**SCIENTIFIC COLLABORATIONS:** INRIA, IRMAR

## Context and Challenges

Very often, indoor localization is thought as a lost user looking at his smartphone to find its position in a big mall. As a consequence, many developments in that field have considered real-time processing to make localization permanently available. However, before he got lost, the user was not looking at his smartphone and many other applications (behavior analysis, crowd sourcing etc.) are interested by his past trajectory rather than his current position. This paradigm, where all data is available at processing time, gives access to more powerful algorithms not constrained by causality and, when it takes place in the cloud, to huge processing power also. Based on an existing real-time particle filter (RT-PF) developed at CEA that performs sensors fusion and map-matching, this first work compares straightforward methods that can be applied to improve efficiency of particle filters when causality and processing power constraints are relaxed.

## Main Results

RT-PF is tracking multiple hypothesis at the same time and has to choose between them to provide a single position to the user. This is illustrated in Figure 1, where the RT-PF is initially assuming that the circle-hypothesis is correct until the associated probability collapses (time  $t_6$ ) because a wall is on the way, then the RT-PF has to switch from circle-hypothesis to diamond one, resulting in a "jump" of the real-time trajectory.

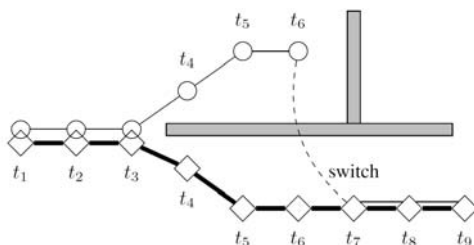


Figure 1: illustration of hypothesis switch when the PF is tracking a wrong trajectory.

Our approach was focusing on the post-processing of the multiple hypothesis delivered by the real-time RT-PF to select, for each

time  $t_k$ , the best one with respect to the entire trajectory, which is known as a smoothing problem. Two smoothing algorithms, forward filtering backward smoothing (FFBSm) and forward filtering backward simulation (FFBSi), and the Viterbi algorithm have been compared over a database comprising more than 600 indoor experiments. Figure 2 shows an example of result where the RT-PF has chosen a wrong hypothesis at start (i.e. black star), contrary to the three non-causal algorithms.

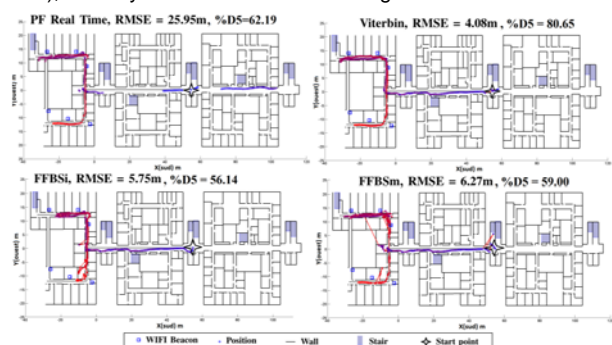


Figure 2: comparison of real-time PF, Viterbi and smoothing algorithms (FFBSm and FFBSi).

Performances have been computed over the entire database using the D5 metric, which corresponds to the percent of time when the error is inferior to 5m. RT-PF has a score of 45%, FFBSm 48.75%, FFBSi 47.03% and Viterbi 50.62%, but those slight improvements (i.e. <10%) with respect to the RT-PF are hiding the fact that many trajectories cannot be further improved by post-processing because there is no better solution among the outputs of RT-PF.

## Perspectives

This first work shows that some straightforward methods can be easily applied to take advantage of a context not constrained by real-time. However these methods produce only a slight improvement (i.e. about 10% for the Viterbi algorithm), because they only consist in an additional layer that is applied on the top of a real time algorithm. We are now investigating new approaches that do not rely on real-time algorithms, and which are intended to be used within a crowd-sourcing context.

## RELATED PUBLICATIONS:

[1] J. Trogh, D. Plets, L. Martens, and W. Joseph, "Advanced real-time indoor tracking based on the Viterbi algorithm and semantic data," *International Journal of Distributed Sensor Networks*, 2015, article ID 271818. [2] Torres-Sospedra, J., Jiménez, A. R., Knauth, S., Moreira, A., Beer, Y., Fetzer, T., ... & Belmonte, O. (2017). The Smartphone-Based Offline Indoor Location Competition at IPIN 2016: Analysis and Future Work. *Sensors*, 17(3), 557. [3] P. Wilk, J. Karciarz, and J. Swiatek, "Indoor radio map maintenance by automatic annotation of crowdsourced Wi-Fi fingerprints," in *Proceedings of the 2015 International Conference on Indoor Positioning and Indoor Navigation (IPIN)*, Banff 2015, Oct. 2015. [4] J. Singh, F. Mokaya, K. Mori, and S. Sidhu, "Indoor hallway structure mapping by matching segments from crowd-sourced mobile traces," in *Proceedings of the 2015 International Conference on Indoor Positioning and Indoor Navigation (IPIN)*, Banff 2015, Oct. 2015. [5] Nurminen, H., Ristimäki, A., Ali-Loytty, S., & Piché, R. (2013, October). Particle filter and smoother for indoor localization. In *Indoor Positioning and Indoor Navigation (IPIN), 2013 International Conference on* (pp. 1-10). IEEE.

# TURBO-FSK, A PHYSICAL LAYER FOR LOW POWER WIDE AREA NETWORKS

## RESEARCH TOPIC:

Low rate, Physical Layer, Low-Power Wide-Area (LPWA), Internet-of-Things (IoT)

## AUTHORS:

Y. Roth, J-B. Doré, L. Ros (GIPSA-lab), V. Berg

## ABSTRACT:

As the Internet-of-Things is becoming a reality, the need for a new Low-Power Wide-Area (LPWA) network emerged for the last few years. Numerous low-cost devices will be connected, and this requires an optimization of the link budget: the physical layer needs to be designed highly energy efficient. The combination of M-ary orthogonal Frequency-Shift-Keying (M-FSK) modulation and coding in the same process has been shown to be a promising candidate when associated with an iterative receiver (turbo principle). This new digital transmission scheme, so-called Turbo-FSK, is studied. The optimization of its parameters is done using a well-known tool designed for iterative receiver, the EXIT chart. The performance is confronted to existing LPWA solutions, demonstrating the potential of this technology.

## Context and Challenges

Existing solutions for LPWA connectivity rely on two main strategies: the use of narrow band signaling (eg. Sigfox) or the consideration of a low spectral efficiency. The technique considered in this work, Turbo-FSK, relies on the second strategy. It combines the use of an orthogonal modulations (Frequency-Shift-Keying, FSK), a convolutional code and repetition, in association with an iterative receiver. The scheme was designed to reach low levels of sensitivity. When considering the theoretical limit of Shannon, the design of a system must allow its performance to be close to the limit. We seek to optimize the parameters of Turbo-FSK to approach the limit [1,2]. The performance of Turbo-FSK should also be evaluated versus the several existing LPWA solutions [3].

## Main Results

Both main parameters of the Turbo-FSK scheme are the size of the orthogonal modulation,  $M$ , and the number of repetitions,  $\lambda$ . To each set of parameters correspond a specific spectral efficiency and energy efficiency. With two degrees of freedom, the asymptotic performance of the Turbo-FSK is evaluated using the Extrinsic Information Transfer (EXIT) chart. The values of  $M$  tested span from 16 to 2048 and the values of  $\lambda$  from 3 to 6. The spectral efficiency of each configuration is given versus the energy efficiency in Fig 1, along with the performance when the block size is set to  $Q = 1000$ .

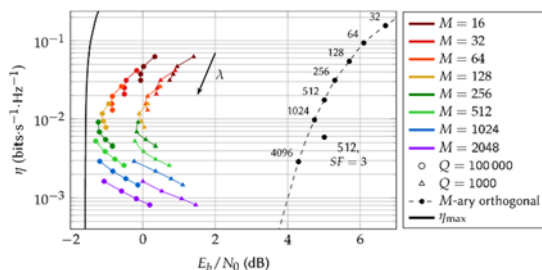


Figure 1: Performance of Turbo-FSK for various values of parameters

The asymptotic performance of Turbo-FSK approach the minimum achievable  $E_b/N_0$  at 0.28dB for parameters  $M=512$

and  $\lambda=3$ . When the information block size is set to 1000, the distance to Shannon's limit is equal to 1.35dB (for a BER of  $10^{-5}$ ). This demonstrates the potential of Turbo-FSK to closely approach the theoretical limits.

Several LPWA solutions are selected for comparison under the AWGN channel. The standard 802.15.4k, notably used by the RPMA technology, a solution based on the principle of the LoRa technology, and the Uplink of Narrow-Band IoT (NB-IoT UL), the preliminary LPWA standard proposed by the 3GPP. This latter technology relies on the use of a powerful Turbo Code (TC). The performance in Packet Error Rate (PER) of the 3 schemes compared to Turbo-FSK with optimum parameters is depicted in Fig 2, versus the Signal-to-Noise Ratio (SNR). Turbo-FSK outperforms the other schemes. The two technologies relying on a turbo receiver offer the best performance, which demonstrates the potential of turbo coded solutions. Also, the ranges of SNR match the requirements of long range operation. Indeed, with a low level of SNR, low levels of sensitivity can be expected.

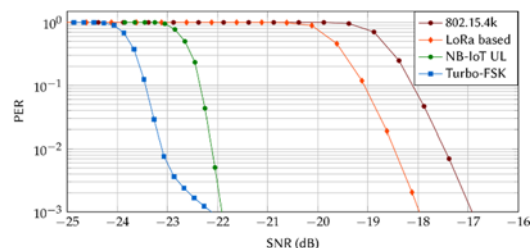


Figure 2: Performance of Turbo-FSK versus existing LPWA solutions.

## Perspectives

Turbo-FSK has been optimized and compared with existing LPWA solutions. However, as presented in Figure 1, the ranges of spectral efficiency are very low. In comparison, NB-IoT can reach significantly higher levels of spectral efficiency. Having a flexibility in spectral efficiency helps to increase the number of possible applications and should be investigated. Finally, other comparisons should be considered such as the performance under frequency selective channels.

## RELATED PUBLICATIONS:

- [1] Y. Roth, J-B. Doré, L. Ros and V. Berg, "Turbo-FSK, a physical layer for low-power wide-area networks: Analysis and optimization", Elsevier Comptes Rendus Physique, 2017. Access: [www.sciencedirect.com/science/article/pii/S163107051630158X](http://www.sciencedirect.com/science/article/pii/S163107051630158X).
- [2] Y. Roth, J-B. Doré, L. Ros and V. Berg, "EXIT Chart Optimization of Turbo-FSK: Application to Low Power Wide Area Networks", 9th International Symposium on Turbo Codes & Iterative Information Processing 2016 (ISTC'16), Brest, France, 2016.
- [3] Y. Roth, J-B. Doré, L. Ros and V. Berg, "A Comparison of Physical Layers for Low Power Wide Area Networks", 11th EAI International Conference on Cognitive Radio Oriented Wireless Networks (Crowncom), Grenoble, France, 2016.



# IMPLEMENTATION AND ANALYSIS OF A TURBO-FSK TRANSCEIVER FOR A NEW LOW POWER WIDE AREA PHYSICAL LAYER

## RESEARCH TOPIC:

Turbo FSK, Implementation, LPWA, Physical Layer

## AUTHORS:

J. Estavoyer, Y. Roth, J-B. Doré, V. Berg, L. Ros (Gipsa Lab)

## ABSTRACT:

Low Power Wide Area Networks aim at connecting low cost devices with high constraints on the link budget. Focusing on the physical layer, the combination of orthogonal modulation and coding in the same process has been proven efficient when associated with a turbo receiver. This work shows how this scheme, based on frequency shift keying modulation, can be efficiently implemented on today low-end platform based on a flexible radio frequency semiconductor component combined with a low power microcontroller. A link budget improvement of 4.6dB is demonstrated with a low-end receiver, enabling a coverage extension by a factor of 1.78 or a reduction of the transmit power by a factor 3, while keeping the same quality of service.

**SCIENTIFIC COLLABORATIONS:** GIPSA-lab

## Context and Challenges

In Low Power Wide Area (LPWA) Networks, terminals are expected to be low cost, have a low power consumption, and be able to communicate over a long range. In previous works, we have introduced a new high performance physical layer, so-called Turbo-FSK, based on the combination of a convolutional code and an orthogonal modulation with an iterative decoder. The considered scheme is particularly interesting for the uplink transmission in a cellular network context. Complexity is dominated by the iterative nature of the decoder and is deported at the base station. The implementation of the scheme on off-the-shelf component is considered to demonstrate the viability of the solution even on low end platforms [1]. The comparison with standard LPWA solutions is done in [2], showing the potential of turbo processing in this context.

## Main Results

Implementation of a transceiver using Turbo-FSK with a 4-FSK modulation is considered. The architecture of the transmitter and the receiver is depicted in Figure 1. The platform used to implement the physical layer is the SmartRF Transceiver Evaluation Board (TrxEB) provided by TI, composed of a MSP430 MCU and a CC1200 RF chip. Programs are developed in C and implemented on two platforms to manage both transmitter and receiver platforms. The TrxEB platform does not allow for the receiver to perform probabilistic demodulation (hard values of the bits are fed to the decoder).

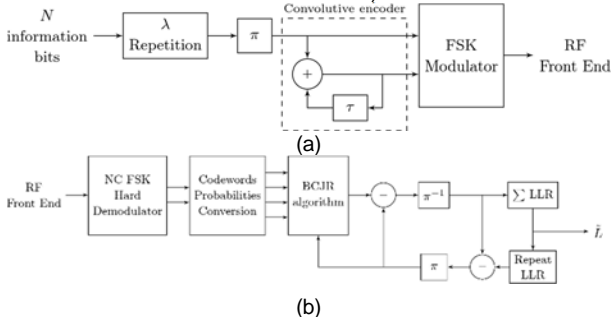


Figure 1: Transmitter (a) and receiver (b) of the implemented Turbo-4FSK.

Also, non-coherent demodulation of the Turbo-FSK is performed. The receiver is thus sub-optimal as better performance could be obtained by considering probabilistic (or soft) decoding. The Turbo-4FSK is compared to a simple repetition scheme. The receiver for the repetition scheme performs majority decoding.

Experimental measurements with the CC1200 platform have been done. The PER measurements versus the received signal power (in dBm) is depicted in Figure 2. The Turbo-4FSK scheme reaches a PER of  $10^{-3}$  for a received power equal to -113dBm, providing a gain of 4.6dB in comparison to the simple repetition scheme. This results was confirmed by simulations.

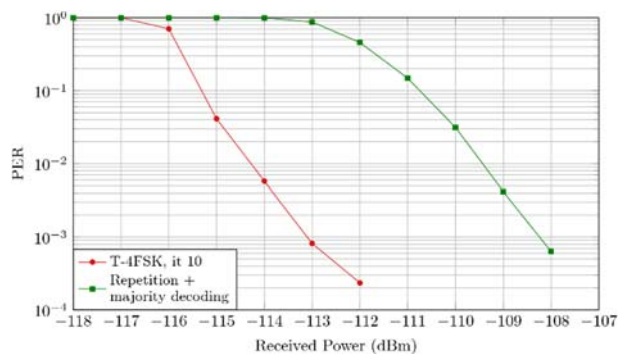


Figure 2: Performance of the Turbo-4FSK obtained with the evaluation board.

## Perspectives

This work is the first implementation of a newly proposed Turbo-FSK receiver. The scheme was designed to provide significant performance gain in comparison to standard repetition schemes. These results of sub-optimal Turbo-FSK receiver performance demonstrate the practical viability of the Turbo-FSK scheme for LPWA applications.

## RELATED PUBLICATIONS:

- 1] J. Estavoyer, Y. Roth, J-B. Doré and V. Berg, "Implementation and Analysis of a Turbo-FSK transceiver for a new Low Power Wide Area Physical Layer", 2016 International Symposium on Wireless Communication Systems (ISWCS): Special sessions (ISWCS'2016 – Special sessions), Poznan, Poland, 2016.
- [2] Y. Roth, J-B. Doré, L. Ros and V. Berg, "A Comparison of Physical Layers for Low Power Wide Area Networks", 11th EAI International Conference on Cognitive Radio Oriented Wireless Networks (Crowncom), Grenoble, France, 2016.

# PROTOCOL DESIGN AND COEXISTENCE STUDIES IN A REALISTIC BODY AREA NETWORK ENVIRONMENT

## RESEARCH TOPIC:

Body Area Network, Body to Body, Network Simulator, Protocol

## AUTHORS:

M. Maman, F. Mani, B. Denis, R. D'Errico (CEA)  
M.M. Alam, D. Ben Arbia, E. Ben Hamida (QMIC)

## ABSTRACT:

To deeply analyze and design wearable applications, an accurate and realistic simulator for body area networks (BAN) and body-to-body networks (B2B) is required. In our semi-deterministic approach, a real-time measurement campaign have been performed, characterized through statistical analysis and included in our network oriented simulator. This enables to generate link-correlated and time-varying realistic traces (i.e., with consistent mobility patterns) for BAN and B2B shadowing and fading, including body orientations and rotations and to support and guide even more efficient system design. Based on this framework, the impact of mutual interference on intra-BAN communications is evaluated while using several MAC strategies.

**SCIENTIFIC COLLABORATIONS:** QMIC, Doha, Qatar

## Context and Challenges

With the continuous and exponential rise of wearable devices and applications, it is anticipated that by 2019, there will be more than 150 million wearable devices worldwide. The assumption of a massive market penetration raises numerous concerns regarding coexistence that must be carefully analyzed and understood. Several interference mitigation schemes have been recently proposed in the literature to cope with multiple collocated Body Area Networks (BAN). Nevertheless, an in-depth analysis of the underlying coexistence issues and challenges is still needed so as to support and guide even more efficient system design. This analysis requires an accurate and realistic simulator for BAN and B2B networks.

## Main Results

WSNet simulator has been adapted in order to accurately model the BAN and B2B channel models, radio link and mobility models and to fulfill the upper layers requirements (i.e., MAC, network and application layers)[2].

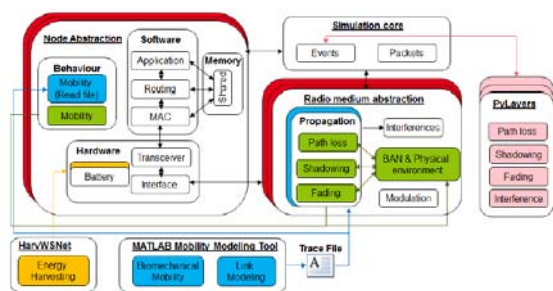


Figure 1: WSNet simulator adaptation to BAN/B2B (green).

An essential feature of our simulation is the semi-deterministic approach of the mobility model that provides improved and extended sets of input parameters (i.e., positions, relative orientations, speeds, obstructions...) for the On-Body and B2B stochastic channel models to generate time-varying realistic traces (i.e., with consistent mobility patterns). For example, On-Body channels can adapt their models based on the human walk according to the BAN speed. B2B channels can

dynamically take into account the mutual body orientations, the (Non) Line-Of-Sight conditions and the room the other BAN belongs to in order to define interfering links. Based on this framework, we have evaluated the impact of the mutual interference on intra-BAN communications while using several access strategies, including unslotted and beacon-enabled (BE) slotted Carrier Sense Multiple Access/Collision Avoidance (CSMA/CA) or Guaranteed TimeSlot (GTS), along with different acknowledgement (ACK) and retransmission (RTX) policies.

Figure 2 shows the Packet Reception Rate (PRR) for up to 10 BANs composed of 3 nodes in a two rooms (5 x 5 m each) area. Each node generates 50-byte data to its BAN coordinator. The data is generated each 125 ms (1 packet per superframe).

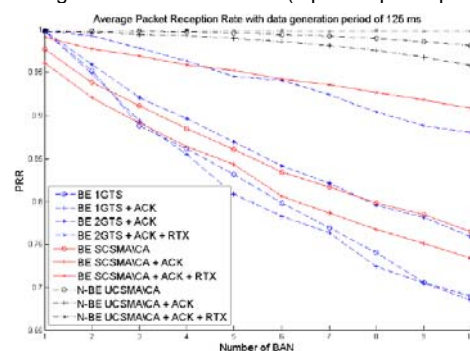


Figure 2: Packet Reception Rate for a 125ms data packet generation as a function of the number of 3-Nodes BANs.

Protocol simulations using an adequate Physical layer abstraction show that GTS communications experience severe degradation and have relatively low resilience against the most harmful interference conditions. On the contrary, unslotted CSMA/CA enjoys the best PRR by avoiding collision of each single communication independently, but requires higher energy consumption due to its 100% duty cycle.

## Perspectives

Future works will exploit the simulation framework here presented in order to evaluate interference mitigation schemes and to further improve the system.

## RELATED PUBLICATIONS:

- 1) M. Maman, F. Mani, B. Denis and R. D'Errico, "Evaluation of multiple coexisting Body Area Networks based on realistic on-body and Body-to-Body channel models", 2016 10th International Symposium on Medical Information and Communication Technology (ISMICT), Worcester, 2016.
- 2) M.M. Alam, E. Ben Hamida, D. Ben Arbia, M. Maman, F. Mani, B. Denis and R. D'Errico, "Realistic Simulation for Body Area and Body-To-Body Networks", Sensors 2016, 16, 561.











# 3.

## ANTENNAS AND PROPAGATION

- Antennas Design, Characterization and Experimentation
- Reconfigurable Transmit Array
- Low Profile Antennas
- Channel Modelling
- Environment Mapping

# COMPACT METASURFACE FOR LOW PROFILE ANTENNA IN THE UHF BAND

## RESEARCH TOPIC:

Low profile, antenna, metasurface, metamaterial, artificial magnetic conductor, unit cell miniaturization

## AUTHORS:

N. Kristou, J-F. Pintos, K. Mahdjoubi (Institut d'Electronique et de Télécommunications de Rennes)

## ABSTRACT:

In this contribution, an alternative technique is proposed to miniaturize the Artificial Magnetic Conductors (AMC) unit cell. Novel unit cell achieves up to 93% surface size reduction at the same operating frequency compared to conventional mushroom-like unit cell. An AMC surface of  $5 \times 5$  cells is designed under a dipole antenna with a distance of  $0.05\lambda_0$ , where  $\lambda_0$  denotes the free space wavelength at 0.9 GHz, for gain enhancement and radiation control. Both the dipole antenna and the AMC surface are fabricated and measured to demonstrate the potential of this new structure.

**SCIENTIFIC COLLABORATIONS:** Institut d'Electronique et de Télécommunications de Rennes

## Context and Challenges

Artificial Magnetic Conductors (AMC) constitutes an attractive reflector for low profile antennas which can take advantage of intrinsic zero reflection phase response to reduce antenna height without the need for thick quarter wave backplane. Main drawback of such structure remains the size of the unit cell which is close to quarter-wavelength in free space. A significant amount of research has been made recently on unit cell miniaturization and several works have been widely proposed in the literature with various miniaturization techniques (complex engineered patterns, volumetric structures with superposed layers and lumped element loading). In this contribution, an alternative technique is proposed to miniaturize an AMC unit cell. Dipole antenna over a new compact AMC surface is designed, simulated and measured to demonstrate the potential of the new approach

## Main Results

The proposed unit cell comprises two superposed substrates. The top metasurface layer (AMC shape) is linked to the bottom layer (back side interconnexion array) by a set of four metallic vias, as explained in [1][2]. All these vias are crossing the entire thickness of the structure and passing through one of the holes of the ground plane with no electrical contact. This results in creating a meandered network at the bottom side of the structure that connect every single unit cell to its near neighbours. The position of the offset four-vias and the phase shift ( $\Delta\phi$ : relative to the meander length for each unit cell) represent the key parameters of this new approach offering a novel way to set the zero-phase frequency of the AMC and to reduce the unit-cell size. Fig. 1 summarizes unit square cell miniaturization effort. Novel unit cells shown in Fig. 1 (b) and Fig. 1 (c) achieve respectively 60% and 73% surface reduction compared to a conventional unit cell shown in Fig. 1 (a). For final design, a square spiral shape is used instead of square shape for bandwidth enhancement while keeping compact size. Final proposed unit cell shown in Fig. 1(d) achieves 93% surface reduction compared to conventional unit cell at the same frequency. As example, the introduced unit cell in Fig. 1(b) is duplicated, to 5 by 5 unit cells, to form the metasurface. Low-cost FR4 ( $\epsilon_r=4.4$ ,  $\tan \delta_e=0.02$ ) is selected as a substrate. The dimensions of the unit cell are  $38 \times 38 \text{ mm}^2$  ( $\lambda_0/9 \times \lambda_0/9$ ).

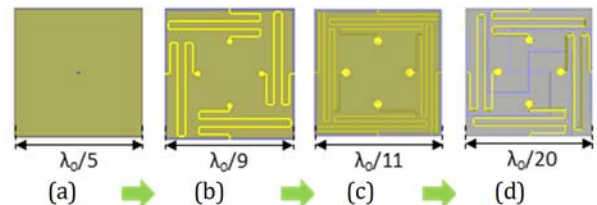


Fig. 1. Unit cell miniaturization effort using the proposed approach.

A dipole antenna of length 150 mm ( $\sim \lambda_0/2$ ) is placed at a distance of 17 mm ( $\lambda_0/20$ ) above the AMC surface [3]. The overall size of the structure is  $\lambda_0/1.8 \times \lambda_0/1.8 \times \lambda_0/15$ . The proposed dipole antenna over the AMC structure is simulated, fabricated and measured, as shown in Fig. 2(b), in anechoic chamber. Experimental results show that, with maintaining low profile and compact size (60% surface size reduction), the antenna system achieves a maximum realized gain measured of 5 dBi. The peak directivity is quite stable from 0.84 GHz to 1 GHz and exceeds 7 dBi. Moreover, low front-to-back ratio (15 dB) and cross-polarization level (-25 dB) is obtained simultaneously. Low radiation performance can be noted at 1 GHz due to surface losses. Good agreement are observed between the measured and simulated results. The small discrepancies are caused by the effect of the coaxial cable, fabrication tolerance and measurement accuracy

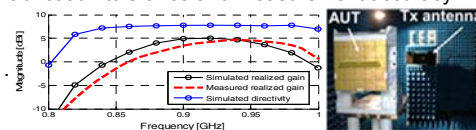


Fig. 2. (a) Measured and Simulated realized gain of the proposed antenna, (b) radiation measurement setup.

## Perspectives

Miniaturized AMCs have been shown to reduce the profile (height) of antennas while maintaining compact lateral dimensions, but at the expense of operating bandwidth. Next steps will focus on adding tunability to the system that would restore the possibility of adjusting the operating frequency over a large bandwidth (LTE band targeted).

## RELATED PUBLICATIONS:

- [1] N. Kristou, J-F. Pintos, K. Mahdjoubi, "Alternative Approach to Miniaturize an AMC Structure", META'16, the 7th International Conference on Metamaterials, Photonic Crystals and Plasmonics, Torremolinos, Spain, 2016.
- [2] N. Kristou, J-F. Pintos, K. Mahdjoubi, "New compact AMC structure for low profile antenna", META'16, the 7th International Conference on Metamaterials, Photonic Crystals and Plasmonics, Torremolinos, Spain, 2016.
- [3] N. Kristou, J-F. Pintos, K. Mahdjoubi, "Low Profile Dipole Antenna Over Compact AMC Surface", 2017 International Workshop on Antenna Technology (iWAT), Athens, Greece.



# DESIGN AND EXPERIMENTAL CHARACTERIZATION OF RECONFIGURABLE TRANSMITARRAYS WITH REDUCED FOCAL DISTANCE

## RESEARCH TOPIC:

High-gain antennas, transmitarray, 5G networks, SATCOM, beamforming

## AUTHORS:

L. Di Palma, A. Clemente, L. Dussopt, R. Sauleau (IETR, Univ. Rennes 1), P. Potier (DGA), and P. Pouliguen (DGA)

## ABSTRACT:

In this contribution, we present the design and experimental characterization of two 400-element reconfigurable transmitarrays with reduced focal distance operating, respectively, in X- and Ka-band. To this end we consider an illumination with four feed horn antennas in case of the X-band antenna and with a planar focal array in the case of the Ka-band. The focal distance and the focal source configuration in the focal plane have been optimized with an in-house simulation tool. The experimental results obtained in radiation are in good agreement with the numerical predictions. The multiple-source transmitarrays exhibit similar radiation performances as the single-source ones in terms of gain, bandwidth and beam tilting capabilities, but with about half its volume.

**SCIENTIFIC COLLABORATIONS:** University of Rennes 1, DGA

## Context and Challenges

Transmitarray antennas are formed by one or more focal sources [1] illuminating a planar array of unit-cells (Fig. 1). Each unit-cell is composed by a receiving antenna, a phase shifting system and a transmitting antenna. Controlling the transmission phase allows collimating the beam in a desired direction and/or generating radiation pattern with a predefined mask. In the case of reconfigurable transmitarrays, the phase shift of each unit-cell can be controlled electronically using varactor diodes, p-i-n diodes [2-4], MEMS switches or tunable materials. These antennas can be used in many defense and civil applications, such as satellite communications, radar systems, and wireless metropolitan area networks (WMAN), point-to-point and point-to-multipoint communication links. Their important volume, if compared with phased arrays, could limit the integration on vehicles and on host platforms where a low-profile solution is a primary concern. The thickness of a transmitarray is mainly related to the focal distance, i.e. the distance between the source and the transmitarray receiving layer (labelled  $F$  in Fig. 1). The length  $F$  is in general several wavelengths in order to optimize the surface illumination. In particular, it should be chosen as a trade-off between the illumination tapering and spillover loss. In this paper two electronically reconfigurable transmitarrays with reduced focal distance operating in X- [2,3] and Ka-band [4], respectively, are presented.

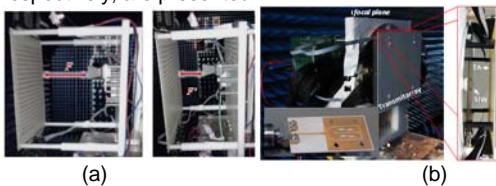


Fig. 1. Photograph of the two transmitarrays with reduced focal distance working in (a) X- and (b) Ka-band, respectively.

## Main Results

In the case of the X-band transmitarray (Fig. 1(a)) four standard gain horns have been used as a focal source. The measurements in radiation show a maximum broadside gain of 23.2 dBi at 10 GHz with side lobe levels below -14.4 dB when the horns are disposed in a square configuration with a focal distance

of 119 mm ( $F/D = 0.39$ ). This focal distance must be compared with the one of the case of the single source, which is equal to 214 mm ( $F/D = 0.71$ ). [2]. Instead, in the case of the transmitarray working in Ka-band an array of four sub-arrays, i.e. 16 slots, separated by a distance  $d$  of 34 mm has been designed (Fig. 1(b)). The focal distance  $F$  has been optimized to 36 mm ( $F/D = 0.36$ ) for a maximum broadside gain. The focal distance in the case of single source was equal to 60 mm. The sub-arrays are fed through three 3-dB power splitters designed in SIW technology in order to mitigate the spurious radiation that would occur with microstrip lines. The measured maximum gain is 16.2 dBi with a cross polarization discrimination of 27 dB at broadside. This gain value is lower than the measured one with a single horn antenna (28.8 dBi) because the planar focal sources and the required feeding network introduce additional losses.

The measured radiation pattern of the transmitarray working in the X-band with a beam steered at  $40^\circ$  on the vertical plane is presented in Fig. 2. In the picture the simulated pattern and the associated phase distribution on the array aperture are presented.

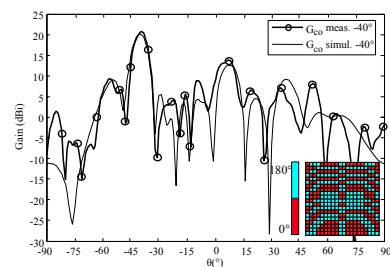


Fig. 2. Measured and simulated gain patterns of the X-band transmitarray at scanning angle  $40^\circ$ .

## Perspectives

The possibility to reduce the focal distance and as a consequence the transmitarray profile and volume has been analyzed and experimentally demonstrated. In the future works, the possibility to reduce the focal distance of a factor  $> 2$  considering innovative techniques for transmitarray illumination will be investigated.

## RELATED PUBLICATIONS:

[[1] A. Clemente, L. Dussopt, R. Sauleau, P. Potier, and P. Pouliguen, "Focal distance reduction of transmit-array antennas using multiple feeds," *IEEE Antennas Wireless Propag. Letters*, vol. 11, Nov. 12. [2] A. Clemente, L. Dussopt, R. Sauleau, P. Potier, and P. Pouliguen, "Wideband 400-element electronically reconfigurable transmitarray in X Band," *IEEE Transaction on Antennas and Propag.*, vol. 61, no. 10, Oct. 13. [3] L. Di Palma, A. Clemente, L. Dussopt, R. Sauleau, P. Potier, and P. Pouliguen, "Design and experimental characterization of a reconfigurable transmitarray with reduced focal distance," *International Journal of Microwave and Wireless Technologies*, vol. 8, no. 3, May 16. [4] L. Di Palma, A. Clemente, L. Dussopt, R. Sauleau, P. Potier, and P. Pouliguen, "Circularly-polarized reconfigurable transmitarray in Ka-band with beam scanning and polarization switching capabilities," *IEEE Transaction on Antennas and Propag.*, Vol. 65, no. 2, Feb. 17.

# CIRCULARLY-POLARIZED RECONFIGURABLE TRANSMITARRAY IN KA-BAND WITH BEAM-SCANNING AND POLARIZATION SWITCHING CAPABILITIES

## RESEARCH TOPIC:

High-gain antennas, transmitarray, 5G networks, SATCOM, beamforming

## AUTHORS:

L. Di Palma, A. Clemente, L. Dussopt, R. Sauleau (IETR, Univ. Rennes 1), P. Potier (DGA), and P. Pouliguen (DGA)

## ABSTRACT:

The design, realization and experimental characterization of a 400-element electronically-reconfigurable transmitarray operating in Ka-band is presented. It is based on linearly-polarized unit-cells with  $180^\circ$  phase-shifting capability. Several sequential rotation schemes have been compared numerically to generate a circularly-polarized beam over a broad frequency band, and a random distribution has been selected to mitigate spurious cross-polarized side-lobes when scanning the main beam. 2D electronic beam-steering capabilities of  $\pm 60^\circ$  have been verified experimentally. The prototype, illuminated by a horn antenna as a focal source, exhibits a broadside gain of 20.8 dBi at 29.0 GHz and a 3-dB bandwidth of 14.6% with radiation efficiency of 58%.

**SCIENTIFIC COLLABORATIONS:** University of Rennes 1, DGA

## Context and Challenges

In the last years, transmitarray antennas have become popular in millimeter-wave applications for the significant benefit offered by spatial feeding in terms of reduced losses and complexity. They are formed typically by an arrangement of half-wavelength unit-cells, which collimate the radiation of a focal source by locally shifting the phase of the transmitted waves. If this phase shift is controlled electronically, a reconfigurable antenna is obtained with beam-forming and beam-steering capabilities. Transmitarray antennas are attractive solutions for many applications operating in Ka-band, such as satellite communications, point-to-point links and heterogeneous wireless networks

## Main Results

In this work, we present a  $20 \times 20$ -element fully reconfigurable circularly-polarized transmitarray (Fig. 1) based on the reconfigurable unit-cell proposed in [1,2] working in Ka-band. 800 p-i-n diodes are integrated on the array to control the transmission phase of each unit-cell enabling beam-steering and circular-polarization switching capabilities. The details of this work and the possibility to use a focal array to reduce the focal length improving the compactness of the transmitarray are presented in [3]. The sequential rotation technique is used, and a random rotation scheme is selected in order to optimize the beam-steering capabilities. The experimental results exhibit very good performance in agreement with the simulations (Fig. 2)). A broadside gain of 20.8 dBi in circular polarization is obtained with a cross polarization discrimination of about 25 dB. The

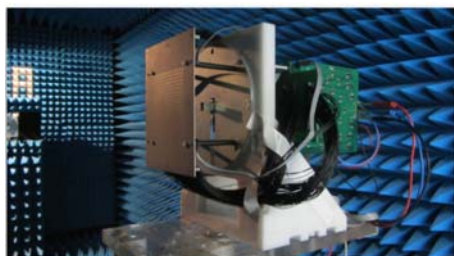


Fig. 1. Photograph of the realized circularly-polarized reconfigurable transmitarray at Ka-band.

LHCP/RHCP switching capability has been demonstrated as well. In all the tested cases, a good agreement with the numerical simulations is obtained and a beam-steering capability of  $\pm 60^\circ$  is demonstrated. The radiation efficiency is about 58%. To our knowledge, this work presents the first demonstration of a circularly-polarized reconfigurable transmitarray in Ka-band with beam-steering and polarization switching capability.

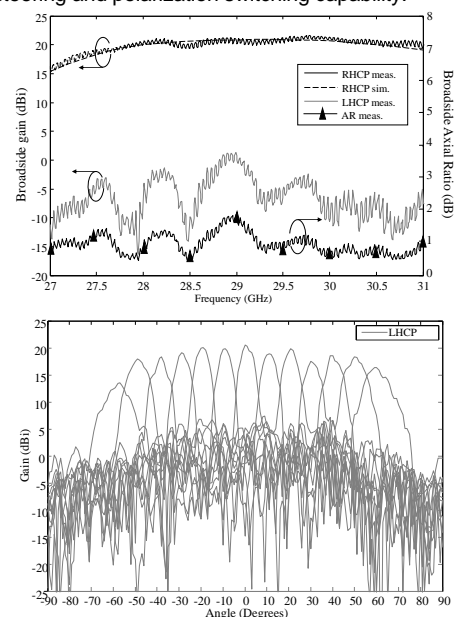


Fig. 2. Measured frequency response and radiation patterns of the realized transmitarray at Ka-band

## Perspectives

A 400-element electronically reconfigurable transmitarray with beam-steering capability has been experimentally demonstrated in Ka-band. In the next works 2bit unit-cell design will be investigated in order to increase the antenna aperture efficiency.

## RELATED PUBLICATIONS:

- [1] L. Di Palma, A. Clemente, L. Dussopt, R. Sauleau, P. Potier, and P. Pouliguen, "1-bit unit-cell for transmitarray applications in Ka-band," In Proc. of *Europ. Conf. Ant. Propag.* (EuCAP), Lisbon, Portugal, 12-17 Apr. 2015.
- [2] L. Di Palma, A. Clemente, L. Dussopt, R. Sauleau, P. Potier, and P. Pouliguen, "1-bit unit-cell for transmitarray applications in Ka-band," *IEEE Antennas Wireless Propag. Letters*, vol. 15, pp. 560-563, 2016.
- [3] L. Di Palma, A. Clemente, L. Dussopt, R. Sauleau, P. Potier, and P. Pouliguen, "Circularly-polarized reconfigurable transmitarray in Ka-band with beam scanning and polarization switching capabilities," *IEEE Transaction on Antennas and Propag.*, Vol. 65, no. 2, pp. 529-540, Feb. 2017.

# WIDEBAND LINEARLY-POLARIZED TRANSMITARRAY ANTENNA FOR 60 GHz BACKHAULING

## RESEARCH TOPIC:

High-gain antennas, transmitarray, 5G networks, backhauling, 60 GHz

## AUTHORS:

C. Jouanlanne, A. Clemente, M. Huchard (Radiall), J. Keignart, C. Barbier (Radiall), T. Le Nadan (Radiall), and L. Petit (Radiall)

## ABSTRACT:

This paper presents the design of a linearly-polarized transmitarray antenna for backhauling applications at V-band (57 – 66 GHz). The antenna is composed of a planar circular-shape array with 1264 unit-cells printed on a three-metal layer standard PCB, an ad-hoc focal source, and a radome. A 3-bit phase resolution has been selected to achieve a gain higher than 31 dBi over the unlicensed 60 GHz-band and low side lobe levels. Experimental results are in line with the theoretical ones provided by an in-house design tool based on analytical model and electromagnetic simulations. The proposed design presents a measured broadside gain of 32.5 dBi at 61.5 GHz with an aperture efficiency of 42.7% and a wide 1-dB gain bandwidth of 15.4% (57 – 66.5 GHz).

**SCIENTIFIC COLLABORATIONS:** Radiall

## Context and Challenges

The rapid growth of mobile data traffic and the use of smartphone or other connected objects have recently drawn increased attention to the large amount of underutilized millimetre wave (mmWave) frequency bands (30 – 300 GHz) as a potential solution to achieve tens or hundreds of times more capacity compared to the current cellular networks. In this scenario, 5G wireless heterogeneous networks will be probably composed of medium-range macro-cells at sub-3 GHz bands, small-cells at sub-6 GHz, and small-cells at mmWave bands (28, 38, 60 GHz or E band 71 – 76 and 81 – 86 GHz) with a target peak capacity of 2 – 7 Gb/s near the access point. High-capacity (peak capacity around 10 – 25 Gb/s) mmWave backhaul links working in line-of-sight (LOS) conditions will also connect the access points to the core network. In this work, a fixed beam transmitarray antenna for backhauling at V-band is designed, optimized and characterized.



Fig. 1. Schematic view of the linearly-polarized transmitarray for backhauling at V-band.

## Main Results

The proposed transmitarray (Fig. 1) uses a 3-bit phase quantization [1], which means a pool of eight unit-cells (called 0°, 45°, 90°, 135°, 180°, 225°, 270°, and 315°), to reach the required performances (maximum gain and Side Lobe Level) over the whole 57 – 66 GHz unlicensed band. The design is pushed to a Technology Readiness Level (TRL) corresponding to an industrial demonstrator. For instance, the focal source, including

a profiled skirt protecting the antenna from its surroundings, is rather more complex than a standard pyramidal horn antenna usually used in the open literature for classical transmitarray antenna design. A polypropylene radome is also included to protect the array from its surrounding environment. It has been taken into account in the unit-cell design and optimization. The aperture phase distribution and the illumination taper are optimized using the in-house software previously demonstrated [2] to obtain a radiation pattern in accordance with the required masks. A wide 1-dB bandwidth of 15.4% (~57 – 66.5 GHz), with a maximum gain of 32.5 dBi at 61.5 GHz and a relatively high aperture efficiency of 42.7% are experimentally demonstrated [3]. The experimental results are presented in Fig. 2.

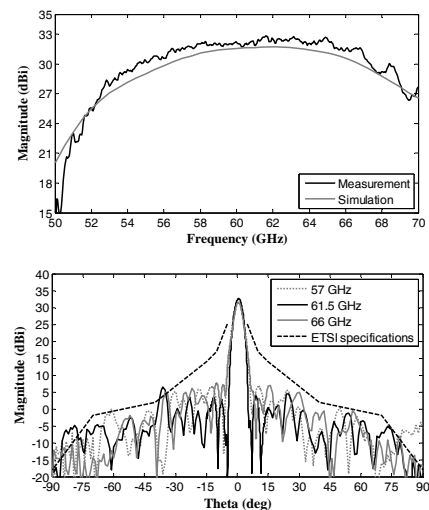


Fig. 2. Measured frequency response and radiation patterns of the linearly-polarized transmitarray for backhauling at V-band.

## Perspectives

A fixed beam transmitarray for backhauling application in the V-band has been successfully demonstrated. In the future works the possibility to reduce the focal distance will be investigated.

## RELATED PUBLICATIONS:

- [1] C. Jouanlanne, T. Le Nadan, M. Huchard, Laurent Petit, and A. Clemente, "Design of a Linearly-Polarized 3-bit TransmitArray Antenna at 60 GHz," *IEEE Intern. Symp. Antenna Propag.* (APS-URSI 2016), 26 Jun. - 1 Jul. 2016, Fajardo, Puerto Rico, USA.
- [2] A. Clemente, L. Dussopt, R. Sauleau, P. Potier, and P. Pouliguen, "Focal distance reduction of transmit-array antennas using multiple feeds," *IEEE Antennas Wireless Propag. Letters*, vol. 11, pp. 1311-1314, Nov. 2012.
- [3] C. Jouanlanne, A. Clemente, M. Huchard, J. Keignart, C. Barbier, T. Le Nadan, and L. Petit, "Wideband linearly-polarized transmitarray antenna for 60 GHz backhauling," *IEEE Transaction on Antennas and Propag.*, vol. 65, no. 3, pp. 1440-1445, Mar. 2017.



# RADIATION EFFICIENCY IMPROVEMENT OF A BALANCED MINIATURE IFA-INSPIRED CIRCULAR ANTENNA

## RESEARCH TOPIC:

Electrically small antenna, inverted-F antenna, radiation efficiency, Ultra NarrowBand antenna, balanced antenna

## AUTHORS:

F. Sarrazin, S. Pflaum, and C. Delaveaud

## ABSTRACT:

The radiation efficiency improvement of an Electrically Small Antenna is presented. We consider a balanced Miniature IFA (inverted F-Antenna)-Inspired Circular Antenna (MIICA) whose radius is  $\lambda/28$  at 433 MHz. By modifying the antenna strip width, we identify an antenna radiation efficiency improvement up to 53 % while keeping its overall dimension and general structure identical. Then, we confirm the simulated antenna performances improvement by radiation efficiency measurements performed inside the large anechoic chamber of CEA-LETI.

**SCIENTIFIC COLLABORATIONS:** This work was supported by the French National Research Agency (ANR) under the "SENSAS"

## Context and Challenges

Electrically Small Antennas (ESAs) have been studied for many years. Indeed, it is a key element for radio communication systems miniaturization and small antenna design is still very challenging. An antenna is generally considered as electrically small if  $ka \leq 0.5$ , where  $k$  is the wavenumber and  $a$  is the radius of the minimal sphere enclosing the antenna. The numerous studies about fundamental limits of ESAs highlight the classical tradeoff between radiation efficiency, size and bandwidth. Several studies focus on enlarging the bandwidth (minimizing the Q-factor) of ESAs for a given size. However, for some specific upcoming applications, only a narrow frequency bandwidth is necessary. As example, Wireless Sensors needs to transmit intermittently and only a few of packets of data. Moreover, the available power of the communication node is usually very low. Thus, the radiation efficiency becomes the most critical parameter of the required UNB antenna.

## Main Results

This work aims to optimize the radiation efficiency of ESA and most particularly to demonstrate how to improve the radiation efficiency of an ESA while keeping its general design and overall dimensions identical. The initial idea is to reduce the ohmic losses of the antenna by enlarging its strip width [1].

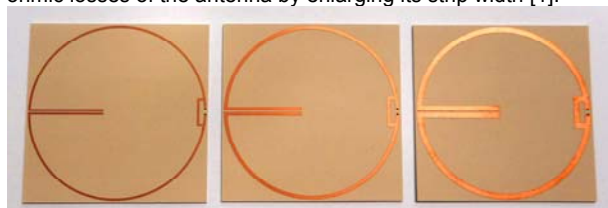


**Figure 1. Pictures of the three realized MIICA with different strip widths: 0.6 mm (left), 1 mm (center) and 1.6 mm (right).**

We consider the antenna topologies presented in Fig. 1 designed to operate at 433 MHz ( $\lambda=70$  cm). It is a balanced Miniature IFA-Inspired Circular Antenna (MIICA) printed on low loss dielectric substrate (0.8 mm thick Rogers RO3003). This antenna combines different miniaturization techniques. The first is related to the presence of a short circuit recalling a quarter

wavelength IFA structure. Then the quarter-wave arm is folded along circular shape. Finally, a capacitive load is introduced at the antenna extremity to artificially elongate the resonant length. This capacitor is constituted of a coplanar twin strip line whose length adjusts the capacitance value. The antenna radius is 25 mm ( $\lambda/28$  at the working frequency or  $ka=0.2267$ ). The short circuit strip close to antenna feeding is equally used for impedance matching. Ten different strip widths from 0.1 mm to 4.1 mm are considered in the study.

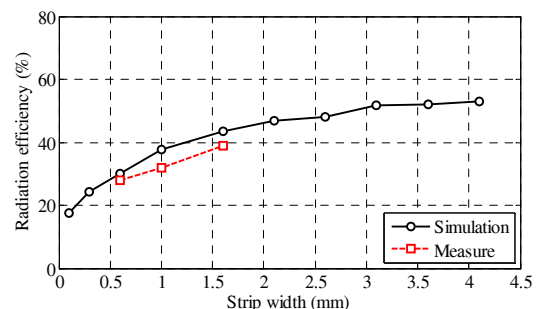


**Figure 2. Radiation efficiency of the MIICA as a function of the strip width, simulated and measured results.**

The simulated radiation efficiency is compared to the measured one (3 prototypes of Fig.1) in Fig. 2 as a function of the strip width. Measured efficiencies are obtained by integrating the antenna gain pattern over the whole sphere [2]. Gain patterns are measured in far field condition using a differential setup [3]. Antenna efficiencies rise from 18 % for the thinnest strip (0.1 mm), up to 53 % for the thickest one (4.1 mm).

## Perspectives

This work present the MIICA antenna whose radiation efficiency can be tuned from 17 % to 53 % by modifying its strip width, while keeping its overall dimension identical. The radiation efficiency improvement predicted by simulation is validated by the measurements performed in far field. The radiation efficiency improvement is obtained simultaneously with Q-factor increase [1], thus respecting the ESAs' fundamental limits. These results constitute a demonstration of the possible control of miniature antenna radiation efficiency.

## RELATED PUBLICATIONS:

- [1] F. Sarrazin, S. Pflaum, C. Delaveaud, "Radiation Efficiency Improvement of a Balanced Miniature IFA-Inspired Circular Antenna," in IEEE Antennas and Wireless Propagation Letters, vol. PP, no. 99, pp.1-1
- [2] L. Huitema, C. Delaveaud, R. D'Errico, "Impedance and Radiation Measurement Methodology for Ultra Miniature Antennas," IEEE Trans. Antennas Propag., vol. 62, no. 7, pp.3463-3473, July 2014.
- [3] R. Bourtoutian, P. Clais, C. Delaveaud and S. Toutain, "A novel method for measuring differential antennas radiation characteristics" in Antenna Measurement Techniques Association AMTA, Nov. 2007.

# HF-RFID IN HARSH ENVIRONNEMENT (MOIST SOIL, METALLIC PARTS &) NEW ANTENNA DESIGN WITH PEEC METHOD ANALYSIS INCLUDING CONDUCTIVE SURFACE MODEL

## RESEARCH TOPIC:

RFID tag, RFID-HF, Inductive antenna, PEEC method, metallic environment

## AUTHORS:

THOMAS Thierry, REVERDY Jacques, DESCHARLES Melanie

## ABSTRACT:

A novel inductive antenna is designed and fabricated for HF-RFID tag in order to maintain efficiency while immersed in a moist environment and to allow large size antenna without inductance value consideration that facilitate the optimization. A simplified partial element equivalent circuit (PEEC) method is implemented on MATLAB where inductive antennas are approximated by filaments loops and metallic objects by ideal conductive surfaces. This method is applied to evaluate the volume coupling, the resonant frequency and all the magnetic parameters of the inductive antenna in order to proceed with a circuit analysis using a SPICE-like tool. It's then possible to adjust the antenna design in presence of metallic object, confirm the RFID chip power supply conditions and evaluate the level of load modulation of the reverse link thanks to an electrical RFID chip model.

## Context and Challenges

RFID is now in widespread use, but applications in harsh environment are still challenges, for example for a range extended beyond 1 m, with a tag buried in dry or sodden soil without *radome* for protection or near a metallic body. The detection range of a tag by an inductive antenna can be extended by increasing the coupling volume that is directly relevant to the antenna size. The coupling volume of a tag is the ratio of the square of the area of its coil-antenna by the self-inductance of this coil. This ratio is multiplied by the vacuum permeability  $\mu_0$  in order to obtain a result homogeneous to a volume. In HF-RFID, the electromagnetic field attenuation in dielectric medium is low, but the stray capacitance of a classical coil is aggravated with the proximity of high dielectric material. A thick enough conductive sheet blocks the magnetic flux and affects the tag, the resonant frequency value decreases and the *apparent* coupling volume is strongly reduced despite a resonant frequency tuning.

## Main Results

The tag detection range capability can be related to the coupling volume by defining a minimal value: from 35 cm<sup>3</sup> for a 1 m range to 350 cm<sup>3</sup> for 1.5m with a 68 cm diameter loop reader antenna supplied with 1 A current. As a comparison, the coupling volume of reference PICC coil is about 60cm<sup>3</sup>. The minimal coupling volume grows rapidly with the required range and can be strongly reduced with angular misalignment, environment weight.

The novel inductive antenna design [1] consists of two spiral wound identical strip lines separated by a dielectric sheet in which several gaps are cut on conductive tracks. The lumped-element equivalent circuit is a distributed series LC in series that reduce the stray capacitance weight by minimizing the voltage along the conductive tracks and allows to increase the coil-antenna size and therefore the coupling volume without turn number consideration. Some experimentations comparing classical coil-antenna to this novel antenna design show a derating on resonant frequency of -40% for the classical case and -3% for the novel design when the tag goes from 'air' to 'water' (the coil-antenna is just protected by a 0.1mm overlay).

The simplified PEEC analysis operated on MATLAB allows to adjust geometrical antenna parameters with the resonant frequency value as target in presence of metallic objects.

For example, as showed in the Fig. 1, a tag (33x230 mm<sup>2</sup>) must be placed close to three parallel conductive cylinders in triangular configuration spaced with a gap of small portion of its diameter.

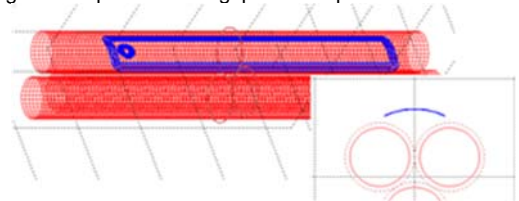


Figure 1: a case of PEEC analysis in presence of metal

The predicted and measured resonant frequency values in presence of cylinders matches together within better than 1%. The resonant frequency (Fig. 2) is lower by 880 kHz when the tag is out of conductive cylinders.

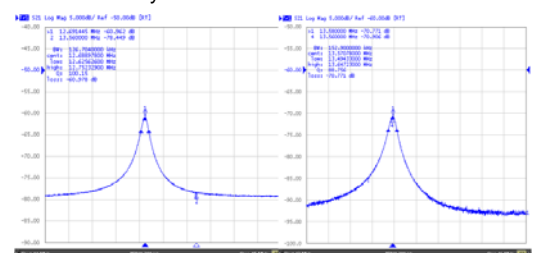


Figure 2: frequency response free at left ( $f_c = 12.69$  MHz) in presence of metal at right ( $f_c = 13.57$  MHz)

The calculated apparent coupling volume is about 70 cm<sup>3</sup>, the measured minimum field strength to activate the tag, is about 40 mA/m rms corresponding to a range of 1.1 m in the same conditions described above.

## Perspectives

It is still possible to increase the current that feeds the reader loop antenna in order to increase the range (1 A in a loop of 68 cm in diameter need roughly 4 W and we can push up to 10 W). Therefore the combination of a strong HF source and great distance brings a sensitivity problem in load modulation detection by the reader. A new challenge will be treated in future works to enhance the performances of the reader.

## RELATED PUBLICATIONS:

[1] US 937 944 B2, Antenna for a Moist Environment, T. Thomas, June 28

# E-BAND MILLIMETER WAVE INDOOR CHANNELS CHARACTERIZATION

## RESEARCH TOPIC:

I Propagation channel, millimeter-waves, 5G

## AUTHORS:

S A. Bamba, F. Mani, and R. D'Errico

## ABSTRACT:

This work presents a propagation channel characterization in the E-Band (80.5-86.5 GHz) in indoor environments, for 5G application. Measurements were performed in an office and conference rooms by means of mechanical steering of directive antennas at both the transmitter and receiver side, allowing a double-directional angular characterization. Specular components have been estimated by means of a detection algorithm. Characterization of the path loss, delay spread, Angle-of-Departure and Angle-of-Arrival spreads are presented for two indoor environments.

## Context and Challenges

The number of wirelessly connected devices along with the number of users are exponentially increasing nowadays owing to, e.g., the advent of tablets and smartphones. The 5th Generation of mobile communications (5G) is expected to offer extreme broadband, pervasive and large connectivity with very low latency. The usual frequency bands for mobile communications systems (i.e., 300 MHz-6 GHz) cannot provide satisfactory quality of service due to the limited bandwidth therein. Therefore, the World Radio-communications Conference (WRC) 2015 identified several of the millimeter wave bands for further study for mobile applications. However, the radio channel ought to be well understood at the millimeter frequencies by the designers of future communications systems. Indeed, the knowledge of the channel state information is important in order to design efficient and optimal communications systems. We present here the channel measurements results in indoor environments in E-band along with the preliminary results of the channel characterization. This work was carried out in the framework of the H2020 mmMAGIC project.

## Main Results

A channel measurement campaign was carried out at CEA LETI in indoor premises (Fig. 1).



Fig. 1: Channel measurement campaign in indoor environments: office (left), conference room (right).

The channel sounder was based on Vector Network Analyzer (VNA) with millimeter wave frequency converters. Two automatic positioners were employed to mechanically steer directive horn antennas. Starting from directive channel measurements and

antenna steering, omnidirectional power delay profiles (PDPs) have been synthesized, and multipath components have been extracted [1].

Large-scale channel parameters (i.e., path loss, delay spread) results were extracted from measurements. It was observed that the path loss is higher in the bigger environment, i.e. conference room due to longer propagation path. The delay spread values have been determined and it was observed a mean value of about 6.10 ns (resp. 5.20 ns) is obtained in the office (resp. conference) room.

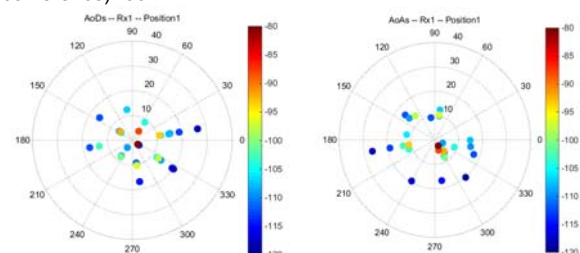


Fig. 2 Example of multipath components extraction in office environment: Angles of departure (left) and arrival (right) of multipath (Office).

Fig. 2 shows an example of estimated multipath. As expected, most of the signal power departs and arrives in the line-of-sight direction. However, the multipath depart and arrive - almost - in all directions. This feature of multipath can be further exploited to achieve optimal beamforming, (i.e., directional transmission or reception for users) for systems with multiple antennas elements.

## Perspectives

Radio channel measurement campaigns with directive antennas have been carried out in millimeter wave frequencies.

Starting from measurement results indoor channel characteristics were extracted and have been used to model multipath and clusters. Further measurements in the V-Band have been also performed. These results are currently being used to develop a stochastic channel model for 5G meter wave application.

## RELATED PUBLICATIONS:

[1] A. Bamba, F. Mani, and R. D'Errico, "E-Band Millimeter Wave Indoor Channel Characterization" in IEEE 27<sup>th</sup> Annual International Symposium on Personal, Indoor, and Mobile Radio Communications (PIMRC), Valencia, Spain, 4-7 September 2016.



# ENVIRONMENT MAPPING WITH MILLIMETER-WAVE MASSIVE ARRAYS FOR PERSONAL RADARS APPLICATIONS

## RESEARCH TOPIC:

Millimeter-waves, massive antenna arrays, indoor mapping, personal radar

## AUTHORS:

Francesco Guidi, Anna Guerra (Uni. of Bologna), Davide Dardari (Uni. of Bologna), Antonio Clemente and Raffaele D'Errico

## ABSTRACT:

This work investigates the feasibility of using massive antenna arrays for localization and mapping applications thanks to the high scanning resolution achievable when a large number of antennas is exploited. In this framework we describe different approaches adopted for indoor environment mapping using massive array architectures. More specifically, thresholding strategies to filter out unwanted received signal components and Bayesian approaches are accounted for and tested with measurement data.

**SCIENTIFIC COLLABORATIONS:** University of Bologna, Italy

## Context and Challenges

Usually, in traditional Simultaneous Localization and Mapping (SLAM), a device with an integrated laser-based radar or a camera moves in an unknown indoor environment and is able to reconstruct a map of it while inferring its own position and orientation inside the generated map. The main shortcomings of traditional approaches are mainly related to technological aspects, as laser-based radar as well as camera-based systems work well only in perfect visibility conditions and they require a mechanical steering in order to perform a scanning operation. To overcome such limitations, The Marie Curie project MAPS investigates the feasibility and the opportunities that can be offered by integrated millimeter-wave massive array that scans the environment in order to reconstruct it [1].



Fig. 1 Radar measurement campaign employing millimeter-wave massive antenna arrays.

## Main Results

Massive arrays have been proposed [1-3], and mapping performance with massive arrays have been investigated as a function of the array characteristics and errors [2]. To achieve our goal, we exploited a measurement campaign performed in a corridor environment and for different positions as shown in Fig. 1 with a 400-elements massive array [3], where a characterization of the backscattering channel delay spread was conducted. Two different approaches have been used: a *hard-decision* [1] and a *soft-decision* [2] based-one. In the first scenario, the received signal was compared with a threshold to mask components due to side-lobes and to decide whether a target is present or not. In particular, the proposed threshold design accounts for the massive array characteristics in order to preserve the array

complexity as low as possible. Fig. 2 shows an example of environment reconstruction where it is possible to observe the reconstructed environment contour.

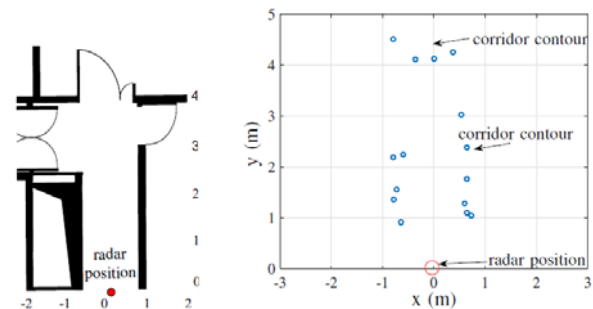


Fig. 2 Example of results, with the real map (left) and the reconstructed environment contour (right).

We then considered a *soft-decision* approach accounting for a grid-based Bayesian algorithm, which discretizes the environment into a grid and directly includes measurement data into the algorithm without the need of a threshold. At the end of the procedure, the radar gives an estimate of the radar cross section assigned to each grid point. Thus, by emulating through measurements the trajectory of a personal radar as in Fig. 1-right, we showed the possibility to attain interesting mapping performance by accounting for real data.

## Perspectives

The obtained results showed the feasibility of the proposed techniques, which were corroborated by real measured data. The mapping precision using millimeter wave massive antenna arrays can be ameliorated by jointly exploiting the *hard* and *soft* approaches described. An alternative is represented by the possibility to conceive an environment-adaptive approach in order to mitigate the side-lobes effects without the need of any a-priori assumption on the threshold design.

The technologies and applications investigated could be exploited to automatically create indoor maps. Such procedure could help supporting a safer navigation in indoor environments for visually impaired people, as well as rescue situations in critical visual conditions.

## RELATED PUBLICATIONS:

- [1] F. Guidi, A. Guerra, D. Dardari, A. Clemente and R. D'Errico, "Joint Energy Detection and Massive Array Design for Localization and Mapping," in IEEE Transactions on Wireless Communications, vol. 16, no. 3, pp. 1359-1371, March 2017.
- [2] F. Guidi, A. Guerra, D. Dardari, A. Clemente; R. D'Errico, "Environment Mapping with Millimeter-wave Massive Arrays: System Design and Performance," in Proc. IEEE Globecom, LION Workshop, Washington D.C., USA, Dec., 2016.
- [3] A. Guerra, F. Guidi, A. Clemente, R. D'Errico and D. Dardari, "Delay spread characterization of millimeter-wave indoor backscattering channel," 2016 10th European Conference on Antennas and Propagation (EuCAP), Davos, 2016.

# MOBILE TO MOBILE INDOOR CHANNEL MODEL

## RESEARCH TOPIC:

Mobile to Mobile channel, time correlation function, channel model

## AUTHORS:

G. Makhoul, F. Mani, R. D'Errico, C. Oestges (ICTEAM Electrical Engineering, Université Catholique de Louvain (UCL), Belgium

## ABSTRACT:

The temporal correlation properties of mobile-to-mobile (M2M) channels is studied based on a measurement campaign carried out in an indoor environment at 2.48 GHz. In order to model the dynamic channel characteristics, short- and long-term fading behaviors are extracted. The autocorrelation function (ACF) is characterized for different types of mobility patterns. Finally the results of a channel model implementation preserving the ACF properties are presented, showing good match with those obtained from measurements.

**SCIENTIFIC COLLABORATIONS:** Université Catholique de Louvain (UCL), Louvain-la-Neuve, Belgium

## Context and Challenges

In recent years, mobile-to-mobile (M2M) communications have attracted much attention in response to a better quality of data service with low energy consumption. The indoor M2M communication is the exchange of information via a direct link between mobile users located in indoor premises. It can be used for a secure short-range communication or as an underlay to the cellular network. Although the indoor M2M systems are a very promising technology, many research challenges have to be studied before their wide deployment. One of the most important challenges is the characterization of M2M propagation channels, in order to test, design and optimize wireless communication protocols.

## Main Results

An indoor M2M channel measurement campaign was carried out at 2.48 GHz at CEA LETI, in order to model the M2M time varying channel [1]. Monopole antennas were mounted on helmets placed on the heads of four moving subjects. The time variant channel responses were collected by means of a channel sounder based on a 4 port-vector network analyzer (VNA) used in time domain. During measurement, different mobility patterns were considered. The outcome of the measurement results were post-processed in order to decompose the time varying channel transfer function into three major components: the path loss, short-term fading and the long term fading.

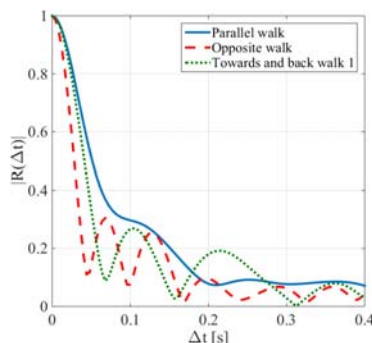


Fig. 1. ACFs of the channel transfer functions

The path characterizes the attenuation of the transmitted signal over distance, while the long-term fading reflects the variation of the average received signal power. The short term fading represents the rapid fluctuation of the received signal due to a small change in position over a short duration.

In order to model the channel time-varying aspects, the second statistical order, i.e. auto-correlation function (ACF) and Doppler spectrum, must be characterized. The ACFs of the channel transfer functions, short- and long-term fading, are presented in [2]. It was shown that the ACF should be analyzed considering the specific pattern mobility (cf. Fig. 1). We have also pointed out that the short-term fading correlation properties have a predominant effect over the ones obtained from the long-term fading. Similarities, in terms of coherence time and shape of ACFs, between the transfer function and its corresponding short-term fading are exhibited. For an average speed of 0.5 m/s, a typical channel coherence time is around 30 ms, while the long-term fading one is above 0.5 s. A channel model implementation preserving the measured time correlation properties is proposed. The method is based on the Cholesky decomposition in order to generate correlated fading processes, whose correlation characteristics are retrieved from the measured ACFs (cf. Fig. 2) [2]-[3].

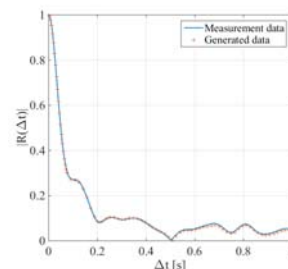


Fig. 2 Short-term fading ACF: measured (blue), model-generated (red)

## Perspectives

Ongoing works includes analyzing the Doppler characteristics and modeling the ACF, and channel stationarity. This model is expected to be extended to different mobile-to-mobile scenarios. model.

## RELATED PUBLICATIONS:

- [1] F. Mani and R. D'Errico, "A Spatially Aware Channel Model for Body-to-Body Communications," in IEEE Transactions on Antennas and Propagation, vol. 64, no. 8, pp. 3611-3618, Aug. 2016.
- [2] G. Makhoul, F. Mani, R. D'Errico and C. Oestges, "Time correlation properties of dynamic mobile to mobile channels in indoor environments," 2016 10th European Conference on Antennas and Propagation (EuCAP), Davos, 2016, pp. 1-5.
- [3] F. Mani, G. Makhoul, C. Oestges and R. D'Errico, "On the Generation of Correlated Short- and Long-Term Fading for Multiple BANs," in IEEE Antennas and Wireless Propagation Letters, vol. 16, no. , pp. 573-576, 2017.



\_\_\_\_\_

\_\_\_\_\_

**SCIENTIFIC COLLABORATIONS:** The authors wish to thank the CNES, French space agency for partially funding this work

Figure 1. 3D view of the low profile dual polarized antenna.

Figure 2. Extracted radiated power for TM and TE modes

SWE tool showed that the proposed antenna could be described as a set of multiple sources. The antenna radiates almost identical and stable  $TE$  and  $TM$  modes. SWE analysis proves that magneto-electric dipole antennas behave as a Huygens source. Further work deal with the representation of ME antennas using the equivalent circuits of  $TE$  and  $TM$  modes.

- [1] K.Belmkaddem, et al. "Electrically small antenna analysis using spherical wave expansion," 15th Intern. Symp. Antenna Techn. and Applied Electromagnetics (ANTEM), Jul. 2012.
- [2] A. Clemente, et al., "Design of a super directive four-element compact antenna array using spherical wave expansion," IEEE Trans. Antennas Propag., vol. 63, no. 11, pp. 4715-4722, Nov. 2015.
- [3] A. S. Kaddour, S. Bories, A. Bellion and C. Delaveaud, "Low profile dual-polarized wideband antenna," 2016 International Symposium on Antennas and Propagation (ISAP), Okinawa, 2016, pp. 86-87.



# LOW PROFILE DUAL-POLARIZED WIDEBAND ANTENNA

## RESEARCH TOPIC:

Wideband Antennas, Magneto-Electric Dipoles, Dual-Polarization, Unidirectional Radiation, 3D Printing

## AUTHORS:

Abdul Sattar Kaddour, Serge Bories, Anthony Bellion (CNES-Toulouse) and Christophe Delaveaud

## ABSTRACT:

A low profile dual-polarized unidirectional wideband antenna based on two crossed magneto-electric dipoles is presented. The antenna consists in folding the radiating element, the height of the radiation element is reduced to  $0.11\lambda_0$  where  $\lambda_0$  is the wavelength at the lowest operation frequency for a standing wave ratio (SWR)  $<2$  corresponding to a reduction factor of 37%. The antenna has been prototyped using 3D printing technology and evaluated in the CEA-LETI anechoic chamber. The measurement results are in excellent agreement with simulations. The measured input impedance matching bandwidth is 54% from 1.8 GHz to 2.9 GHz with  $SWR < 2$ .

**SCIENTIFIC COLLABORATIONS:** The authors wish to thank the CNES, French space agency for partially funding this work.

## Context and Challenges

Recently, many efforts have been made to design wideband antennas satisfying telecommunication requirements such as wide impedance matching, unidirectional and stable radiation pattern with low profile and light weight design. The state of art shows that "Magneto Electric" dipole antennas are promising solutions with excellent radiation characteristics and wide impedance matching. These antennas are based on the concept of complementary antenna or Huygens source [1]. However, these antennas suffer from large height ( $\lambda/4$ ). In order to reduce the antennas height many techniques were proposed as dielectric loading materials or folding structure. Here a method for reducing the height of the dual-polarized wideband magneto-electric dipole antenna uses the geometric folding technique [2].

## Main Results

A 3D view of the proposed antenna is presented Fig. 1a, the antenna consists of four horizontal plates operate together as two crossed electric dipoles. Each horizontal plate is shorted to the ground plane through two vertical folded plates. Each adjacent vertically oriented plates and the ground between them act like a magnetic dipole. These elements form two crossed magneto-electric dipoles generating a dual polarization at  $\pm 45^\circ$ . The antenna is excited by two "I" shaped probes built using three portions of PCB (RT5870). These probes are orthogonally placed in the gaps between the vertical folded plates. To improve the radiation characteristics the antenna can be mounted on a square cavity.

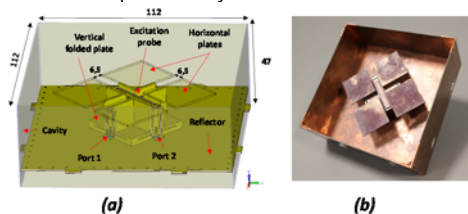


Figure 1. a) 3D view of the proposed dual polarized antenna b) Photograph of the fabricated prototype.

The position and the dimensions of the folded part of the vertical plates are optimized to obtain the widest impedance bandwidth while maintaining an electrically small size of the

radiation element. The antenna radiation elements were prototyped using 3D printing technology (Laser Sintering) in Plastic PC/ABS and electroplated with a  $50\ \mu\text{m}$  copper thickness see Fig 1b. The simulated and measured standing wave ratio (SWR) and realized gain from "Port 1" and "Port 2" are shown in the Fig. 2a. It can be seen that the antenna have a common bandwidth from 1.7 GHz to 3.14 GHz (54% relative bandwidth for  $SWR < 2$ ). Over the operating frequency the measured broadside gain at  $(\theta=0^\circ)$  for "Port 1" and for "Port 2" is  $7.2\ \text{dBi} \pm 1.5\ \text{dB}$ . The difference between "Port 1" and "Port 2" is due to the dissymmetry between the two excitation probes.

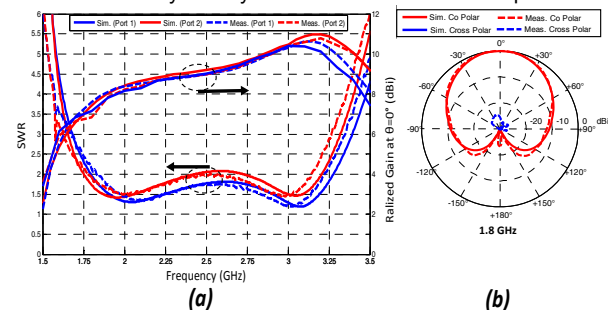


Figure 2. Simulated and measured a) SWRs and gains of the low profile dual polarized antenna, b) Radiation pattern

The simulated and measured normalized realized gain radiation pattern at  $1.8\ \text{GHz}$  at  $\phi=45^\circ$  for "Port 1" is depicted in Fig. 2b. The  $-3\text{dB}$  beam width is  $72^\circ$ . Antenna miniaturization can be achieved by increasing the current path length. The proposed radiation element of the antenna has a dimension of  $0.36\lambda_0 \times 0.36\lambda_0 \times 0.11\lambda_0$  compared to the antenna in literature where the radiation element has a dimension of  $0.33\lambda_0 \times 0.33\lambda_0 \times 0.18\lambda_0$  where  $\lambda_0$  is the wavelength at the lowest operation frequency for  $SWR < 2$  (without taking into account the ground plane dimension).

## Perspectives

Further work deals reconfigurable magneto-electric. This will be able to cover an additional octave while maintaining stable radiation pattern regarding frequency. The trade-off between hardware complexity and radiation performance over large frequency band will be encompassed

## RELATED PUBLICATIONS:

- [1] A. S. Kaddour, S. Bories, A. Clemente, A. Bellion and C. Delaveaud, "Radiation modes investigation of Huygens source type antenna using spherical wave expansion," 2016 International Symposium on Antennas and Propagation (ISAP), Okinawa, 2016, pp. 664-665.
- [2] A. S. Kaddour, S. Bories, A. Bellion and C. Delaveaud, "Low profile dual-polarized wideband antenna," 2016 International Symposium on Antennas and Propagation (ISAP), Okinawa, 2016, pp. 86-87.

# LARGE-SIGNAL ANALYSIS AND CHARACTERIZATION OF A RF SOI-BASED TUNABLE NOTCH ANTENNA FOR LTE IN TV WHITE SPACE FREQUENCY SPECTRUM

## RESEARCH TOPIC:

Tunable notch antenna, TV white space, tunable capacitor, LTE, linearity

## AUTHORS:

S. Bories, E. Ben Abdallah, D. Nicolas, A. Giry, C. Delaveaud

## ABSTRACT:

A compact frequency-agile notch antenna for LTE low-band using TV White Space frequencies is designed and fabricated. The antenna aperture tuning is provided by a SOI CMOS tunable capacitor. The slot size is only 18 mm by 3 mm (which correspond to  $\lambda/33$  by  $\lambda/200$  at 510 MHz) etched on a ground plane size of 103 mm by 50 mm ( $\lambda/6$  by  $\lambda/12$  at 510 MHz), a typical smartphone size. The tunable capacitor RF non linearity analysis is studied and characterized experimentally. The simulated and measured performances are presented and demonstrate antenna tuning features from 500 MHz down to 800 MHz. High linearity is validated with an over the air measured adjacent channel leakage ratio (ACLR) lower than -30 dBc up to 22 dBm input power in the considered frequency range.

## Context and Challenges

The concept of Cognitive Radio (CR) used with TV White Space (TVWS) is one of solutions to solve spectrum resources shortage. They enable the unlicensed users to dynamically locate the unused spectrum segments and to communicate into. In Europe, this spectrum is located from 470 MHz to 790 MHz.

The antennas usually used for this band are physically large to cover the entire frequency band. Reconfigurable antennas, which are much more compact and have a low profile structures, are the most compelling for TVWS where instantaneous bandwidth is only a narrow part of the overall band. Moreover transmit signal linearity is a critical parameter to prevent distortions of modern waveforms.

## Main Results

The presented miniaturized antenna can be tuned on the selected channel (10 MHz instantaneous bandwidth) over the TVWS bands by controlling the Tunable Capacitor (TC) value between 1 and 7 pF, Fig. 1. The TC used in this study is a LETI made SOI CMOS integrated circuit based on a network of binary-weighted switched capacitors [1]. Multiple FET transistors are stacked in series in order to prevent breakdown in OFF-state by providing voltage division of the high-power RF signal once put on the non 50  $\Omega$  part of the antenna.

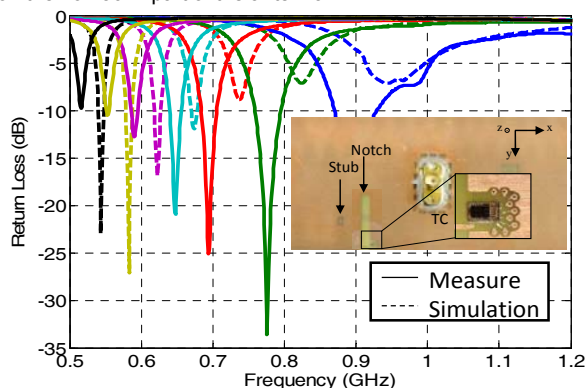


Figure 1 Simulated and measured antenna return loss for seven states (colored lines) of the SOI CMOS tunable capacitor.

The maximum gain is measured in the CEA-Leti anechoic chamber with our test-bench dedicated to electrically small antenna. The gain decreases as expected when the antenna is tuned toward lower frequencies (physical laws): -8 dBi at 770 MHz where the notch length is in  $\lambda/21$  and -15 dBi at 510 MHz (notch in  $\lambda/33$ ). In fact, higher currents run on the miniaturized surface and the TC series resistance (ESR) causes higher insertion losses.

A large signal analysis and characterization of the tunable antenna has been performed by realizing adjacent channel leakage Ratio (ACLR) measurements on the signal radiated through the antenna. A dedicated over the air test-bench has been developed. The tunable antenna respects the 3GPP standard ACLR specification of -30 dBc up to 22 dBm input power at 770 MHz, Fig. 2.

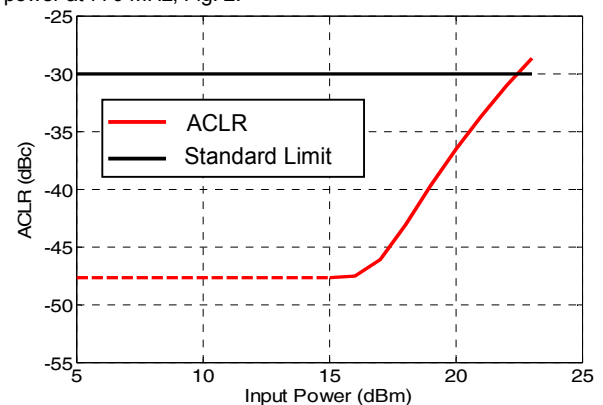


Figure 2 Measured ACLR versus input power with a LTE 16 QAM 10 MHz signal at 770 MHz on the radiated signal

## Perspectives

For frequency reconfigurable antenna, the trade-off between miniaturization, radiation efficiency and linearity will be improved by co-designing the antenna topology and the tunable capacitor IC architecture. In the future, SOI technology Figure of Merit (RonCoff) progress will allow a lower impact of ESR on small antenna radiation efficiency.

## RELATED PUBLICATIONS:

- [1] Nicolas, D.; Giry, A.; Ben Abdallah, E.; Bories, S.; Tant, G.; Parra, T.; Delaveaud, C.; Vincent, P.; Po, F.C.W., "SOI CMOS tunable capacitors for RF antenna aperture tuning," in Electronics, Circuits and Systems (ICECS), 2014 21st IEEE International Conference on , vol., no., pp.383-386, 7-10 Dec. 2014.
- [2] E. Ben Abdallah, S. Bories, D. Nicolas, A. Giry, C. Delaveaud, "Large-Signal Analysis and Characterization of a RF SOI-based Tunable Notch Antenna for LTE in TV White Space Frequency Spectrum" published in Cognitive Radio Oriented Wireless Networks: 11th International Conference, CROWNCOM 2016, Grenoble, France, May 30-June 1, 2016, Proceedings (Vol. 172, p. 536). Springer.







## 4.

## SENSORS AND SYSTEMS, ENERGY AND NANO TECHNOLOGIES

- Nano systems
- Energy Harvesting
- Emotional Sensing
- Battery Energy Management
- Mems Devices
- Shape Capture
- Context Recognition

# SURFACING CURVE NETWORKS WITH NORMAL CONTROL

## RESEARCH TOPIC:

Shape capture, curve networks, smooth surface, normal vector input, shape monitoring

## AUTHORS:

S T. Stanko, S. Hahmann (LJK, INRIA), G.-P. Bonneau (LJK, INRIA), N. Saguin-Sprynski

## ABSTRACT:

Recent surface acquisition technologies based on microsensors produce three-space tangential curve data which can be transformed into a network of space curves with surface normals. We address the problem of surfacing a closed 3D curve network with given surface normals. The surface is computed as the solution of a new variational optimization method based on the mean curvature vectors. The intuition behind this original approach is to guide the standard variational methods by the curvature information extracted from the input normals. The normal input increases shape fidelity and allows to achieve globally smooth and visually pleasing shapes.

**SCIENTIFIC COLLABORATIONS:** Université Grenoble Alpes, CNRS (Laboratoire Jean Kuntzmann), INRIA

## Context and Challenges

Traditionally, digital models of real-life shapes are acquired with 3D scanners, providing point clouds for surface reconstruction algorithms. However, there are situations when 3D scanners fall short, e.g. in hostile environments, for very large or deforming objects.

In the last decade, alternative approaches to shape acquisition using data from microsensors have been developed [3,4]. Small size and low cost of these sensors facilitate their integration in numerous manufacturing areas; the sensors are used to obtain information about the equipped material or equipped structure, such as spatial data or deformation behavior. Ribbon-like devices incorporated into soft materials [3] or instrumented mobile devices moving on the surface of an object [2] provide tangential and positional data along geodesic curves.

In this context, we focus on the resulting problem of surface reconstruction and leave aside all issues related to acquisition and transformation of sensor signals into geometric data.

## Main Results

We propose an algorithm for computing a globally smooth surface given a curve network (positions  $\mathbf{x}$  and normal vectors  $\mathbf{n}$ ) lying on this surface [1, 2]. Efficiency and robustness are achieved by using a linearized objective functional, such that the global optimization amounts to solving a sparse linear system of equations.

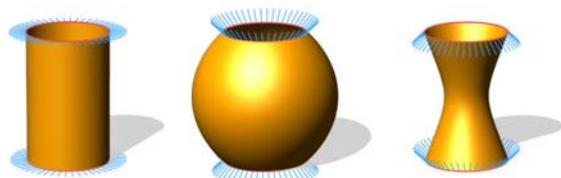


Fig. 1: The input normals guide the reconstruction of the smooth surface. In this example, various sets of normal vectors (blue) along the two parallel circles (red) yield different final shapes.

The algorithm proceeds as follows. Raw data are first interpolated with cubic splines and resampled uniformly with respect to the arc

length parameter; the uniform curves are then triangulated. By solving two bi-harmonic systems  $\Delta^2 \mathbf{X} = 0, \Delta^2 \mathbf{N} = 0$ , we propagate the curve positions  $\mathbf{x}$  and the curve normals  $\mathbf{n}$  to the surface. This initial guess (the positions  $\mathbf{X}$  and the normal field  $\mathbf{N}$ ) allows us to estimate the mean curvature  $H$ . Finally, we solve an optimization problem computing a surface that best matches the mean curvature vectors  $H\mathbf{N}$ . To this end, we minimize the energy

$$\int \|\Delta \mathbf{X} + 2H\mathbf{N}\|^2$$

subject to positional constraints along the input curves (Fig. 1).

The surface is represented as a triangle mesh and the Laplacian operator is discretized via a (sparse) set of linear equations. This means that for a typical input network (Fig. 2), the algorithm runs at interactive rates (order of 100ms for a mesh with 10k vertices and 1k constraints).

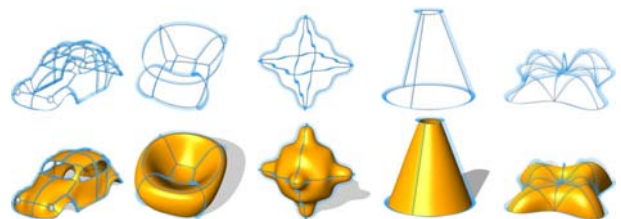


Fig. 2: Networks surfaced using our algorithm.

## Perspectives

The presented framework is intended to serve for curve networks with normal vectors acquired by mobile devices equipped with sensors. For this application we plan the following extensions. The method, currently requiring a closed curve network, could be modified to work with open curve networks. Since our current implementation runs at interactive time rates, we plan to allow the user to scan shapes interactively by incrementally adding curves. We therefore want to investigate how to update the optimization when the input data changes locally.

## RELATED PUBLICATIONS:

- [1] T. Stanko, S. Hahmann, G.-P. Bonneau and N. Saguin-Sprynski. "Smooth interpolation of curve networks with surface normals," in Proc. Eurographics -short papers, pp. 21-24, May 2016.
- [2] T. Stanko, S. Hahmann, G.-P. Bonneau and N. Saguin-Sprynski. "Surfacing curve networks with normal control," in Computers & Graphics, vol. 60, pp. 1-8, Elsevier, Nov. 2016.
- [3] N. Saguin-Sprynski, L. Jouanet, B. Lacolle, L. Biard. "Surfaces Reconstruction via Inertial Sensors for Monitoring," in Proc. EWSHM, July 2014.
- [4] N. Sprynski, D. David, B. Lacolle, L. Biard. "Curve Reconstruction via a Ribbon of Sensors," in Proc. IEEE ICECS, pp. 407-10, 2007.

# HUMAN STRESS EVALUATION USING WEARABLE SENSORS FROM LABORATORY TO REAL LIFE

## RESEARCH TOPIC:

human stress, sensors, wearable, physiological, heart rate, electrodermal activity, stress observer

## AUTHORS:

Christelle Godin, Simon Ollander, Gaël Vila, Etienne Labyt, Audrey Vidal, (Sylvie Charbonnier, Aurélie Campagne)

## ABSTRACT:

We develop wearable systems for real time evaluation of human stress. Our focus is on data fusion algorithms that interpret raw sensor raw to deliver one single indicator of human stress. For developing such algorithms, we used already existing datasets available online and conducted our own experiments. In a first experiment, we considered voluntarily induced stressors of several types (social, physical and cognitive). In a second experiment real life stressors are observed in controlled situation. From all the collected data our aim is to develop algorithms that should be robust to sensor quality, stressor type and inter-individual variability.

**SCIENTIFIC COLLABORATIONS:** LPNC UMR 5105, Gipsa-Lab (Univ. Grenoble Alpes)

## Context and Challenges

Human stress is a common health issue in the modern society. Finding a way to evaluate it during real life activity could be of interest for prevention of psychosocial illness, but also for enhancement of psychological conditions during several activities like driving, travelling, learning, working, negotiating, and gaming. Physiological wearable sensors being less and less obtrusive and expensive, it becomes possible to use them for consumer application. Stress estimation is one of them. For doing that it is necessary to develop robust algorithms that extract a realistic stress indicator from temporal sensor raw data. Several studies have been made but none of them consider together real life and laboratory condition and sensors in order to infer indicators of stress robust to inter-individual, stressor type, sensor type and collecting condition variability. With this objective, we designed, conducted and analyzed a new experimental database of physiological sensor data related to chosen varying conditions.

## Main Results

First of all we used the MIT Database for Stress Recognition in Automobile Drivers, available online to analyze the relevance of sensors and of the features extracted from them [1]. In this database, we extracted features from heart rate, skin conductivity, electro muscular activity and respiration. We studied two classification tasks. The first one was to distinguish rest versus driving, the second one city versus highway driving. The driving was supposed to be more stressful than resting while driving on the highway was supposed less stressful than in the city. We considered mono-user and multi-user classification. Mono-user corresponds to a model adapted for each person. Multi-user supposes a model that takes into account inter-individual variability. Classification rates for the set of most relevant features are given in Table 1. Mean heart rate, mean and maxima of skin conductivity and respiration has been found to be the most relevant features.

	Rest vs driving	Highway vs city
Mono-user	94.6%	78.1%
Multi-user	87.3%	72.1%

Table 1: correct classification rates for rest several configurations using MIT driver database [1].

We designed and conducted our own experimental protocol considering several cases from the laboratory to real life. It includes, well-known protocols like trier social stress test (TSST), Socially Evaluated Cold-Pressor Test (SECPT) and real life experiments during oral presentation and a whole work week. During laboratory experiments we used both stationary sensors (AD Instruments PowerLab) and wearable sensors (Empatica E4 wrist) in order to assess the validity of wearable sensors to estimate stress [2]. Errors in heart rate derived from Empatica E4 sensor in Table 2, show that heart rate is not always available and valid. However, receiver-operating characteristic curve for control versus stress classification show equivalent performances by using mean heart rate and better results using Empatica E4 and integral under skin conductance responses feature.

	rest	control	Stress
Missed pulses	26%	57%	61%
heart rate relative error	2%	4%	6%

Table 2: missed heart pulses (%) and heart rate relative error (%) for rest, control and stress conditions in TSST experiments.

## Perspectives

Next steps are to analyze further the variability induced by stressor types and to calibrate a model for each individual with less calibration phase as possible. Real life experiments during a work week will be also conducted and analyzed.

## RELATED PUBLICATIONS:

- [1] S. Ollander, C. Godin, S. Charbonnier, and A. Campagne, "Feature and Sensor Selection for Detection of Driver Stress," presented at the 3rd International Conference on Physiological Computing Systems, 2017, pp. 115–122.  
 [2] O. Simon, C. Godin, A. Campagne, and S. Charbonnier, "A Comparison of Wearable and Stationary Sensors for Stress Detection" in IEEE International Conference on Systems, Man, and Cybernetics, 2016.



# LARGE BAND ACOUSTIC MEMS DEVICES MADE WITH AMORPHOUS CARBON AS NANOMETRIC SUSPENDED MEMBRANES

## RESEARCH TOPIC:

MEMS, micro-C-MUTS, carbon, membranes, mechanical properties, resonances, large bandwidth acoustic transducer

## AUTHORS:

S. Thibert, M; Delaunay, A Ghis

## ABSTRACT:

Amorphous carbon is used to make self standing 10nm thick membranes. This material provides exceptional mechanical properties. Vibrations of the suspended membranes are observed and measured using an AFM. Significant displacement is demonstrated both at low and high frequencies. These innovative devices are premises for acoustic transducers operating from DC to several tens of Mhz.

## Context and Challenges

Carbon based materials appear with several atomic arrangements such as graphene, diamond, nanotubes etc. We paid attention to an amorphous arrangement of the carbon atoms that bring exceptional mechanical properties to nanometer thick membranes, so flexibility and tenacity can be combined with the pristine chemical inertia of diamond like carbon materials. Relevant use of this material may be foreseen in various applicative fields, namely in sensors and actuators devoted to operate in either harsh (SHM) or fragile (bioMEMS) environments.

As a first demonstration of the feasibility and capabilities of a:C implementation, we focus on devices based on ultrathin suspended membrane. Classical MUTS (Micromachined Ultrasonic Transducer) are based on the plate-like mechanical behavior of a mobile layer which thickness is in the micrometer range. The challenge for a:C ultrathin membranes is to differentiate by a broader operating frequency range, as this would open to tunable ultrasonic transducers.

## Main Results

We use an AFM in two different modes to measure at the nanoscale the deflection of the membranes under electrostatic actuation [1]. Note that the experiments are done at ambient pressure and room temperature.

The current devices are 10nm thick a:C based membranes bridging over 2.3 $\mu$ m wide 200nm deep 50 $\mu$ m long trenches. In one measurement mode, we map the topology of the suspended membrane by scanning an area of a few square micrometer including trench and wedges (Fig 1 left).

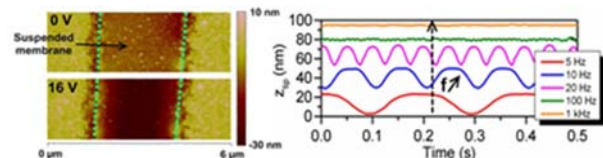


Figure 1 : DC and low frequency excitation Left: AFM scans of the membrane surface at 0V and 16VDC. Right: time deflection of the center of the membrane under 16Vpp low frequency excitation.

In a second measurement mode, the AFM tip is fixed at the center of the trench and the local deflection is registered depending on time. It is quite noticeable that large deflection of up to twice the membrane thickness and 1% of the suspended width are achieved at low frequency and low voltage (Fig1 right).

For frequencies higher than the natural frequency of the AFM cantilever, the measurement obtained is the envelope of the local amplitude of vibration. This allows for spectral analysis of the vibratory behavior beyond 100MHz, together with the mapping of resonance modes. The remarkable flexibility of the membrane allows for high amplitude high order vibration mode (Fig2).

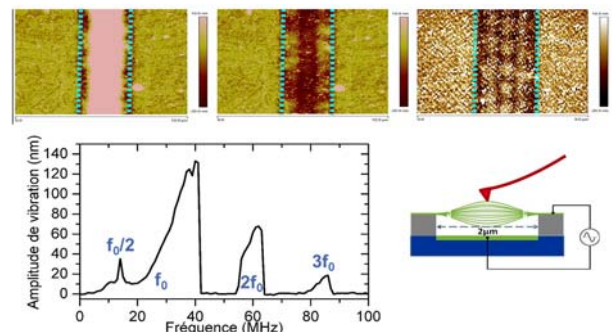


Figure 2: High frequency excitation: Top: scans of the membrane surface at 16 MHz, 50 MHz and 86 MHz from left to right. Bottom: left: frequency spectrum; right: artist view of vibration envelope measurement with an AFM tip under high frequency excitation.

## Perspectives

Next step is the demonstration of large frequency range acoustic pressure generation. The device dimensions may be enlarged to diameters of several tens of micrometers.

The observed membrane-type behavior opens the current panel of resonators, pressure and ultrasonic transducers. The combination of large operating frequency range with micrometric dimensions allows for multiple frequency beam steering capabilities with interest for imaging, Identification or localization, in domains such as medicine, security, or robotics.

## RELATED PUBLICATIONS:

- [1]S. Thibert, A. Ghis, and M. Delaunay, "AFM study of 2D resonators based on Diamond-Like-Carbon," in Nanotechnology (IEEE-NANO), 2016 IEEE 16th International Conference on, 2016, pp. 479–482.BEST PAPER AWARD of IEEE NANO 2016.
- [2]S. Thibert, A. Ghis, and M. Delaunay, "Mechanical Characterization of Ultrathin DLC Suspended Membranes for CMUT Applications," Physics Procedia, vol. 70, pp. 974–977, 2015.
- [3]A. Ghis, N. Sridi, M. Delaunay, and J.-C. P. Gabriel, "Implementation and mechanical characterization of 2nm thin diamond like carbon suspended membranes," Diamond and Related Materials, vol. 57, pp. 53–57, Aug. 2015.

# TRANSPORTATION MODE RECOGNITION BASED ON SMARTPHONE EMBEDDED SENSORS FOR CARBON FOOTPRINT ESTIMATION

## RESEARCH TOPIC:

Context Recognition, Carbon Footprint, Big Data, Machine Learning, Sensors, Smartphone, Mobility observer

## AUTHORS:

Oana Lorintiu and Andrea Vassilev

## ABSTRACT:

Thanks to the increase in processing power and in the number of sensors present in today's mobile devices, context-aware applications have gained a renewed interest. This paper focuses on a particular type of context, the transportation mode used by a person for carbon footprint estimation and it summarizes a method for automatically classifying different transportation modes with a smartphone. The method was evaluated with real data presenting promising results: a performance of around 95% was obtained when classifying 7 different classes with a random forest followed by a Discrete Hidden Markov Model (DHMM) filtering and accelerometer and magnetometer based features, while the addition of the GPS improved the performance up to 97%.

## Context and Challenges

The field of context recognition has gathered a lot of attention in recent years mostly thanks to the widespread of smartphones and wearable devices. With the continuous integration and miniaturization of new sensors, their ever increasing computing power and their virtual omnipresence, these devices have become ideal tools for context recognition. Here, our interest is the recognition of the transportation modes used by a person for the estimation of transportation's environmental impact. We aim at constructing a classification system that can run in real-time on a smartphone equipped with accelerometer, magnetometer and GPS. Though, in order to save battery consumption the use of the GPS is optional. The system should be convenient to use without any location or orientation constraint.

## Main Results

The classification problem addressed is complex because the number of different modes considered is ambitious and high (up to 15), and some modes are very close, for e.g. 'car' and 'bus', 'tram' and 'train'. We chose to tackle a simpler problem, considering 3 different classes relative to motorized transportation mode: 'rail' (regrouping 'tram', 'metro' and 'train'), 'road' (regrouping 'car' and 'bus') and 'plane'; 'boat' data were discarded. This reduction leads to a 7 classes' problem: 'bike', 'plane', 'rail', 'road', 'run', 'still', 'walk'.

We use a supervised learned approach. We first develop an Android Smartphone Application (App) to perform data collection. This App stores the raw data of several sensors: accelerometer (A), magnetometer (M), GPS, etc. and asks the user to annotate his trips.

A crucial step is data cleaning. Indeed, for e.g., each time the subject is moving and stops for a particular reason (for e.g., when walking to look to a map, or to wait for the red-light, or in a train that stops at a station), the user annotation should be changed to 'still'; we therefore develop a preprocessing step that automatically changes the user annotation [2].

Another key aspect is to be invariant to the smartphone's orientation; we therefore develop a procedure [1] that estimate horizontal and vertical linear acceleration, from the raw accelerometer data.

From the preprocess data, 13 features are extracted [1]. They are computed over 5 sec non overlapping windows, and related to

the standard deviation of the norm of the magnetic field and of the linear acceleration components, the proportion of energy in different frequency bands of the vertical acceleration, the spectral centroid and spread of the vertical acceleration and of the magnetic field, and the median of GPS speed.

We build two classifiers, according to GPS availability and test two well-known classifiers: decision tree and random forest (RF).

As transportation mode does not change erratically over time, and as some transitions between transportation modes are forbidden, we implement a post classification step using a Discrete Hidden Markov Model (DHMM).

To develop and evaluate our approach, we collect about 180 hours of transportation data from 22 users and 12 different smartphones. We randomly split 5 times our database and perform Cross Validation using 2/3 of the data for training and 1/3 for testing [2].

Fig. 1 compares the accuracy for different configurations: with or without GPS, with or without DHMM. The best results, about 95-97%, are obtained with DHMM.

Transportation Mode	RF		RF+DHMM	
	AM	AM & GPS	AM	AM & GPS
perfect still	97%	96%	92%	95%
walk	89%	94%	94%	97%
run	95%	95%	97%	98%
bike	73%	88%	90%	96%
road	92%	96%	96%	98%
rail	94%	95%	97%	98%
plane	91%	95%	97%	98%
other	51%	70%	59%	77%
Total	89,8±0,1%	93,5±0,1%	93,7±0,1%	96,3±0,3%
Total w/ other	91,7±0,1%	94,6±0,1%	95,4±0,2%	97,3±0,3%

Fig. 1 Comparison of RF and RF+DHMM recall results by class

## Perspectives

There are several perspectives to further improve this mobility observer, such as like tackling the problem of fine grained classification, using opportunistically other sensors (barometer, audio), and reducing the device consumption. The proposed tool is dedicated to low power applications for energetic efficiency, but it can be also applied for modes-centric services, inter-modality, social and urban sensing uses.

## RELATED PUBLICATIONS:

[1] F. Masculo and A. Vassilev, "Reconnaissance de modes de transport avec capteurs embarqués," presented at the GRETSI, 2015.

[2] O. Lorintiu and A. Vassilev, "Transportation mode recognition based on smartphone embedded sensors for carbon footprint estimation," in 2016 IEEE 19th International Conference on Intelligent Transportation Systems (ITSC), 2016, pp. 1976–1981.

# ON-CHIP INTEGRATION OF INDIVIDUALLY CONTACTED PIEZOELECTRIC NANOWIRES FOR FORCE SENSOR

## RESEARCH TOPIC:

Nanosystem, ZnO nanowire, force sensor, microfabrication, microelectronics

## AUTHORS:

E. Saoutieff, E. Leon Perez, M. Allain, Y-R. Nowicki-Bringuier, A. Viana, E. Pauliac-Vaujour

## ABSTRACT:

A very high-resolution fingerprint sensors based on a matrix of interconnected piezoelectric ZnO nanowires (NWs), reaching level 3 of fingerprint details resolution is developed. Using the local deformation of an array of individually contacted piezoelectric NWs, we aim to reconstruct an image of the distribution of the charges collected from the ZnO NWs into adjacent bottom or top-bottom contacts. Heterogeneous integration of nano-piezotronic objects onto microelectronics chips, considering process compatibility at the wafer scale, contacting, and encapsulation steps, are among the CEA-Leti fabrication challenges.

**SCIENTIFIC COLLABORATIONS:** MTA EK MFA, IMEP-LAHC, Fraunhofer IAF, ULEI, Specific Polymers, OT-Morpho, KTU, Tyndall

## Context and Challenges

Increase the reliability and develop robust fingerprint sensors beyond today's 500dpi international standards is one motivation for designing a new technology of fingerprint sensor. The work carried out over the course of a 3-year doctorate, in parallel with the PiezoMAT European project, aims at developing and demonstrating a concept based on a matrix of inter-connected piezoelectric NWs grown directly onto a microelectronics chip. The interest of vertically-integrated piezoelectric NWs for high sensitivity sensor applications lies in high densities of integration, which occur through the size diminishing of individual pixels. The high spatial resolutions that it is possible to obtain - 3000 dpi for our proof-of-concept chip - should enable the detection of level 3 minutiae of fingerprints (pores, ridge-edge recognition).

## Main Results

2 types of sensors were developed, one in bending configuration and the other in compression mode. For each of them, a NW or a bundle of NWs, respectively, form a pixel. The feasibility of both the bending (Fig. 1) and the compression (Fig. 2) architectures was demonstrated, and piezoelectric signals were measured for the bending case. Signal measurements on compressive mode devices are still on-going

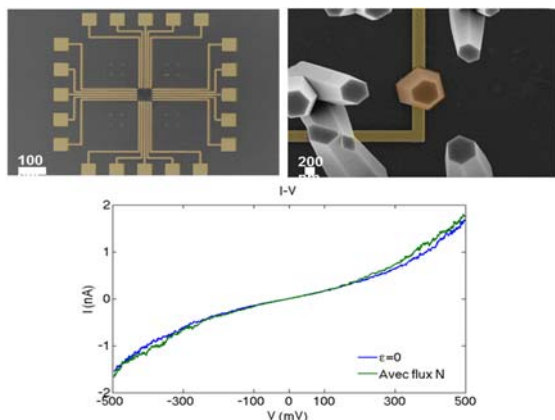


Fig. 1. Légende ((top left) Top-view SEM image of one device with an  $80 \times 80 \mu\text{m}^2$  NW growth area in the centre, surrounded by metal lines of increasing widths (200 nm to  $5 \mu\text{m}$ ) and 20 metallic pads of  $50 \mu\text{m} \times 50 \mu\text{m}$  for signal collection; (top right) Zoomed-in SEM image of one of the  $10 \times 10$  pixels within the growth area, where one single vertical NW is interconnected by the two metallic lines. (bottom) I-V characterizations of a pixel in resting state and under  $\text{N}_2$  blowing.

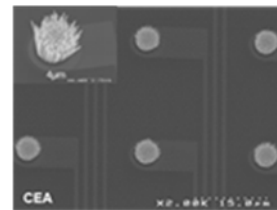


Fig. 2. Top-view SEM image of interconnected ZnO NW bundles grown directly and selectively on-chip within individually interconnected pixels of a  $10 \times 10$  array of pitch  $20 \mu\text{m}$ . The chip was fully processed in a 200mm clean-room prior to NW growth

ZnO nanowires were grown directly and selectively on-chip following clean-room processing (Fig. 1 and 2). Preliminary measurements in bending configuration (Fig. 1), confirmed the response of one pixel when applying an intermittent  $\text{N}_2$  flow. Several technological barriers were raised such as, in particular, the clean-room process compatibility at the wafer scale (200mm), the alignment of metallic contacts with 200 nm wide growth sites, and the successful selective growth of ZnO NWs on chip».

## Perspectives

A proof-of-concept chip with top-bottom contact and a matrix of  $10 \times 25$  interconnected bundles of nanowires (1000 dpi resolution) is under development with project partners, including fingerprint-compatible encapsulation and top contact electrode deposition steps. A specific PCB design was also implemented for characterisation tests yet to come.

## RELATED PUBLICATIONS:

- [1] E. Leon Perez et al., "On-chip integration of individually contacted piezoelectric nanowires for fingerprint sensing applications", NGPT, Rome (2016)
- [2] E. Saoutieff et al., "Interconnected array of piezoelectric nanowires integrated onto a microelectronics chip: the PIEZOMAT project", NGPT, Rome (2016)
- [3] E. Saoutieff et al., "Integration of piezoelectric nanowires matrix onto a microelectronics chip", Procedia Engineering 168 (2016) pp1638 – 1641
- [4] E. Saoutieff, M. Allain, Y-R. Nowicki-Bringuier, A. Viana, E. Pauliac-Vaujour, "PiezoMAT project", EuroSensors workshop, Budapest (2016)
- [5] A. Bouvet-Marchand et al., "UV-crosslinked polymeric materials for encapsulation of ZnO nanowires in piezoelectric fingerprint sensors", Procedia Engineering 168 (2016) pp1135 – 1139.



# BATTERY AGING-AWARE ENERGY MANAGEMENT OF GREEN SMALL CELLS POWERED BY THE SMART GRID

## RESEARCH TOPIC:

Green communication, battery management system, renewable energy harvesting, smart grid, system optimization,

## AUTHORS:

M. Mendil, A. De Domenico, V. Heiries, R. Caire (UGA, G2Elab), and N. Hadjsaid (UGA, G2Elab)

## ABSTRACT:

Energy harvesting mobile networks are increasingly deployed due to their advantages such as self-sustainable capability and reduced operating expenditure. However, the energy storage is subject to irreversible aging, requiring management policies that consider both the energy cost and the battery life cycle. In this study, we investigate energy management strategies for a small cell powered by renewable energy, a battery, and the smart grid, to simultaneously minimize electricity expenditures and enhance the battery life span of the storage device.

**SCIENTIFIC COLLABORATIONS:** Grenoble Electrical Engineering Lab, Univ. Grenoble Alpes

## Context and Challenges

The Information and Communications Technologies industry is seen as an increasingly important contributor of the worldwide energy consumption. The increasing growth of data traffic has led to a massive deployment of Small cell Base Stations (SBSs). As a consequence, the energy demand of cellular networks is growing. Based on this, managing the energy usage is primordial for Mobile Network Operators (MNOs) to ensure the economic and environmental sustainability of the future heterogeneous cellular Networks. Different from existing works, we propose an energy flow management framework for on-grid energy-harvesting SBSs, which focuses on the battery control. The decision making by the supervisor is done at the battery level and uses realistic models to capture the SBS power consumption, the renewable energy (RE) production, and the non-linear battery behavior and aging mechanisms.

## Main Results

The proposed architecture illustrated in Fig. 1, in which the SBS is jointly powered by the Smart Grid (SG) and REs. Moreover, a battery is used as a local storage device. The system is interconnected to the SG in a two-way energy flow such that energy can be sold and bought. First, we have investigated the optimal battery and solar panel sizing. Then, we have designed an Energy Supervision System (ESS) in charge of scheduling the energy flow to guarantee the mobile service, reduce the operational expenditure, and preserve the battery life span. In parallel to the energy flow management, the ESS collects information about the power consumption, production, and price.

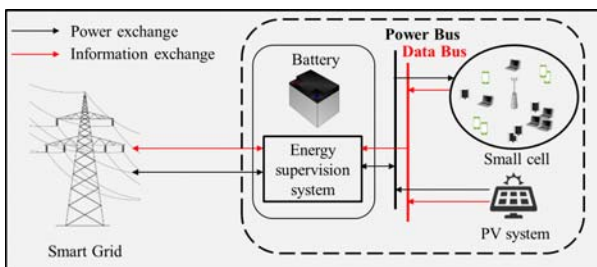


Figure 1 . System architecture of the small cell energy supervision

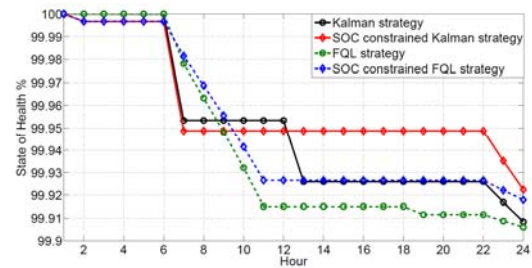


Figure 2 Average battery calendar aging of the ideal strategy under the constraint sets C1, C2, and C3.

The ESS developed is based on reinforcement learning algorithm (Fuzzy Q-Learning) to determine the optimal energy management strategy without prior deep knowledge of the system components. We investigated the energy cost savings achieved by our FQL algorithm scheme compared to three baseline solutions: 1) the reference strategy that systematically buys energy from the SG (battery and solar panel are not used). 2) The naive strategy that seeks to reduce the immediate energy cost with the PV production (the battery is never used). 3) The ideal strategy with PV and battery, that upper-bounds the performances of the system by using a perfect knowledge of the stochastic variables (SBS load, energy production, and energy price).

Our results show that the solution achieves very large cost reduction compared to basic strategies while respecting the battery constraints. Additionally, the battery aging constraints taken into account in the ESS allows to considerably reduce the calendar and cycle degradation (51% per year) (see Fig. 2). Furthermore, the respect of these constraints resulted in only ten point's decrease of the OPEX cost saving, which is negligible considering current battery costs.

## Perspectives

As future work, we aim to extend this study by investigating the energy management of an entire mobile network in a collaborative fashion. In such network, the BSs of different tiers are expected to share energy and balance their traffic loads to optimize the overall network OPEX while fulfilling their individual operational constraints..

## RELATED PUBLICATIONS:

- [1] Mouhcine Mendil, Antonio De Domenico, Vincent Heiries, Raphael Caire and Nouredine Hadjsaid, "Battery Aging-Aware Energy Management of Green Small Cells Powered by the Smart Grid", EURASIP Journal on Wireless Communications and Networking, 2017.
- [2] Mouhcine Mendil, Antonio De Domenico, Vincent Heiries, Raphael Caire and Nouredine Hadjsaid, "Fuzzy Q-Learning based energy management of small cells powered by the smart grid", 2016 IEEE 27th Annual International Symposium on Personal, Indoor, and Mobile Radio Communications (PIMRC).
- [3] Mouhcine Mendil, Antonio De Domenico, Vincent Heiries, Raphael Caire and Nouredine Hadjsaid, " Battery-Aware Optimization of Green Small Cells: Sizing and Energy Management", IEEE Transactions on Green Communications and Networking, submitted.

# SHOCK ENERGY HARVESTERS FOR GUN-FIRED MUNITION

## RESEARCH TOPIC:

Energy Harvesting, Shock, Electromagnetic transducer, High acceleration, Munition

## AUTHORS:

J. Willemin, S. Boisseau

## ABSTRACT:

We report on a shock energy harvester dedicated to high-G gun-fired munitions and based on a high-stiffness mass-spring architecture. During the firing phase, the 20000G acceleration projects the mass, which stores mechanical energy in the spring at the same time. After the shock, the mass-spring system starts to oscillate and the mechanical energy is converted thanks to an electromagnetic transducer into electricity. The harvester is modeled and designed to support the acceleration and to generate 200mJ in 150ms. The prototype has generated 210mJ in a test bench and 140mJ during a gun-fired munition test. The device sizes 11cm<sup>3</sup> and weighs 370g, corresponding to a mean energy density of 7.9mW/cm<sup>3</sup> (0.9W).

## Context and Challenges

Shocks are a rich source of mechanical energy which can be harvested to supply several kinds of applications (transport, sport, public works...). Nevertheless, three different kinds of challenges must be faced when using such harvesters. First, they must be mechanically reliable, especially if the application deals with high acceleration shocks. Then, as shocks happen very quickly, a high power and short duration input energy must be efficiently converted into electrical energy. Finally, power densities have to be maximized (regarding both size and weight) in order to develop application-compatible devices.

## Main Results

Our system targets to generate 200mJ in 150ms from a 10ms shock peaking at 22700G (Fig 1). Due to cost issues, this shock energy harvester is based on an electromagnetic transducer coupled to a mass-spring system. This architecture enables to store mechanical energy during the shock and to release it progressively as mechanical oscillations. Thus, it decreases the size of the electric transducer and reduces the power issues.

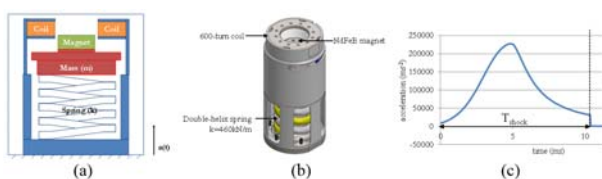


Figure 1. (a) Simplified and (b) CAD views of the energy harvester; (c) high-G input shock

The key parameter is the resonant frequency of the mass-spring system which has been determined by simulations at 299Hz. The mass and the stiffness have been optimized at  $m=130g$  and  $k=460kN/m$  and the theoretical quality factor was estimated at 50. The transducer is made of a 600-turn coil and a NdFeB magnet.

A double helix spring (Fig 2) and guiding parts have been used in order to ensure a good stability and to avoid buckling issues as well as energy transfers between resonant modes during oscillations. The spring is made of round steel wires and has been optimized (diameters, nb of coils) to keep the stress under 1GPa. Then we have manufactured the spring and the complete

device (which sizes 11cm<sup>3</sup> for 370g). Next, we have used a test-bench (Fig 2) with a tensile specimen in order to move the mass at the start-up position (8mm) and suddenly release the spring-mass system, simulating the system right after the shock.

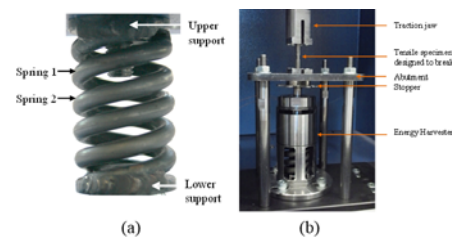


Figure 2. (a) Double helix spring (b) system test-bench

With the test-bench, the prototype has generated 210mJ in 150ms with 289Hz oscillations. Finally, it has been tested in a gun-fired munition, the results are shown in Fig 3 with 140mJ output energy (4,83W peak output power and 41.3mW/cm<sup>3</sup> power density).

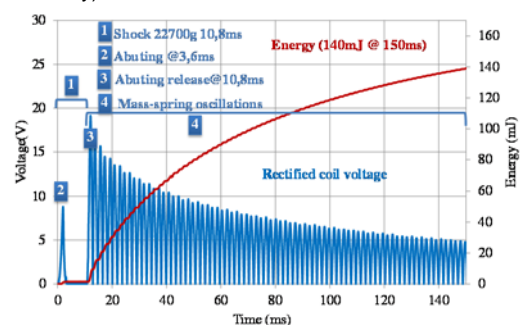


Figure 3. Test results in a gun-fired munition

## Perspectives

Future research will be focused on the reduction of the stress (in order to increase the quality factor) and on the size reduction. Furthermore, dedicated optimizations will be carried out for other applications with different specifications regarding size, weight, cost and input acceleration.

## RELATED PUBLICATIONS:

[1] J Willemin, S Boisseau, L Olmos, M Gallardo, G Despesse, T Robert, " 20000G shock energy harvesters for gun-fired munition ", Proc. PowerMEMS 2016.









# 5.

## SECURITY

- On-Chip Technique
- Deployment of large-scale security protocols
- Lightweight cryptography
- Homomorphic Encryption
- Side-channel-attacks
- Automated Security Testing

# SIDE-CHANNEL-ATTACKS: KERNEL DISCRIMINANT ANALYSIS TO COUNTERACT MASKING COUNTERMEASURE

## RESEARCH TOPIC:

Higher-order SCA, dimensionality reduction

## AUTHORS:

E. Cagli, C. Dumas, E. Prouff (Safran Identity & Security)

## ABSTRACT:

When a  $(d-1)^{\text{th}}$  order masking countermeasure is implemented to thwart Side Channel Attacks, the fundamental preliminary attack phase consisting in selecting Points of Interest which is a very hard task: almost all existing methods have a combinatorial complexity explosion, since they require an exhaustive search among all possible  $d$ -tuples of points. The exploitation of the Kernel Discriminant Analysis leads to an efficient method for informative feature extraction in presence of masking countermeasure, whose complexity does not grow with  $d$ .

**SCIENTIFIC COLLABORATIONS:** Safran Identity & Security

## Context and Challenges

In cryptography, Side Channel Attacks (SCAs) are attacks that target physical implementations of cryptographic algorithms. Information is gained about intermediate sensitive variables of the algorithm by observing the variation of physical properties of the hardware executing the latter algorithm, e.g. power consumption or electromagnetic radiation. In practice, running a SCA requires computing on data of huge dimensions. In SCA context, for attacks against unprotected implementations, a vast literature is dedicated to the problem of dimensionality reduction. The Linear Discriminant Analysis (LDA) technique stands out [2]: it provides an optimal linear combination of the signals time samples, which concentrates the sensitive information over few points. The literature is more scattered in the context of implementations protected with masking countermeasure: extracting information in such a case requires the exploitation of non-linear combinations, and the choice for such combinations is very complex.

## Main Results

In [1], the Kernel Discriminant Analysis technique is proposed. It consists in completing the LDA with a so-called kernel trick. The latter trick allows to implicitly map the data into a larger feature space by means of a non-linear function.

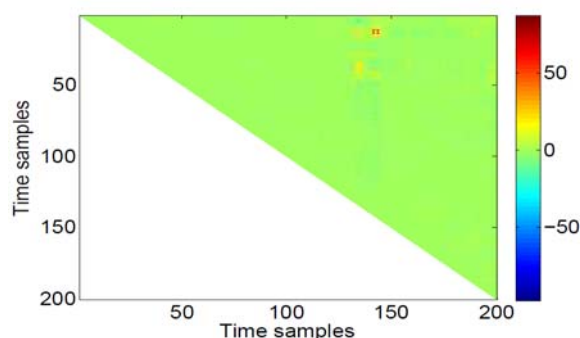


Fig. 1: The 20,100 KDA implicit linear combination coefficients used for the second order attack. High coefficients are assigned to the informative time samples.

In such a larger space, sensitive features are present and the LDA optimally combines them linearly. Since the non-linear mapping is not explicitly performed, this technique is not affected by the drawbacks due to the combinatorial enlargement of the feature space. The KDA requires the choice of a so-called kernel function. The authors of [1] proposed the use of the polynomial function  $K(x,y) = \langle x,y \rangle^d$ . This function is associated to a feature space of size  $\binom{D+d-1}{d}$ ,  $D$  being the original size of data.

Experiments shown in the paper are run over  $D = 200$ -sized data, off orders  $d=2, 3$  and  $4$ . The size of the feature space in these cases equals respectively to 20,100, 1,353,400 and 68,685,050.

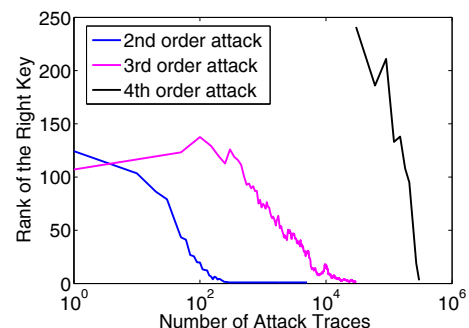


Fig. 2 : Number of side-channel traces vs rank of the right secret key. The goal of a SCA is to rank the correct key first. A  $d$ th order attack is an attack performed against a  $(d-1)$ th order masking countermeasure.

For the three experiments the complexity of the KDA research for linear combining coefficients in the feature space is the same, not being influenced by the size of such a space. Such coefficients are only implicitly computed (in Fig. 1 we explicitly computed them to see the leaking time samples). The SCAs performed over data compressed using the KDA technique are efficient (as shown in Fig. 2), proving the efficiency of such a dimensionality reduction method.

## Perspectives

This work is part of a fruitful transfer of techniques from machine learning to side-channel context, which is to be pursued.

## RELATED PUBLICATIONS:

- [1] E. Cagli, C. Dumas, and E. Prouff. "Kernel Discriminant Analysis for Information Extraction in the Presence of Masking." International Conference on Smart Card Research and Advanced Applications. Springer, Cham, 2016.
- [2] E. Cagli, C. Dumas, and E. Prouff. "Enhancing dimensionality reduction methods for side-channel attacks." International Conference on Smart Card Research and Advanced Applications. Springer International Publishing, 2015.



# AUTOMATED AND REMOTE SECURITY FUZZ TESTING TOOL FOR IOT DEVICES

## RESEARCH TOPIC:

Fuzzing, automated security testing, physical interfaces, network protocols, detection of vulnerabilities, fault injection, embedded

## AUTHORS:

J.C. Fonbonne

## ABSTRACT:

In the IoT economic environment security testing of hardware devices needs to be fast, automated and low cost. This study describes an IoT oriented fuzzing testing tool that provides seamless physical interactions with the device under test and its hardware interfaces. Taking into account the heterogeneity of IoT devices in terms of physical interface, communication protocol, applications... a security fuzz testing tool has been developed with enough modularity to ensure that the targets can easily be connected through any physical channels. Feedback-driven fuzzing on connected devices has also been demonstrated, paving the way for further exploitation of the physical behavior of the devices during the testing procedures.

## Context and Challenges

Fuzzing is a dynamic analysis technique for which a large amount of deliberately malformed or unexpected packets are sent onto the interfaces of a device. The goal is to detect failures to correctly manage such packets, which can result in security vulnerabilities. It is an interesting candidate for security testing in the IoT environment because it corresponds to a "blackbox testing" scheme enabling genericity and speed of testing. The following requirements are necessary to adapt the fuzzing techniques to IoT devices: physical adaptability and modularity (in the sense of being agnostic of the target specifics, such as nature and number of physical links communication protocols and channels, operating system, usage domain...), automated misuse and abuse scenario generation, automated target monitoring and feedback, automated indicator of completeness.

## Main Results

A new fuzzing tool [1] was developed based on the architecture described in Fig.1.

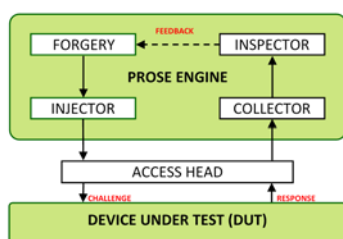


Fig.1 Fuzzing tool general architecture.

The forgery module generates challenge packets according to a pattern database and a scenario manifest. Patterns are generated using a Protocol Description Language which defines the high-level message structure, with its vocabulary and grammar. The malformed fields are computed automatically depending on a collection of data "mutators" described in the scenario manifest. The access head is responsible for low layer communication management, ensuring the physical modularity. The inspector module detects faulty or suspicious responses based on assertions provided in the inspection manifest to detect

inappropriate responses or behavior. Feedback-driven fuzzing (FDF) is a feature that allows the mutation operated by the forgery module to depend on the previous responses and on the behavior of the target, as provided by the inspector.

The fuzzing tool has been tested with three different devices: an IoT device running a 6LoWPAN communication stack, a multiple interface Industrial Control System (ICS) device and a HCI secure element (SE) for a smartwatch (H2O project). The fuzzing tool successfully found vulnerabilities such as buffer overflow, endless loop and stack overflow.

The physical timing-based FDF has been tested successfully on the SE test case. The measurement of the TOE's response delays, combined with supervised data clustering, was used to drive better error mutations. Comparing the response time distribution with and without feedback (Fig.2.) shows that the fuzzer can explore all the paths of the control flow graph equally and can test more potential vulnerabilities. Moreover the convergence of the clustering is an indicator of completeness of the fuzzing session in terms of embedded code coverage.

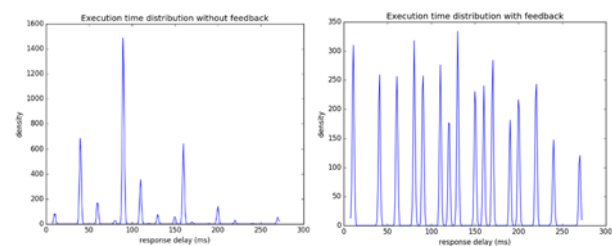


Fig.2 Response time distribution with and without FDF.

## Perspectives

On-going work focuses on supporting more protocols, including composite stateful protocols and adding new FDF features such as power consumption. Application of advanced machine learning techniques and optimized mutation process is also envisioned. Industrial partners have already expressed interest in these technologies. Another objective is their eventual adoption by security evaluation schemes or certification methodologies.

## RELATED PUBLICATIONS:

[1] J.C Fonbonne, "Automated and Remote Security Fuzz testing Tool for IoT Devices", C&ESAR 2016.

# AN ON-CHIP TECHNIQUE TO DETECT HARDWARE TROJANS AND ASSIST COUNTERFEIT IDENTIFICATION

## RESEARCH TOPIC:

FPGA, Hardware Trojan, counterfeit, process variations

## AUTHORS:

Maxime Lecomte, Jacques J.A. Fournier and Philippe Maurine

## ABSTRACT:

This work introduces an embedded solution for the detection of Hardware Trojans (HTs) and counterfeits. The proposed method, which considers that HTs are necessarily inserted on production lots and not on a single device, is based on the fingerprinting of the static distribution of the supply voltage ( $V_{dd}$ ) over the whole surface of an IC. The measurement of this fingerprint is done through an array of sensors sensitive to the local  $V_{dd}$  value and fingerprint extraction is based on a novel variation model of CMOS logic performance. This model takes into account not only process variations but also the impact of the design (layout, supply routing...). The efficiency of the whole detection methodology is experimentally demonstrated on a set of 24 FPGA boards.

**SCIENTIFIC COLLABORATIONS:** CEA Tech DPACA & LIRMM.

## Context and Challenges

Because of the globalization of their manufacturing process, integrated circuits (ICs) have become increasingly vulnerable to malicious alterations. An adversary can modify an IC from the specification step up to the packaging stage. This threat raises concerns as ICs are used in a wide variety of critical applications. This kind of malicious alteration, called a hardware trojan (HT) insertion, can have different effects, which can be parametric or functional.

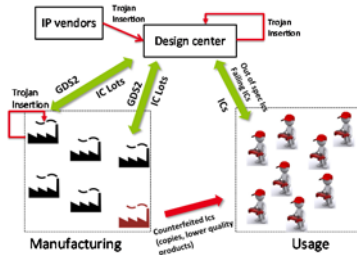


Fig 1: Main threats to IC integrity.

## Main Results

We devised a method, using a matrix of embedded ring oscillators (ROs), for detecting any malicious modification of the IC's structure in way that process variations and the influence of environmental conditions are taken into account. The detection methodology is based on the assumption that an entire lot is corrupted and it is the statistical analysis of this corrupted lot, compared to a reference unaffected lot, that allows to determine the integrity of the first lot. Suppose that we have a lot of  $m_{lot}$  chips where each chip bears  $q$  ROs. If  $T$  is the period for each RO such that

$$T = T_0 + \Delta T_{intra} + \Delta T_{inter} + \Delta T_{design}$$

with  $\Delta T_{inter} \approx N(0, \sigma_{inter}^2)$  and  $\Delta T_{intra} \approx N(0, \sigma_{intra}^2)$ . The fingerprint corresponding to each lot is given by

$$fingerprint = [\Delta T_{design}^1, \dots, \Delta T_{design}^q, \sigma_T^1, \dots, \sigma_T^q]$$

where

$$\Delta T_{design}^i = \frac{1}{m_{lot}} \sum_{j=1}^{m_{lot}} T_i^j - T_0; \sigma_T^i = \sqrt{\frac{1}{m_{lot}} \sum_{j=1}^{m_{lot}} (T_i^j - T_0 - \Delta T_{design}^i)^2}$$

$$\text{for } T_0 = \frac{1}{m_{lot} \times q} \sum_{j=1}^{m_{lot}} \sum_{i=1}^q T_i^j$$

We implemented our proof-of-concept on a Xilinx Spartan-3E 1600E FPGA where a matrix of 60 ROs are integrated. To illustrate counterfeit detection, we implemented two circuits where AES blocks were place-and-routed differently. To illustrate Trojan detection, we modelled a HT as a 64-bit LFSR.



Fig 2: A reference circuit, a 'counterfeit' and a corrupted one.

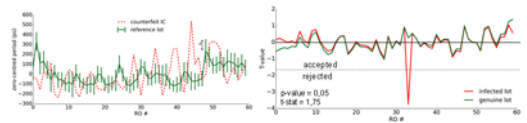


Fig 3: Curves showing counterfeit and HT detections.

More detailed discussions on the sensitivity of our methodology is given in [1].

## Perspectives

Now that the scheme has been shown to work quite efficiently on FPGAs, our next goal is to transpose the concept to the ASIC world.

## RELATED PUBLICATIONS:

[1] Maxime Lecomte, Jacques J.A. Fournier and Philippe Maurine, "An On-Chip Technique to Detect Hardware Trojans and Assist Counterfeit Identification", IEEE Transactions on Very Large Scale Integration (VLSI) Systems, vol.PP, no.99, pp.1-14, 2016.

# ON THE IMPORTANCE OF CONSIDERING PHYSICAL ATTACKS WHEN IMPLEMENTING LIGHTWEIGHT CRYPTOGRAPHY

## RESEARCH TOPIC:

Side channel attacks, fault attacks, light weight cryptography, IoT

## AUTHORS:

Alexandre Adomnicaï, Benjamin Lac, Anne Canteaut, Laurent Masson, Renaud Sirdey, Assia Tria and Jacques J.A. Fournier

## ABSTRACT:

Pervasive IoT devices are usually deployed in hostile environments where they are physically accessible to potential hackers. As lightweight cryptography is designed for such devices, it has to be particularly resistant to physical attacks. We illustrate how active and passive physical attacks against the lightweight block cipher PRIDE can be carried. A side channel attack and a fault attack have been successfully implemented on the same software implementation of the algorithm. In both cases, we were able to recover the entire encryption key. We also discuss about possible countermeasures.

**SCIENTIFIC COLLABORATIONS:** CEA List, CEA Tech DPACA, Inria & Trusted Objects.

## Context and Challenges

As an exponential number of connected devices are being deployed for the Internet of Things (IoT), security concerns have become an issue of utmost importance [1]. To address some of those security requirements in the IoT while respecting the constraints of high performance and low resources (memory, power...), a dedicated field of cryptography, called Light Weight Cryptography (LWC), is currently being developed. In this paper we highlight the importance of securing the implementations of LWC against side channel and fault attacks by showing how such attacks have been carried against an exemplar LWC algorithm called PRIDE.

## Main Results

The PRIDE algorithm is touted as one of the fastest light weight cryptography algorithms when software implementations are considered. It is an iterative block cipher of 20 rounds which uses a 128-bit key to encrypt a 64-bit input. We implemented PRIDE on a COTS 32-bit processor classically used in IoT devices.

We first devised how such an implementation could be attacked by analyzing the Electromagnetic (EM) signals emitted by the processor during a PRIDE calculation. By performing a Correlation Electromagnetic Analysis (CEMA), we were able to retrieve the 128 bits of the encryption key using 1000 measured EM curves [2]. With this we showed how a passive side channel attack can be mounted against a LWC algorithm like PRIDE.

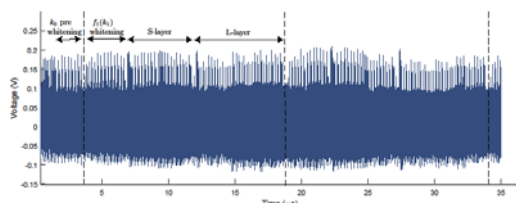


Fig 1: EM emanations of the first two rounds of PRIDE

To illustrate the feasibility of an active fault attack against PRIDE, we first proposed a Differential Fault Attack (DFA) scheme that mathematically allows to retrieve the algorithm's secret key. We

then implemented our DFA against the aforementioned PRIDE implementation using EM pulses as fault injection means. Using the EM pulses, we were able to corrupt the one before last round of the PRIDE algorithm and by applying our DFA scheme on the resulting faulty cipher text and the expected correct cipher text, we were able to recover the 128 bits of the encryption key [2].

A direct consequence of our results is that countermeasures against such attacks have to be integrated into the implementation of algorithms like PRIDE when deployed in IoT devices. We show in [2] how using intermediate random 'masks' can reduce the vulnerability of PRIDE against side channel attacks. Furthermore we also discuss about the use of majority vote using duplication as a means to detect fault injections.

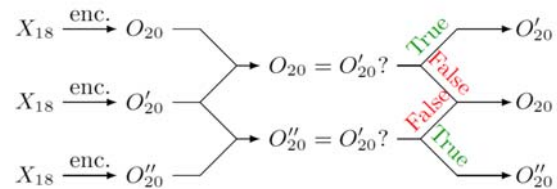


Fig 2: Majority voting using duplication

## Perspectives

The countermeasures that have been proposed so far have a direct negative impact on the performance and the memory footprint of the implemented LWC algorithm. The next step is to investigate how those LWC algorithms can mathematically be redesigned to be intrinsically resistant to physical attacks while keeping them fast and low resource/power consuming.

## RELATED PUBLICATIONS:

- [1] J. Fournier & A. Tria, "Securing the IoT Jungle", C&ESAR 2016 Conference, Rennes, France, November 2016.
- [2] Alexandre Adomnicaï, Benjamin Lac, Anne Canteaut, Laurent Masson, Renaud Sirdey, Assia Tria and Jacques J.A. Fournier, "On the importance of considering physical attacks when implementing lightweight cryptography", NIST Workshop on Light Weight Cryptography, October 2016.



# PROCESSOR HANDLING CONFIDENTIAL DATA

## RESEARCH TOPIC:

Secure processor, homomorphic encryption, confidential data processing

## AUTHORS:

Olivier Savry, Thomas Hiscock and Louis Goubin

## ABSTRACT:

Side-channel attacks allow the successful extraction of sensitive data like cryptographic keys from a number of devices, even presumably secure ones. The general approach to secure such implementation is to modify the circuit, to reduce data-dependent physical emanation using masking and balanced logic, which remain algorithm-specific. In this work, we present a secure processor architecture capable of doing computation on encrypted data thus removing by construction any risk of data leakage. It leverages the modern homomorphic encryption schemes with a bootstrapping method which highly contains the required computational resources.

**SCIENTIFIC COLLABORATIONS:** Université de Versailles St Quentin en Yvelines (UVSQ)

## Context and Challenges

Many applications require to guarantee the confidentiality of handled data both in the binaries, to avoid reverse engineering, and during execution where side-channel attacks can leak secrets like cryptographic keys. Solutions have been proposed based on masking with random numbers but they imply a new treatment for each program. Our study takes advantage of recent advances of homomorphic encryption (HE) following Gentry's thesis in 2009. This scheme enables to run computations on ciphered data without having to decipher them. It calls for lattice properties and in particular the LWE (Learning with Error) NP-problem. A drawback of HE is that the accumulation of operations on ciphered data will increase this error in such a way that no more decryption is possible. With an efficient bootstrapping method called FHE for Fully Homomorphic Encryption which deciphers in the homomorphic field, it is possible to evaluate a program of any size but at the cost of a considerable expansion of the ciphered data and keys sizes. We have found a way to limit those non-practicable constraints for embedded devices while maintaining any depth of the program.

## Main Results

To circumvent the heaviness of bootstrapping, we orientated our work towards a "somewhat HE" based on a light version of the Braberski, Gentry and Vaikutanatan (BGV) scheme. It is capable of evaluating only one arithmetic multiplication or addition which requires to add a patented homomorphic masking method to address deeper program. On Fig. 1, the application of the "recrypt" block can be seen. It will apply a masking by an XOR with a noise generated by an embedded RNG. This masked data is then deciphered (as a consequence it will not appear in clear text but masked) to be subsequently ciphered in order to recalibrate the noise. Finally, an unmasking is carried out before the storing of ciphered result in memory. Thus, there is no way to learn anything about the underlying message at the intermediate decryption step. Side channel attacks of the first order like SPA, DPA, CPA are no longer feasible due to the masking and the impossibility for the attacker to choose the corresponding plain text.

Our processor implements a MIPS instructions set with specific homomorphic instructions and dedicated large registers. The

ALU is modified to treat 8 bit data, ciphered using a polynomial of degree 1024 with coefficients on 64 bits whereas normally such a polynomial enables the encryption of only one bit. The homomorphic encryption relies on a sampling from discrete Gaussian distribution fed by a high throughput RNG based on a stream cipher Trivium. The polynomial multiplication is carried out thanks to a NTT using a butterfly architecture with a 2-port DPRAM followed by a Barrett's modular reduction. This implementation was verified on an FPGA.

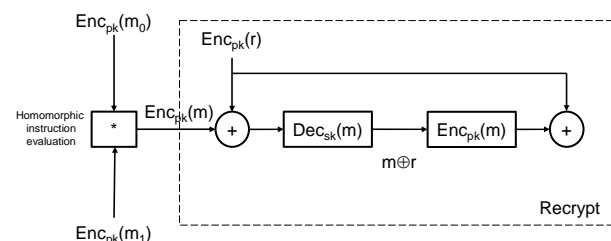


Fig. 1: Recrypt for bootstrapping and recalibrating the noise.

A C-language-adapted compilation chain based on LLVM enables to remove loops, branches which depends on dynamic values and to map arithmetic operations towards homomorphic instructions.

## Perspectives

Our proof-of-concept has been implemented on an FPGA platform. The next step would be to adapt the technology into a secure core embedded into an ASIC design.

## RELATED PUBLICATIONS:

[1] Patent FR1651502 "Méthode d'exécution confidentielle d'un programme opérant sur des données chiffrées par un chiffrement homomorphe", inventors: O. Savry, T. Hiscock, 24/2/2016.

# CELTIC PROJECT "TILAS": DEPLOYMENT OF LARGE-SCALE SECURITY PROTOCOLS FOR SMART CITY APPLICATIONS

## RESEARCH TOPIC:

End-to-End security, Security by design, IoT platform, Elliptic Curves Cryptography, Smart City

## AUTHORS:

Christine Hennebert and Sylvie Mayrargues

## ABSTRACT:

The Celtic project "TILAS" aims at introducing scalable solutions for the large-scale deployment of sensors in an IoT platform for Smart City applications. Innovative security solutions for the secure connection of sensors to the IoT network, device authentication, authorization and maintenance of the end-to-end communications have been proposed to ensure the security of the infrastructure throughout its lifecycle. The TILAS project was evaluated as Excellent and won the prize of the best "Smart City" project awarded in Stockholm on April 28th, 2016 at the Celtic-Plus event.

## Context and Challenges

One of the objectives in the TILAS project was to investigate about the use of asymmetric cryptography for the large-scale deployment of remote, stand-alone and resource-constrained sensors, particularly for Smart City applications. The context of Smart City field is particular because the equipment is deployed in public environment, accessible to all citizens and often difficult to access for maintenance.

Our contribution was twofold. On the one hand, innovative security protocols have been introduced to address the specific need of large-scale deployment in the public sector to limit operator maintenance in the field and to ensure the security of routing packets in the Wireless Sensors Network (WSN). On the other hand, solutions for ensuring end-to-end communications' security throughout the sensors' lifecycle have been implemented on Wismote technology nodes.

(<http://www.aragosystems.com/fr/wisnet-item/wisnet-wismote-item.html>).

## Main Results

A demonstrator was realized showing the feasibility of embedding the compressed version of the IPsec protocol in a node constrained in memory resources, in computing capacity and in bandwidth on the Contiki operating system. We have shown that even the most constrained nodes can be reached securely via an IP address.

Another demonstrator has been developed to show that the DTLS protocol handshake mode can be used in constrained nodes using an asymmetric cryptographic technique based on elliptic curves, enabling nodes to authenticate themselves Autonomous, without having to share common secret pre-installed (Fig #1). This capability facilitates deployment, reduces human intervention costs, increases the autonomy of nodes, raises the level of security of the system and enables maintenance to maintain the desired security level throughout the life cycle of the system.

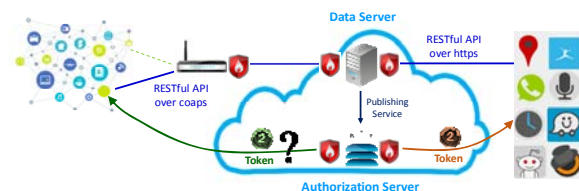


Figure 1: Architecture of the secured IoT platform

The TILAS project has been evaluated "Excellent" by the Celtic program during the final review that occurred in the city of Santander in Spain. The project has won the award of the best « Smart City » project delivered at Stockholm on April 28th, 2016 during the Celtic-Plus event (Fig.#2).



Figure 2: Delivery of the Awards

A scientific paper has been published in the IEEE journal of IoT and a patent has been delivered following the work realized for this project.

## Perspectives

In the following of this project, we would like to address the data protection, in particular to ensure the privacy of the measures issued from the sensors.

## RELATED PUBLICATIONS:

- [1] C.Hennebert, J. Dos Santos "Security Protocols and Privacy Issues into 6LoWPAN stack: A synthesis" IEEE Internet of Things Journal, Vol. 1, Issue 5, pp. 384-398] October 2014.
- [2] Patent: C.Hennebert "Authentication of constrained and remote wireless devices, for achieving end-to-end security", Brevet français 1561408 déposé le 26/11/2015.
- [3] Dos Santos, C. Hennebert, C. Lauradoux [Preserving privacy in secured ZigBee Wireless Sensor Network][IEEE World Forum on Internet of Things, Milan, Italy December 2015.

# SIDE-CHANNEL-ATTACKS: KERNEL DISCRIMINANT ANALYSIS TO COUNTERACT MASKING COUNTERMEASURE

## RESEARCH TOPIC:

Higher-order SCA, dimensionality reduction

## AUTHORS:

E. Cagli, C. Dumas, E. Prouff (Safran Identity & Security)

## ABSTRACT:

When a  $(d-1)^{\text{th}}$  order masking countermeasure is implemented to thwart Side Channel Attacks, the fundamental preliminary attack phase consisting in selecting Points of Interest which is a very hard task: almost all existing methods have a combinatorial complexity explosion, since they require an exhaustive search among all possible  $d$ -tuples of points. The exploitation of the Kernel Discriminant Analysis leads to an efficient method for informative feature extraction in presence of masking countermeasure, whose complexity does not grow with  $d$ .

## Context and Challenges

In cryptography, Side Channel Attacks (SCAs) are attacks that target physical implementations of cryptographic algorithms. Information is gained about intermediate sensitive variables of the algorithm by observing the variation of physical properties of the hardware executing the latter algorithm, e.g. power consumption or electromagnetic radiation. In practice, running a SCA requires computing on data of huge dimensions. In SCA context, for attacks against unprotected implementations, a vast literature is dedicated to the problem of dimensionality reduction. The Linear Discriminant Analysis (LDA) technique stands out [2]: it provides an optimal linear combination of the signals time samples, which concentrates the sensitive information over few points. The literature is more scattered in the context of implementations protected with masking countermeasure: extracting information in such a case requires the exploitation of non-linear combinations, and the choice for such combinations is very complex.

## Main Results

In [1], the Kernel Discriminant Analysis technique is proposed. It consists in completing the LDA with a so-called kernel trick. The latter trick allows to implicitly map the data into a larger feature space by means of a non-linear function.

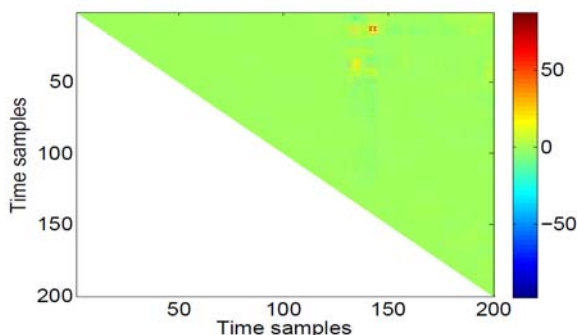


**Fig. 1: The 20,100 KDA implicit linear combination coefficients used for the second order attack. High coefficients are assigned to the informative time samples.** In such a larger space, sensitive features are present and the

LDA optimally combines them linearly. Since the non-linear mapping is not explicitly performed, this technique is not affected by the drawbacks due to the combinatorial enlargement of the feature space. The KDA requires the choice of a so-called kernel function. The authors of [1] proposed the use of the polynomial function  $K(x,y) = \langle x,y \rangle^d$ . This function is associated to a feature space of size  $\binom{D+d-1}{d}$ ,  $D$  being the original size of data.

Experiments shown in the paper are run over  $D = 200$ -sized data, off orders  $d=2, 3$  and  $4$ . The size of the feature space in these cases equals respectively to 20,100, 1,353,400 and 68,685,050.

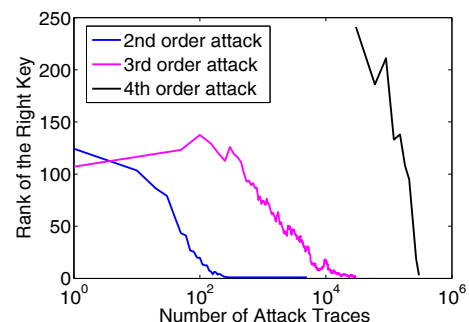


**Fig. 2: Number of side-channel traces vs rank of the right secret key. The goal of a SCA is to rank the correct key first. A  $d^{\text{th}}$  order attack is an attack performed against a  $(d-1)^{\text{th}}$  order masking countermeasure.**

For the three experiments the complexity of the KDA research for linear combining coefficients in the feature space is the same, not being influenced by the size of such a space. Such coefficients are only implicitly computed (in Fig. 1 we explicitly computed them to see the leaking time samples). The SCAs performed over data compressed using the KDA technique are efficient (as shown in Fig. 2), proving the efficiency of such a dimensionality reduction method.

## Perspectives

This work is part of a fruitful transfer of techniques from machine learning to side-channel context. Some improvements could be made by optimum choice of the parameters. Moreover It would be interesting to use this method in the non-supervised context.

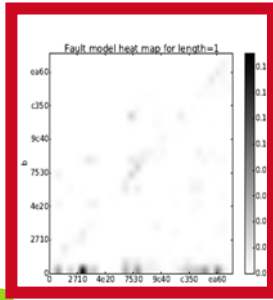
## RELATED PUBLICATIONS:

- [1] E. Cagli, C. Dumas, and E. Prouff. "Kernel Discriminant Analysis for Information Extraction in the Presence of Masking." International Conference on Smart Card Research and Advanced Applications. Springer, Cham, 2016.
- [2] E. Cagli, C. Dumas, and E. Prouff. "Enhancing dimensionality reduction methods for side-channel attacks." International Conference on Smart Card Research and Advanced Applications. Springer International Publishing, 2015.



6.

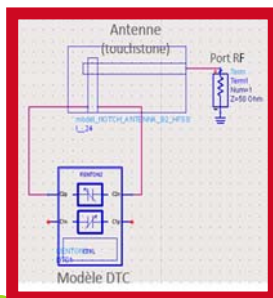
PHD DEGREE  
AWARDED IN 2016



**LOUIS DUREUIL**  
**CODE ANALYSIS AND EVALUATION PROCESS FOR**  
**VULNERABILITY DETECTION AGAINST FAULT INJECTION**  
**ON SECURE HARDWARE**  
*Université Grenoble Alpes (France)*

Vulnerability detections for smart cards require state of the art methods both to attack and to protect the secure device. A typical type of attack is fault injection, most notably performed by means of laser techniques. To prevent some of the consequences of this kind of attacks, several analyses are conducted at the software level. Being able to define criteria and to propose automated tools that can survey the robustness of an application to fault injection is thus nowadays a hot topic, even more so since the hardware attack techniques allow today an attacker to perform several attacks in a single software execution. Indeed, recent research works evaluate the effectiveness of counter-measures against fault injection[1], or attempt to develop models of fault injection at the C level[2]. This thesis project addresses the issue of multiple faults injection, albeit by adding the distinctive aspect of static and dynamic analysis interaction in a context of binary-level fault injection. An objective of the thesis is to achieve a configurable framework to simulate fault

injections in the way they are currently performed by the CESTI-LETI laboratory on the actual hardware. To do so we will develop a generic intermediate model that will allow us to specify hardware constraints, such as the various kinds of memories (RAM, EEPROM, ROM), whose different properties can induce either permanent or volatile faults. Combining the static code analysis with dynamic fault injections should prevent the combinatory explosion of the executions while attack patterns will guide the analysis. A taxonomy of attacks and new attack modelisations could emerge from this work. An adaption of the tools for static analysis is also required, because dynamic fault injection can deeply change the code by modifying the interpretation of the instructions, in a similar manner to dynamic compilation. This thesis project falls within the CESTI-LETI's innovation strategy, et could lead to an automated code verifier that could be used by the CESTI-LETI evaluation specialists.



**ESSIA BEN ABDALLAH**  
**ACTIVE ANTENNA DESIGN FOR FUTURE COMPACT AND**  
**HIGH EFFICIENT RF FRONT-END**  
*Université Grenoble Alpes (France)*

The recent development of cellular communication standards has led to an increasing RF front-end complexity due to the ever increasing number of RF supported frequency bands. This is not optimal for cost and occupied space area. In order to optimize the RF performances and energy consumption, the approach used in this thesis is to share the constraints between the PA and the antenna of the front-end: this is called co-design. In this thesis, the considered co-design approach is twofold and in near future both results should be simultaneously considered and integrated into one fully reconfigurable RF front-end design. The first study addresses the co-design of an antenna and its associated power amplifier (PA), which are traditionally designed separately. We first determine the antenna impedance specifications to maximize the tradeoff between the energy transfer and PA linearity. Then, we propose to remove the impedance matching network between antenna and PA, while demonstrating that a low impedance antenna can

maintain the RF performances. Thus the proposed co-design keeps the PA linearity for high power levels (> 20 dBm). The second study focuses on the co-design of an antenna and its tunable aperture components. The miniaturization effort is balanced regarding the resistive losses between the antenna structure and a tunable capacitor (DTC). The achieved developments are based on EM simulations, modeling, system characterization (linearity and switching time) and radiation measurements (efficiency) of miniature reconfigurable antenna prototypes in the 4G low bands. The radiator occupies only 18 x 3 mm<sup>2</sup> ( $\lambda_0/30 \times \lambda_0/180$  at 560 MHz), and suitable for a possible integration onto smartphones. The antenna resonance frequency is tuned between 560 MHz and 1030 MHz. For the first time, the impact of SOI DTC implemented on the antenna radiating structure on linearity is measured with a dedicated test bench. The linearity specified by 4G is maintained up to 22 dBm of transmitted power.



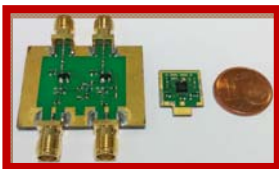
## HÉLÈNE PIRET

### EMBEDDED BROADBAND MEASUREMENT OF ELECTRICAL IMPEDANCE : APPLICATION TO BATTERY

*Université Grenoble Alpes (France)*

Many applications rely on batteries, for instance in the field of transport, of smart grid, of connected objects. Therefore, the development of battery has become a crucial issue. Unfortunately, a battery is a complex electrochemical system which depends of many parameters and whose performance deteriorates over time. Thus the development of an efficient battery management system (BMS) is a priority. One way to obtain interesting information representative of the present state of the battery is to estimate its electrochemical impedance. This thesis presents time frequency impedance identification methods which can be easily embedded in vehicles or nomad devices. The first developed method not only allows an accurate impedance estimation but also a tracking of its temporal evolution contrary to classical electrochemical spectroscopy techniques. This method based on Fourier transform relies on recursive local average controlled by a single parameter, managing a trade-off between tracking and estimation performance. The ability of the

method to monitor the impedance over time is demonstrated on a simulator, then on a real lithium ion battery, on which a repeatability study is carried out, and finally applied to follow the impedance evolution of a drone battery during a flight. The second method based on wavelet transform is developed to deal with long-range dependence phenomena such as ion diffusion-limited reactions which occur in the battery. Battery models using electrical equivalent circuit often include Constant Phase Elements (CPE) to account for these phenomena. After compared wavelet to Fourier method on a CPE simulator thanks to a Monte Carlo procedure, the wavelet approach and its irregular time-frequency tiling appears to be an interesting method, specifically for its minor bias error. To develop a powerful BMS, different battery indicators or parameters are then estimated from the impedance to be able to follow the state of the battery in real time and avoid damages. Several examples are given.



## BATEL LOTFI

### ACTIVE DIRECTIVE SMALL ANTENNAS

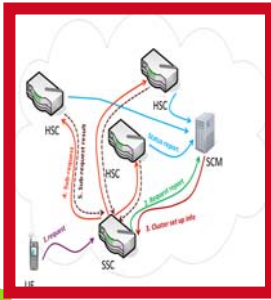
*Université Rennes 1(France)*

In a context of wireless communication systems generalization, the need of small antennas for integration into smart objects is increasing. Trade-off are often required between the main performance characteristics of small antennas and their electrical size because of the limitations of the fundamental physics. Few studies deal with the directivity of small antenna and the fundamental limitations of this radiation property are not yet mature.

Directive antennas, used to focus the radiation in useful directions, offer new perspectives for wireless applications. Nevertheless, usual techniques to enhance antennas' directivity lead to larger antennas and their integration into small objects would be difficult. That becomes critical when antennas working at less than 1 GHz frequencies have to be integrated in small objects (around few centimeters). Radiation control through directive antennas is being an important issue for the future communications. This kind of antennas allows reducing electromagnetic

pollutions which limit wireless systems and communicants objects cohabitation. Recent state of the art has shown new perspectives to establish small antennas with super directive radiation using parasitic antenna arrays. A super directive antenna is a small antenna that exceeds its natural and low directivity. Moreover, these last few years, researches on active antennas and associated results could be considered for modern approach to deal with small and directive antennas' issues. In this work, we propose to evaluate the enhancement perspectives brought by the active electronic circuits to solve the small and directive antennas' issues. Typically, special active circuits known as Negative Impedance Converters have been designed in this thesis. Those circuits have been experimentally evaluated to materialize the small and super directive antennas perspectives. This work has demonstrated for the first time the possibility to establish a super directive radiation pattern within a large frequency bandwidth using a small antenna with Non-Foster elements.

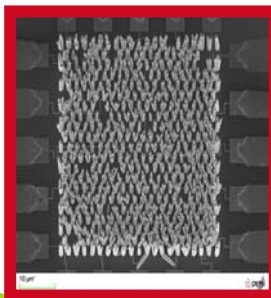




**OUEIS JESSICA**  
**JOINT COMMUNICATION AND COMPUTATION**  
**RESOURCES ALLOCATION FOR CLOUD-EMPOWERED**  
**FUTURE WIRELESS NETWORKS**  
*Université Grenoble Alpes (France)*

Mobile Edge Cloud (MEC) brings the cloud closer to mobile users by moving the cloud from the internet to the mobile edge. In this PhD research we adopt a local MEC computing architecture, where small cells are empowered with computational and storage capacities. In this PhD research we adopt a local MEC computing architecture, where small cells are empowered with computational and storage capacities. Mobile users' offloaded computational tasks are executed at the cloud-enabled small cells. We propose the concept of small cells clustering for MEC, where small cells cooperate in order to execute offloaded computational tasks. A first contribution of this thesis is the design of a multi-parameter computation offloading decision algorithm (SM-POD). In the second part of this thesis, we tackle the problem of small cell clusters set up for MEC computing for both single-user and multi-user cases. The clustering problem is formulated as an optimization that jointly optimizes the computational and communication resource

allocation, and the computational load distribution on the small cells participating in the computation cluster. In the multi-user case, the optimization problem is not convex and we propose a convex reformulation of the problem, proving that both problems are equivalent. As third contribution, we propose the new concept of computation caching for edge cloud computing. With the aim of reducing the edge cloud computing latency and energy consumption, we propose caching popular computational tasks for preventing their re-execution. Our contribution here is two-fold: first, we propose a caching algorithm that is based on requests popularity, computation size, required computational capacity, and small cells connectivity. This algorithm identifies requests that, if cached and downloaded instead of being re-computed, will increase the computation caching energy and latency savings. Second, we propose a method for setting up a search small cells cluster for finding a cached copy of the requests computation. The proposed method



**LEON PEREZ EDGAR**  
**INTERCONNECTED PIEZOELECTRIC NANOWIRE MATRIX**  
**FOR HIGH RESOLUTION SENSOR APPLICATIONS:**  
**TECHNOLOGICAL CHALLENGES AND SOLUTIONS**  
*Université Grenoble Alpes (France)*

Over the past few years, a variety of nanomaterial-based devices have arisen, revealing micro-actuators and micro-sensors with improved performances (resolution, sensitivity, selectivity). Here we will focus on Zinc Oxide (ZnO) nanowires by exploiting the piezoelectric effect combined with their semiconducting properties. When submitted to a mechanical constraint or displacement, piezoelectric nanowires generate an electrical potential (piezopotential). If, in addition to this, nanowires are also semiconducting, the piezopotential can be exploited to control an external current as a function of the mechanical constraint imposed to the nanowire (piezotronic effect). The advantage of using one-dimensional nanostructures lies into the modularity of both their mechanical and piezoelectric properties. Moreover, their integration is now possible and compatible with micro-electronic processes (CMOS/MEMS). These considerations make it possible to design very high performance devices combining the very small dimension of their functional unit elements

(high spatial resolution) and their sensitivity to nanoscale phenomena. In the thesis, we develop a proof-of-concept prototype of vertically-aligned ZnO-piezoelectric-nanowire matrix-type sensors. First, the design process is elaborated based on finite element multiphysics models (FEM) of the piezoelectric response of a single bent nanowire. Technological solutions could be implemented through the fabrication of elementary pixels suitable for characterization and whose piezoelectric response could be predictively modeled. The technological part of the work covered several development stages, including the chemical growth of ZnO nanowires (clean-room compatible seed layer and selective growth process development) and the design of the electrode matrix contacting the nanowires individually. The second part of the fabrication work focused on defining and optimizing the technological stack with respect to all the above mentioned considerations and implementing the technological processes yielding the final targeted matrix.



### VINCENT RÉMY

#### PASSIVE IDENTIFICATION IN ACOUSTICS: ESTIMATORS AND APPLICATIONS TO SHM

*Université Grenoble Alpes (France)*

Passive identification relies on retrieving the impulse response of a propagation medium using only ambient and uncontrolled sources. This domain has been in expansion since the 2000's due to fundamental results obtained in seismology. In 2011, Cea-Leti proposes an application of these results in the acoustic framework. A new formulation of the theory has been derived to be adapted to viscous acoustic waves which is the most relevant existing model in that context. In particular, a new Ward identity has been obtained and validated with real data experiments. The objective of this PhD was to apply the results in the Structural Health Monitoring (SHM) domain for sensors network localization, time of arrival estimation and modal analysis. Firstly, we develop an estimation theory adapted to the passive acoustic identification context. We derived a new Cramer-Rao lower bound for the time of arrival estimation and we compared it to the classical bound known in the active context. Those results have been published in the IEEE Signal Processing journal. Secondly, we defined experimentations to

evaluate the performances of the methodology for SHM applications. These experimentations highlighted the feasibility of the new concept introduced on passive acoustic sensors network localization and applied to geometry retrieval of structures (as concrete and metallic beams, for example). All of the results on SHM application of our passive identification technique has been presented to the International Workshop on Structural Health Monitoring in Stanford in 2015. The perspectives of this work are, in one hand, to develop algorithms adapted to signals acquired in real contexts meaning algorithms able to detect signals which contribute to passive identification and signals which do not (as the sound generated by a rotary machine which generates a structured signal). On the other, a new Ward identity can be established with no a priori on the damping. This perspective has a relevant impact on all passive identification domains as it does not require a knowledge on the true damping which is tricky to evaluate in practice.



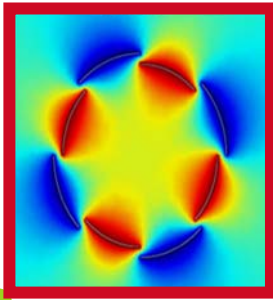
### ARTIGES NILLS

#### FROM INSTRUMENTATION TO OPTIMAL PREDICTIVE CONTROL TOWARDS BUILDINGS ENERGY EFFICIENCY

*Université Grenoble Alpes (France)*

Nowadays, reducing the environmental impact of buildings is a major concern, and Model Predictive Control (MPC) of buildings is seen as a key for energy optimization in this sector. This thesis aims to identify the links between MPC and instrumentation in buildings, through a MPC strategy based on a generic method of simulation and optimization of detailed building models. This method implements the adjoint approach to provide a fast computation of gradients used for optimization. The control strategy is here tested on the case of an experimental home at INES (National Solar Energy Institute), both in simulation and on the real building, allowing us to explore the instrumentation needs. Furthermore, we show that this approach for optimal control and gradients computation can lead to sensitivity studies for selecting the parameters to calibrate and eventually choose the most relevant sensors for predictive models calibration. Keywords: Model Predictive Control, zonal-nodal

models, buildings models calibration, state estimation, sensitivity analysis, adjoint method



**MATTHIAS PEREZ**

**ELECTROSTATIC CONVERSION FOR AIRFLOW ENERGY HARVESTING**

*Université Grenoble Alpes (France)*

This thesis was aimed at converting airflows into electrical energy through electrostatic converters.

The electrical energy produced is intended to supply low power sensors for structural health monitoring, environmental follow-up, buildings monitoring...

Two categories of airflow energy harvesters have been developed: (i) the rotational harvesters which transform the kinetic energy of airflows into a mechanical energy of rotation (micro-turbines) and (ii) the aeroelastic harvesters which use wind energy to produce a mechanical energy of periodical oscillations (like flags in the wind).

These two types of harvesters have been associated with different electrostatic converters, polarized by the addition of electrets or self-polarized by triboelectricity.

The energy harvesters have been optimized and the benefit of the electrostatic conversion

for small-scale devices (a few  $\text{cm}^2$ ) operating at low speeds ( $<3\text{m/s}$ ) has been proven. The power densities reach  $5\mu\text{W}/\text{cm}^2@1\text{m/s}$  for rotational devices and in the range of  $10\mu\text{W}/\text{cm}^2@10\text{m/s}$  for aeroelastic devices.

The micro-generators were finally combined with power management circuits to supply autonomous and communicating sensors. A self-starting power management circuit able to work without battery has been developed to maximize the useful output power of the energy harvesters by implementing a Maximum Power Point technique, compatible with the parallelization of energy harvesters.

This last stage completes the energy harvesting chain and also shows the high benefit of active circuits (synchronous electric charge extraction, maximum power point) compared to standard passive power managements, with usable output powers multiplied by 10.





## GREETINGS

**Sébastien Dauvé**

Head of Systems Division  
sebastien.dauve@cea.fr

**Jean-Louis Amans**

Deputy Head of Systems Division  
jean-louis.amans@cea.fr

**Emilio Calvanese-Strinati**

Scientific Manager  
emilio.calvanese-strinati@cea.fr

**Jean-Michel Léger**

Program Manager  
jean-michel.leger@cea.fr

**Fabien Clermidy**

Head of Wireless Technology Department  
fabien.clermidy@cea.fr

**Stéphanie Riché**

Head of Sensor Autonomy and Integration Department  
stephanie.riche@cea.fr

**Bruno Charrat**

Head of Electronics and components Department  
bruno.charrat@cea.fr

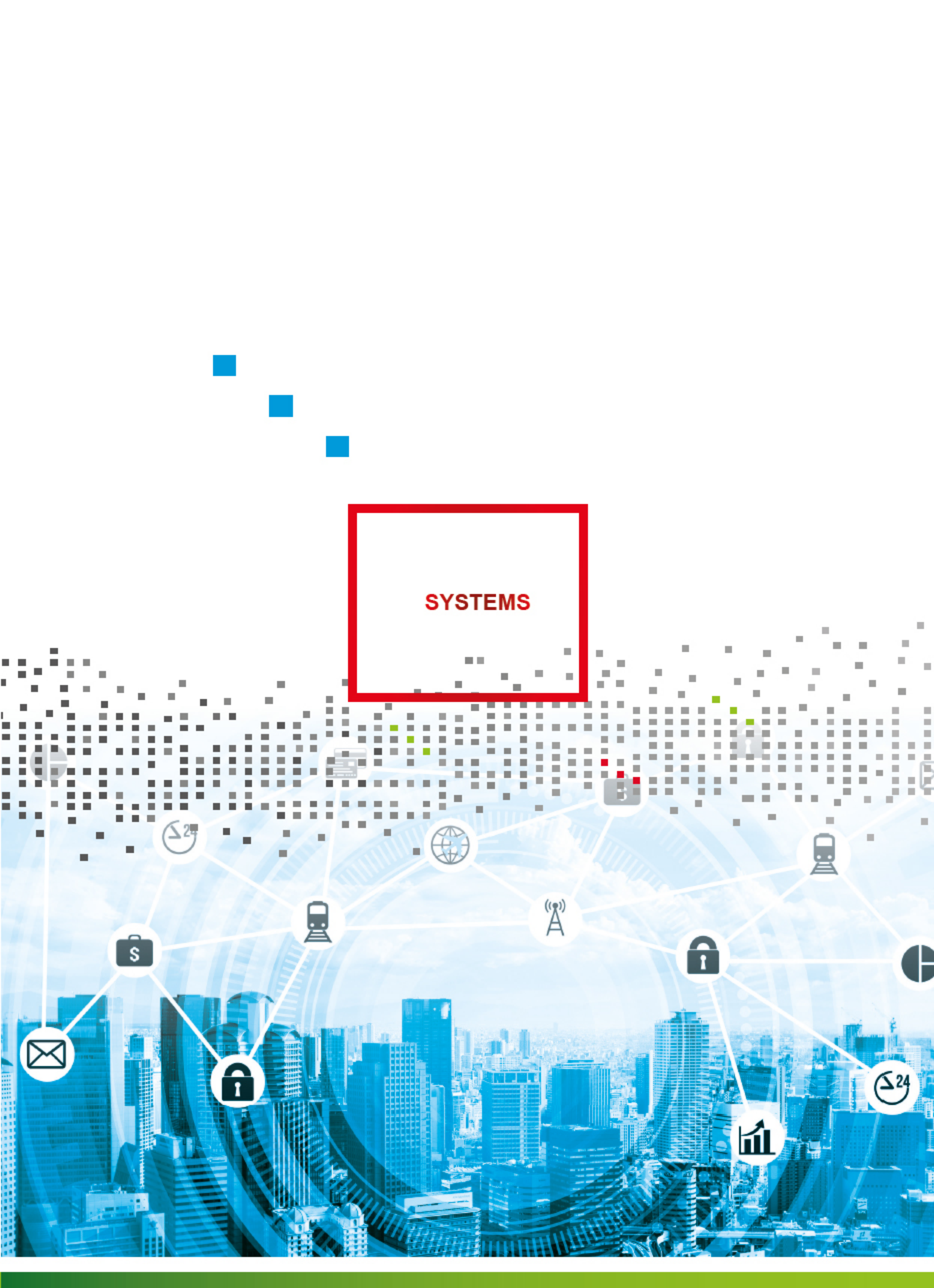
**Sylvie Mayrargue**

International Telecom Expert  
sylvie.mayrargue@cea.fr





**SYSTEMS**







## SYSTEMS

## ANNUAL RESEARCH REPORT 2016

### CONTACTS

**Sébastien Dauvé**

Head of Systems Division  
sebastien.dauve@cea.fr

**Jean-Louis Amans**

Deputy Head of Systems Division  
jean-louis.amans@cea.fr

**Emilio Calvanese-Strinati**

Scientific Manager  
emilio.calvanese-strinati@cea.fr

**Jean-Michel Léger**

Program Manager  
jean-michel.leger@cea.fr

**Fabien Clermidy**

Head of Wireless Technology Department  
fabien.clermidy@cea.fr

**Stéphanie Riché**

Head of Sensor Autonomy and Integration Department  
stephanie.riche@cea.fr

**Bruno Charrat**

Head of Electronics and components Department  
bruno.charrat@cea.fr

**Sylvie Mayrargue**

International Telecom Expert  
sylvie.mayrargue@cea.fr

**Leti, technology research institute**

Commissariat à l'énergie atomique et aux énergies alternatives

Minatec Campus | 17 rue des Martyrs | 38054 Grenoble Cedex 9 | France

[www.leti.fr/en](http://www.leti.fr/en)